BENTHIC MICROBIAL FOOD WEBS: SPATIAL AND TEMPORAL VARIATIONS AND THE ROLE OF HETEROTROPHIC PROTISTS IN SALT MARSH SEDIMENTS

by

MATTHEW ROBERT FIRST

(Under the Direction of James T. Hollibaugh)

ABSTRACT

In order to determine if the loss of bacterial biomass varies over time, I investigated the microbial food web structure at two time scales in the salt marsh sediments of Sapelo Island, Georgia. Samples were collected monthly for one year at three contrasting subtidal locations: a high energy sandy beach, a muddy *Spartina* marsh, and a tidal creek bed. Concentrations of benthic microalgae (BMA), bacteria, heterotrophic protists, and metazoan meiofauna were measured at each location. Additionally, short-term dynamics of sediment microbial populations and bacterivory rates were investigated over a diel period in an intertidal creek bed to determine if variable rates of protist grazing could significantly impact bacterial standing stock. Although bacterivory rates were variable throughout the day, there were no periods of the day when protists could effectively reduce bacterial biomass. Yearly sampling revealed high variation in the microbial food web structure, mostly among sample locations. However, I observed a shift from a BMA-dominated community in the spring/ early summer months to a bacterial-dominated food web in the late summer/fall at all locations. Bacteria and heterotrophic protist concentrations were significantly related to porewater volume ($6.9 \pm 1.2 \times 10^9$ and $5.1 \pm 1.1 \times 10^3$ cells $ml^{-1}$, respectively, ±SE). The low abundance of protists (relative to high bacterial

concentrations) may be due to top-down pressure by large ciliates and nematodes. This top-down pressure in the autumn months (when BMA are proportionally less abundant) may contribute to high concentrations of bacteria during this season. Microbenthos displayed a clumped distribution pattern in Fluorescently Labeled Embedded Cores (FLEC). The aggregation of microbenthos indicates that the importance of protists in microenvironments may be overlooked by their total concentrations in the sediments. The common benthic ciliate, *Uronema marinum*, was capable of ingestion of fluorescently-labeled dextran (a high molecular weight carbohydrate) at low concentrations (3 μM DOC). However, the ingestion of starch, glucose and acetate did not significantly improve the growth or biomass production for this ciliate. Instead, I hypothesize that the initial breakdown of recalcitrant organic carbon compounds (and egestion of fermentation byproducts) can stimulate sulfate reducing bacteria and indirectly benefit bacterivorous protists through increased bacterial production.

INDEX WORDS: Benthic microbial food webs, Sapelo Island, salt marsh, sediments, microbenthos, dissolved organic carbon, dextran, FLEC, bacteria, microphytobenthos

# BENTHIC MICROBIAL FOOD WEBS: SPATIAL AND TEMPORAL VARIATIONS AND THE ROLE OF HETEROTROPHIC PROTISTS IN SALT MARSH SEDIMENTS

by

MATTHEW ROBERT FIRST

B.S., Ohio University, 1997

M.S., The University of Akron, 2002

A Dissertation Submitted to the Graduate Faculty of The University of Georgia in Partial Fulfillment of the Requirements for the Degree

DOCTOR OF PHILOSOPHY

ATHENS, GEORGIA

2008

© 2008

Matthew Robert First

All Rights Reserved

# BENTHIC MICROBIAL FOOD WEBS: SPATIAL AND TEMPORAL VARIATIONS AND THE ROLE OF HETEROTROPHIC PROTISTS IN SALT MARSH SEDIMENTS

by

MATTHEW ROBERT FIRST

| | |
|---|---|
| Major Professor: | James T. Hollibaugh |
| Committee: | Joan M. Bernhard<br>Mark A. Farmer<br>Samantha B. Joye<br>Christof Meile |

Electronic Version Approved:

Maureen Grasso
Dean of the Graduate School
The University of Georgia
May 2008

# DEDICATION

My wife, Angela Modugno stood by me during the many years it took to complete this work. My children, Ian and Isaac learned to stand during these years and have grown into beautiful boys. They sustained me through the rough times and shared in my good times. My parents (by birth and by marriage) selflessly encouraged and supported this endeavor. I dedicate this work to these people, a small token in repayment towards all they have given.

ACKNOWLEDGEMENTS

Advising and mentoring students is an enormous task. Theoretically, it is a mutualistic relationship where both advisor and student benefit. In practice, the tremendous benefit that students derive from the dedication of their advisors is seldom repaid in kind. Knowing these circumstances well, Tim Hollibaugh accepted me into his lab. For this, and all the advice, assistance and support he has given me over the years, I am truly thankful. Tim has been both a friend and a mentor, and has taught me countless lessons.

Likewise, my committee members have generously offered their time and advice. They have assisted me in my research and writing and advocated for me on numerous occasions. I am especially grateful that each member of my committee gave up their limited time to help me on my path to matriculation. Drs. Joye and Farmer have also inspired me in the classroom in the fields of microbial ecology, biogeochemistry, cell biology, and microscopy. I have benefited tremendously from Dr. Meile's perspective and numerical approaches to problem solving. Dr. Bernhard has sacrificed a great deal to participate in my dissertation work and this project is largely inspired by her work.

Dr. Nasreen Bano has graciously offered her time and knowledge, especially with molecular techniques where her knowledge is extensive. She and others in the Hollibaugh lab (Gary Lecleir, Jen Fisher, Karen Kalanetra) have helped me by offering support and friendship. Lanny Miller was a mentor and a friend during my time in Athens. I have learned tremendously from him. I also owe a tremendous amount to Dr. Catherine Teare Ketter. She is a strong advocate for instructional excellence and a tireless worker. I have learned both by her instruction

and her example. I am truly grateful to consider her a mentor and a friend. I also acknowledge all my professors (Drs. Moran, Sun, Cai, Burd, Joye, Farmer, Shields, Keith, Binder, Di Iorio, Teare Ketter), and the professors I have worked with as a teaching assistant (Drs. Hodson, Tilburg, Moran, Alber).

I am grateful for the hospitality I have received at the University of Georgia Marine Institute (UGAMI), where this field work was conducted. Jon Garbisch and Mary Price were especially helpful on the island, providing advice and logistical support. Chris Lasher helped during some of the sampling and almost all of the driving. In the Department of Marine Sciences, Dr. Daniela Di Iorio and Paul McKay, generously loaned their CTD and helped analyze the data. Chris Fleisher (Geology Dept., UGA) advised and assisted on the diamond saw operation. I also benefited from the help I received from Drs. Keith and Shields at the Center for Ultrastructural Research (UGA). Julie Nelson, at the UGA Flow Cytometry Lab, was tremendously helpful in teaching me the basics of flow cytometry (including operating the instruments and analyzing the data). This work was supported by NSF Georgia Coastal Ecosystems LTER grant (OCE-9982133). I also received support through the UGA graduate school.

The work in this document could not have been completed without the support from my wife, Angela Modugno. Because of her, I never lost focus on my goals. Vince and Carolyn Modugno dedicated several years to caring for their grandchildren when their father was at the lab. Bob and Joyce First encouraged me throughout graduate school.

At the time of writing, the list of contributed publications from Marine Institute from 1955 to the present approaches one thousand. I am proud, but humble, to be among the distinguished scientists who have worked to unravel the secrets of the Sapelo Island salt marsh. I have gained much from their insight, learned from their examples and admired their wisdom.

The research chapters in this work are, in order, contribution numbers 967, 952, 957, and 961 to the University of Georgia Marine Science Institute.

TABLE OF CONTENTS

Page

LIST OF TABLES

Page

LIST OF FIGURES

Page

# CHAPTER 1

## INTRODUCTION AND LITERATURE REVIEW

Salt marshes flourish along temperate and sub-tropical coastlines where low tidal energy permits the accumulation of fine sediment and the establishment of marsh grasses tolerant of brackish waters. In the United States, salt marshes make up over 70% of total intertidal wetland area – nearly 4 million acres in total (Dahl 2005). These wetlands provide habitat and sustenance to many important commercial fisheries, such as penaeid shrimp and blue crabs (Zimmerman et al. 2002). Substantial amounts of organic material and nutrients are exchanged between salt marshes and estuaries, highlighting the dynamic linkages and interdependence of these systems (Childers et al. 2000). Salt marshes also provide food to transient consumers, such as birds and nekton (Vernberg 1993). These functions emphasize the value of salt marshes and underscore the need for both conservation and a deeper understanding of them.

### PRIMARY PRODUCTION IN SALT MARSHES: LINKAGES TO SEDIMENTS

Early studies of salt marsh ecology focused on marsh grasses, the most obvious of the primary producers. The common cordgrass, *Spartina alterniflora,* is the dominant intertidal macrophyte in the Southeast United States (Higinbotham et al. 2004). Only a small portion (~ 10%) of standing *Spartina* biomass is used directly by grazers, such as insects and snails (Teal 1962). These plants are composed largely of lignocellulose, which is not readily hydrolyzed except by fungi and bacteria (Benner et al. 1984). Indeed, the marsh periwinkle (a snail commonly found on *Spartina* plants) depends upon fungi that grow on plant wounds and radulations rather than on

directly ingested plant material (Silliman & Newell 2003). Burial of above-ground plant matter and the extensive below-ground root and rhizome structures (e.g. Schubauer & Hopkinson 1984) supply salt marsh sediments with organic matter to fuel an extensive microbial food web (Howarth & Hobbie 1982)

The biomass of microalgae in the sediments and the water column is a fraction of the enormous biomass of salt marsh macrophytes, yet microalgal production can be substantial in shallow coastal waters. The rapid growth of benthic microalgae (BMA) allows for high production rates and short turnover times (MacIntyre et al. 1996, Miller et al. 1996). Benthic diatoms can divide up to three times per day under optimal conditions (Williams 1964). The overall annual BMA production is estimated to be greater than 33% of *Spartina* production (Gallagher & Daiber 1974, Sullivan & Currin 2000). Benthic algal production is rapidly transferred through the benthic food web. For example, the signal from $^{13}$C-labeled algal photosynthate appears in nematodes within 1 h and in bacterial phospholipid fatty acids within several hours after introducing $^{13}$C-labeled bicarbonate to sediments (Middelburg et al. 2000). This suggests that heterotrophic production in the sediments is tightly linked to benthic algal photosynthesis.

The focus of this study is the benthic microbial food web that is fueled by the large inputs of primary production in salt marshes (See Fig. 1.1). The benthic microbial food web regulates the rate of carbon decomposition and the amount of primary production returned to larger grazers. The trophic pathway in which detrital carbon is returned to higher trophic levels is described below.

## THE BENTHIC MICROBIAL LOOP

The flow of energy from dissolved organic carbon (DOC) through heterotrophic bacteria to phagotrophic protists is termed the "microbial loop" (Azam et al. 1983). Bacteria are too small or dispersed to support large grazers, and thus, phagotrophic protists play a key role in reintroducing DOC into the grazing food web. Food web efficiency is a measurement of the amount of DOC returned to the grazing food web, compared to what is lost to microbial respiration. The importance of the microbial loop in returning DOC to higher trophic levels has been debated (Ducklow et al. 1986, Sherr et al. 1987), and is largely dependent upon protist feeding efficiency and the number of trophic transfers among protists.

There is a growing, but still considerably smaller when compared to pelagic environments, body of work available on the microbial loop in benthic communities. In general, concentrations of sediment bacteria are several orders of magnitude greater than in pelagic environments (Rublee 1982). This high bacterial biomass suggests that the flow of carbon through the microbial loop is potentially substantial (Kemp 1990). Yet, bacterial production often exceeds the loss to bacterivores (Posch et al. 2001, Wieltschnig et al. 2003). In freshwater sediments, bacterial production was extremely high in the summer, estimated up to 250 x $10^6$ cells $cm^{-3}$ $h^{-1}$ (Starink et al. 1996). Heterotrophic nanoflagellates were the most abundant bacterivore in these sediments and consumed less than 5% of this bacterial production. Viral lysis does not appear to substantially reduce benthic bacteria standing crop in sediments as rates of viral infection and lysis are estimated to be low in sediment environments (Glud & Middelboe 2004, Filippini et al. 2006). Given that benthic bacterial concentrations are relatively constant

over time (Schmidt et al. 1998), the disparity between production and loss rates justifies closer examination of the microbial loop to resolve this enigma.

Two potential explanations for the imbalance between bacterial production and grazing mortality are: 1) methodological problems with bacterial rate measurements; and 2) temporal uncoupling between bacterial production and grazing loss. Methodological problems (such as selection of particle-attached or motile bacteria over tracer cells) may complicate grazing estimates (Kemp 1988). For example, the ciliate *Euplotes sp.* was able to ingest bacteria attached to surfaces at rates several orders of magnitude greater than suspended tracer particles (Lawrence & Snyder 1998). This bias could lead to underestimations of protist grazing when only suspended tracer particles are offered (Starink et al. 1994).

Microbial communities have rapid growth rates and short turnover times, thus high frequency variations in bacterial production and grazing may be missed with a low-frequency (i.e. >1 d) sampling scheme. Also, the composition of the microbial food web can vary over seasonal cycles. For instance, benthic phagotrophic protists displayed seasonal patterns in grazing rate and prey preference (Epstein 1997). During the winter and spring, micro- and nano-grazers preferentially consumed sediment diatoms while bacterivory was high in the late summer and fall. These examples illustrate that sampling should be frequent enough to detect both long term (seasonal) and short term (daily) patterns, yet it rarely is. One of the factors considered in designing the study reported here was to capture variability in microbial loop dynamics of typical salt marsh sediments over a range of frequencies.

## THE MICROBIAL LOOP OBSERVED AT TWO TIME SCALES

Abundance of bacteria in sediments (when scaled to sediment porosity) remains relatively constant at approximately $10^9$ cells $ml^{-1}$ across a range of marine environments (Schmidt et al. 1998). This observation raises many questions regarding the fundamental controls on the biomass of benthic bacteria. For example, why are benthic bacteria three orders of magnitude more concentrated than in the water column? What physical/chemical characteristics of the sediment prevent the more complete consumption of bacterial biomass by grazers? This study addresses these questions by measuring the biomass of BMA, bacteria, heterotrophic protists, and meiofauna at two temporal scales. First, I sampled three contrasting subtidal locations monthly for one year (**Chapter 2**). Seasonal cycles of temperature and solar irradiation were superimposed on the divergent physical/chemical characteristics of sediments at each location: a sandy, high energy beach (Nannygoat Beach), a tidal creek bed (Dean Creek), and the boarder of a *Spartina* marsh (Marsh Landing) (See Fig. 1.1). Second, I sampled intertidal sediments at a site in Dean Creek every three hours for a day (**Chapter 3**). I measured the rate of protist bacterivory at each time point using a technique that permits the simultaneous estimate of grazing on both free-living and particle-attached bacteria (Starink et al. 1994). These studies were designed to test the hypothesis that protists are able to control the biomass of benthic bacteria. Control can be identified by a high bacterivore:bacteria biomass ratio at times of the year or through variable rates of ingestion over a short (daily) time period. Production of organic carbon available to bacteria by BMA and marsh macrophytes varies with incident solar irradiation (Smith & Underwood 1998) and seasonal patterns of marsh grass production and burial will lead to uneven rates of plant-derived carbon input throughout the year. Consequently, bacterial production can be expected to vary over daily and seasonal cycles. Since the structure of the microbial food web

is strongly influenced by bacterial production, it will also vary over short and long-term cycles. The impact of protist grazing on bacterial production may vary temporally. The increased importance of bacterial grazing during parts of the day (or seasons) could explain the observations that bacterial production greatly exceeds grazing loss.

## MICROBENTHOS DISTRIBUTIONS IN INTERTIDAL SEDIMENTS

Sediment ecosystems are heterogeneous environments with steep chemical gradients. Within intertidal sediments, these chemical gradients are constantly shifting over diel cycles of solar irradiation and tidal flow. Exposure to sunlight drives high primary production and oxygen generation in the surficial sediments of intertidal mudflats (Pinckney & Zingmark 1993). Consequently, the changing depth of the oxycline restructures the vertical distributions of benthic heterotrophic protists over the course of a day. For example, many benthic protists are highly motile and can quickly locate zones of optimal oxygen concentrations (e.g. Fenchel & Bernard 1996). As a consequence, distributions of aerobic ciliates and flagellates were highly correlated to oxygen penetration in intertidal sediments (Böttcher et al. 2000). Conversely, microaerophilic taxa are sensitive to high oxygen concentrations originating from algal production in the surface photic zone (Berninger & Epstein 1995) and in some cases, sulfide concentration effectively limits the distributions of protists. For example, the common benthic ciliates *Uronema marinum* and *Euplotes sp*. differ in their tolerance to high sulfide concentrations (survival time in 5 mM sulfide is 2 h and 24 h, respectively) (Fenchel & Finlay 1995).

Vertical migrations of BMA occur over the course of a day in intertidal sediments (reviewed by Consalvey et al. 2004). The downward migration may allow BMA to access

nutrients deeper in the sediments (Kingston 2002). The vertical distributions of heterotrophic protists, BMA, and metazoan meiofauna in sediments can provide insights as to their metabolic strategies, oxygen requirements, and associations with other organisms. Subsectioning sediment cores (e.g. MacIntyre & Cullen 1995) is one approach to observe how the vertical distribution of sediment biota changes over time. However, this approach does not capture the three dimensional spatial relationships that occur among microbenthos. These spatial relationships (e.g. the distance between organisms and the clustering of cells) can provide insight into the ecology and associations among the benthic microbial community. The Fluorescently Labelled Embedded Core (FLEC) technique (Bernhard et al. 2003) provides a method to observe these spatial relationships with submillimeter resolution.

I applied the FLEC technique to observe the distributions of microbenthos in intertidal sediments over a diel cycle. The results of this study are reported in **Chapter 4.** The resulting data were used to test the null hypothesis that microbenthos were randomly distributed throughout the sediment core. The implications of non-random distributions (e.g. clumped or evenly distributed) imply that interactions among microbenthos may be important. Associations among microbenthos may become more important throughout parts of the day. For example, benthic eukaryotes aggregate near sulfide-oxidizing bacteria, perhaps avoiding higher sulfide concentrations (Bernhard et al. 2003). These aggregations may be more important when oxygen is depleted throughout the sediment. This study was conducted in tandem with the diel sampling described in **Chapter 3** to provide information on the spatial relationships among microbenthos in addition to data on variation in food web structure and bacterivory over the course of a day.

## THE DOC-CILIATE LINK

The high input of primary production to the sediments results in a large DOC pool. Part of this DOC pool is resistant to bacterial hydrolytic enzymes, resulting in slow rates of decomposition (Arnosti 2004). Ciliates may be able to compete with bacteria for these compounds, as the ingestion of these compounds (if occurring as a result of feeding activities) would not require additional energy expenditures. The ingestion of DOC by benthic ciliates has been suggested as a supplemental energy source for benthic ciliates when the rate of particle ingestion appears lower than required for cell maintenance (Epstein 1997). Ciliates are very abundant in marine sediments (Fenchel 1967), thus their role in processing sediment DOC could be significant.

Ingestion and assimilation of DOC has been shown to occur in some free-living bacterivorous protists. For example, water column flagellates can directly ingest dissolved organic carbon at low ambient concentrations (Sherr 1988). Ciliates have been reported to directly ingest DOC and can survive in bacterial-free, carbon rich environments (Soldo & Van Wagtendonk 1969, Orias et al. 2000). This ability may not be universal, as Tranvik et al (1993) reported that a pelagic ciliate could not ingest high molecular weight (HWM) DOC. In **Chapter 5**, I tested the hypothesis that direct ingestion of DOC can occur in benthic ciliates, using the common benthic bacterivorous ciliate *Uronema marinum*, as a model. Fluorescein-labelled dextran (2,000 kDa) was used as an analogue for HWM-DOC in the sediments. The growth and production of *U. marinum* on other DOC compounds (soluble starch, glucose, and acetate) were measured to determine if *U. marinum* could benefit from DOC at concentrations typical for coastal sediments. The direct ingestion and utilization of DOC by ciliates can increase the efficiency of the benthic microbial loop.

## THE ROLE OF HETEROTROPHIC PROTISTS IN SALT MARSH SEDIMENTS

Heterotrophic protists play crucial roles in aquatic food webs. These roles include: regenerating nutrients (Sherr et al. 1982); selectively grazing bacterial populations (Lavrentyev et al. 1997); and releasing labile carbon compounds to stimulate microbial growth (Biagini et al. 1998). Also, heterotrophic protists are an important dietary component of large consumers, including microinvertebrates (Calbet & Saiz 2005) and filter-feeding bivalves (LeGall et al. 1997).

The overall goal of this project is to build upon previous investigations of the benthic microbial food web in salt marsh sediments. The focus on heterotrophic protists will provide insights into the other components of the sediment food web. For example, concentrations of bacteria (when scaled to sediment porosity) are relatively constant across a range of marine environments (Schmidt et al. 1998). How do concentrations of benthic heterotrophic protists vary between sediments and over time? What characteristics of marine sediments control the concentrations of heterotrophic protists in the sediments and how do these controls differ from pelagic environments? Separately, these four studies address different questions regarding the role of heterotrophic protists in the benthic microbial food webs. Together, this work attempts to converge on a greater understanding of the flow of salt marsh primary production through the sediment microbial food web and to elucidate the role of heterotrophic protists in regulating this flux.

## REFERENCES


Arnosti C (2004) Speed bumps and barricades in the carbon cycle: substrate structural effects on carbon cycling. Mar Chem 92:263-273

Azam F, Fenchel T, Field JG, Gray JS, Meyer-Reil LA, Thingstad F (1983) The ecological role of water-column microbes in the sea. Mar Ecol Prog Ser 10:257-263

Benner R, MacCubbin AE, Hodson RE (1984) Anaerobic biodegradation of the lignin and polysaccharide components of lignocellulose and synthetic lignin by sediment microflora. Appl Environ Microbiol 47:998-1004

Bernhard JM, Visscher PT, Bowser SS (2003) Submillimeter life positions of bacteria, protists, and metazoans in laminated sediments of the Santa Barbara Basin. Limnol Oceanogr 48:813-828

Berninger UG, Epstein SS (1995) Vertical distribution of benthic ciliates in response to the oxygen concentration in an intertidal North Sea sediment. Aquat Microb Ecol 9:229-236

Biagini GA, Finlay BJ, Lloyd D (1998) Protozoan stimulation of anaerobic microbial activity: enhancement of the rate of terminal decomposition of organic matter. FEMS Microbiol Ecol 27:1-8

Calbet A, Saiz E (2005) The ciliate-copepod link in marine ecosystems. Aquat Microb Ecol 38:157-167

Childers DL, Day Jr JW, McKellar Jr HN (2000) Twenty more years of marsh and estuarine flux studies: revisiting Nixon (1980). In: Concepts and controversies in tidal marsh ecology. Kluwer Academic Publishers, Dordrecht, p 391–424

Consalvey M, Paterson DM, Underwood GJC (2004) The ups and downs of life in a benthic biofilm: migration of benthic diatoms. Diatom Res 19:181-202

Dahl TE (2005) Status and trends of wetlands in the conterminous United States 1998 to 2004. US Dept. of the Interior, US Fish and Wildlife Service

Ducklow HW, Purdie DA, Williams PJL, Davies JM (1986) Bacterioplankton - a sink for carbon in a coastal marine plankton community. Science 232:865-867

Epstein SS (1997) Microbial food webs in marine sediments. 2. seasonal changes in trophic interactions in a sandy tidal flat community. Microb Ecol 34:199-209

Fenchel T (1967) The ecology of marine microbenthos I. the quantitative importance of ciliates as compared with metazoans in various types of sediments. Ophelia 4:121-137

Fenchel T, Bernard C (1996) Behavioural responses in oxygen gradients of ciliates from microbial mats. Eur J Protistol 32:55-63

Fenchel T, Finlay BJ (1995) Ecology and evolution in anoxic worlds. Oxford University Press, Oxford

Filippini M, Buesing N, Bettarel Y, Sime-Ngando T, Gessner MO (2006) Infection paradox: high abundance but low impact of freshwater benthic viruses. Appl Environ Microbiol 72:4893-4898

Gallagher JL, Daiber FC (1974) Primary production of edaphic algal communities in a Delaware salt marsh. Limnol Oceanogr 19:390-395

Glud RN, Middelboe M (2004) Virus and bacteria dynamics of a coastal sediment: implication for benthic carbon cycling. Limnol Oceanogr 49:2073-2081

Hayward BH, Droste R, Epstein SS (2003) Interstitial ciliates: benthic microaerophiles or planktonic anaerobes? J Eukaryot Microbiol 50:356-359

Higinbotham CB, Alber M, Chalmers AG (2004) Analysis of tidal marsh vegetation patterns in two Georgia estuaries using aerial photography and GIS. Estuaries 27:670-683

Howarth RW, Hobbie JE (1982) The regulation of decomposition and heterotrophic microbal activity in salt marsh soils: a review. In: Kennedy VS (ed) Estuarine comparisons. Academic Press, New York, p 183-207

Kemp PF (1988) Bacterivory by benthic ciliates - significance as a carbon source and impact on sediment bacteria. Mar Ecol Prog Ser 49:163-169

Kemp PF (1990) The fate of benthic bacterial production. Rev Aquat Sci 2:109-124

Kingston MB (2002) Effect of subsurface nutrient supplies on the vertical migration of *Euglena proxima* (Euglenophyta). J Phycol 38:872-880

Lavrentyev PJ, Gardner WS, Johnson JR (1997) Cascading trophic effects on aquatic nitrification: Experimental evidence and potential implications. Aquat Microb Ecol 13:161-175

Lawrence JR, Snyder RA (1998) Feeding behaviour and grazing impacts of a *Euplotes sp.* on attached bacteria. Can J Microbiol 44:623-629

LeGall S, Hassen MB, LeGall P (1997) Ingestion of a bacterivorous ciliate by the oyster *Crassostrea gigas*: protozoa as a trophic link between picoplankton and benthic suspension-feeders. Mar Ecol Prog Ser 152:301-306

MacIntyre HL, Cullen JJ (1995) Fine-scale vertical resolution of chlorophyll and photosynthetic parameters in shallow-water benthos. Mar Ecol Prog Ser 122:227-237

MacIntyre HL, Geider RJ, Miller DC (1996) Microphytobenthos: the ecological role of the "secret garden" of unvegetated, shallow-water marine habitats. I. distribution, abundance and primary production. Estuaries 19:186-201

Middelburg JJ, Barranguet C, Boschker HTS, Herman PMJ, Moens T, Heip CHR (2000) The fate of intertidal microphytobenthos carbon: An in situ $^{13}$C-labeling study. Limnol Oceanogr 45:1224-1234

Miller DC, Geider RJ, MacIntyre HL (1996) Microphytobenthos: The ecological role of the "secret garden" of unvegetated, shallow-water marine habitats. II. role in sediment stability and shallow-water food webs. Estuaries 19:202-212

Orias E, Hamilton EP, Orias JD (2000) *Tetrahymena* as a laboratory organism: useful strain, cell culture, and cell line maintenance. In: Asai DJ, Forney JD (eds) *Tetrahymena thermophila*, Vol 62. Academic Press, San Diego, p 189-211

Pinckney J, Zingmark RG (1993) Biomass and production of benthic microalgal communities in estuarine habitats. Estuaries 16:887-897

Rublee PA (1982) Bacteria and microbial distribution in estuarine sediments. In: Kennedy VS (ed) Estuarine comparisons. Academic Press, New York, p 159 - 182

Schmidt JL, Deming JW, Jumars PA, Keil RG (1998) Constancy of bacterial abundance in surficial marine sediments. Limnol Oceanogr 43:976-982

Schubauer JP, Hopkinson CS (1984) Above-ground and belowground emergent macrophyte production and turnover in a coastal marsh ecosystem, Georgia. Limnol Oceanogr 29:1052-1065

Sherr BF, Sherr EB, Berman T (1982) Decomposition of organic detritus - a selective role for microflagellate protozoa. Limnol Oceanogr 27:765-769

Sherr EB (1988) Direct use of high molecular-weight polysaccharide by heterotrophic flagellates. Nature 335:348-351

Sherr EB, Sherr BF, Albright LJ (1987) Bacteria - link or sink. Science 235:88-88

Shimeta J, Sisson JD (1999) Taxon-specific tidal resuspension of protists into the subtidal benthic boundary layer of a coastal embayment. Mar Ecol Prog Ser 177:51-62

Silliman BR, Newell SY (2003) Fungal farming in a snail. PNAS 100:15643-15648

Smith DJ, Underwood GJC (1998) Exopolymer production by intertidal epipelic diatoms. Limnol Oceanogr 43:1578-1591

Soldo AT, Van Wagtendonk J (1969) Nutrition of *Paramecium aurelia*, Stock 299. J Protozool 16:500-506

Starink M, BarGilissen MJ, Bak RPM, Cappenberg TE (1996) Bacterivory by heterotrophic nanoflagellates and bacterial production in sediments of a freshwater littoral system. Limnol Oceanogr 41:62-69

Starink M, Krylova IN, Bargilissen MJ, Bak RPM, Cappenberg TE (1994) Rates of benthic protozoan grazing on free and attached sediment bacteria measured with fluorescently stained sediment. Appl Environ Microbiol 60:2259-2264

Sullivan MJ, Currin CA (2000) Community structure and functional dynamics of benthic microalgae in salt marshes. Concepts and controversies in tidal marsh ecology. M. Weinstein and D. Kreeger (Eds.), Kluwer Academic Publishers, Dordrecht, 81–106

Teal JM (1962) Energy flow in salt marsh ecosystem of Georgia. Ecology 43:614-624

Tranvik LJ, Sherr EB, Sherr BF (1993) Uptake and utilization of colloidal DOM by heterotrophic flagellates in seawater. Mar Ecol Progr Ser 92:301-309

Vernberg FJ (1993) Salt-marsh processes: a review. Environ Toxicol Chem 12:2167-2195

Williams RB (1964) Division rates of salt-marsh diatoms in relation to salinity and cell size. Ecology 45:876-880

Zimmerman R, Minello T, Rozas L (2002) Salt marsh linkages to productivity of penaeid shrimps and blue crabs in the northern Gulf of Mexico. In: Concepts and Controversies in Tidal Marsh Ecology, Kluwer Academic Publishers, Dordrecht, p 293-314

**Figure 1.1.** Simplified conceptual model of the benthic microbial marine food web in shallow water marine sediments. Arrows indication carbon flow through ingestion of viral lysis. The shaded area represents the dissolved organic carbon (DOC) pool available to bacteria. White boxes indicate groups considered in this study.

**Figure 1.1**

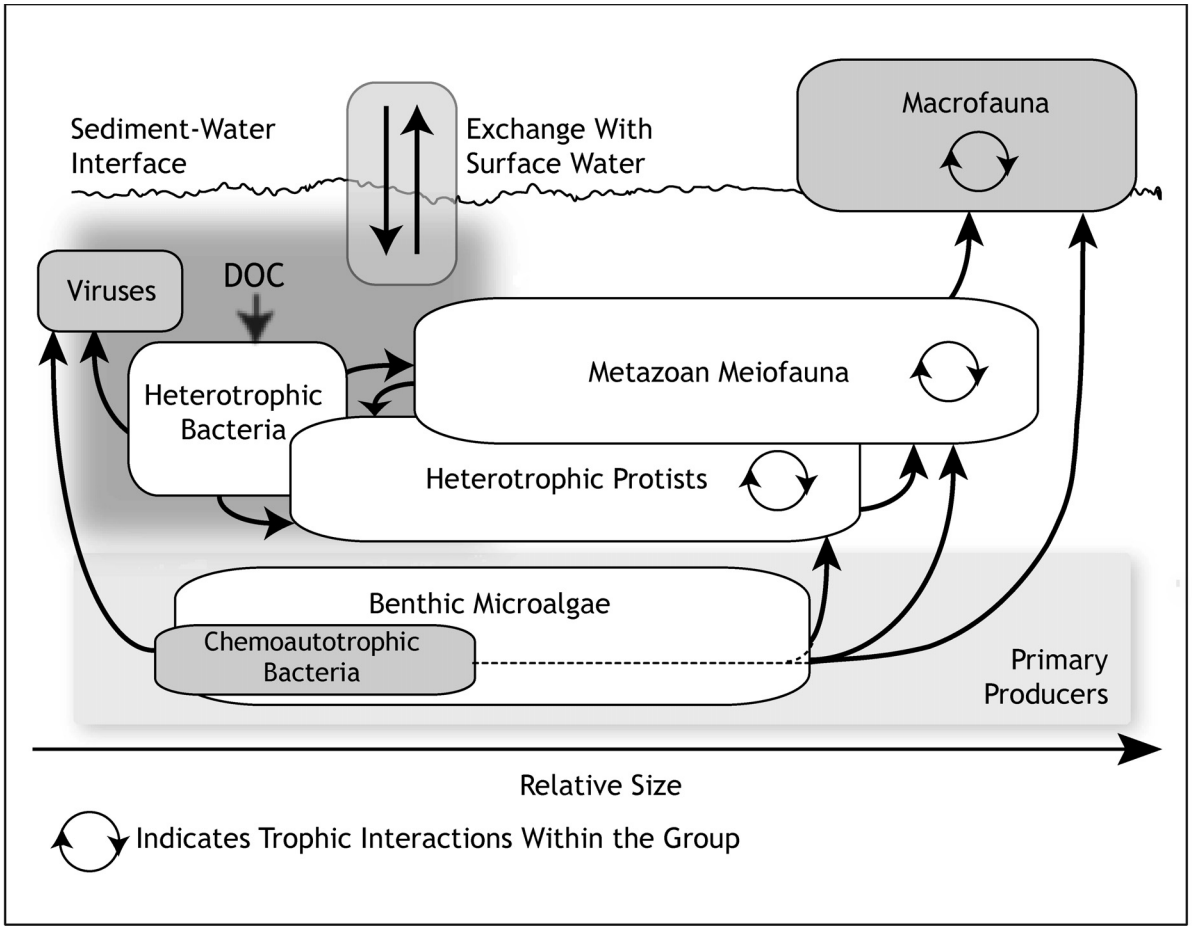
Sediment-Water
Interface
Exchange With
Surface Water
Macrofauna
Viruses
DOC
Heterotrophic
Bacteria
Metazoan Meiofauna
Heterotrophic Protists
Benthic Microalgae
Chemoautotrophic
Bacteria
Primary
Producers
Relative Size
Indicates Trophic Interactions Within the Group

**Figure 1.2** Map of Sapelo Island, GA indicating sampling locations: Marsh Landing (ML), Dean Creek (DC), and Nannygoat Beach (NGB). See Table 2.1 for sediment characteristics.

**Figure 1.2**

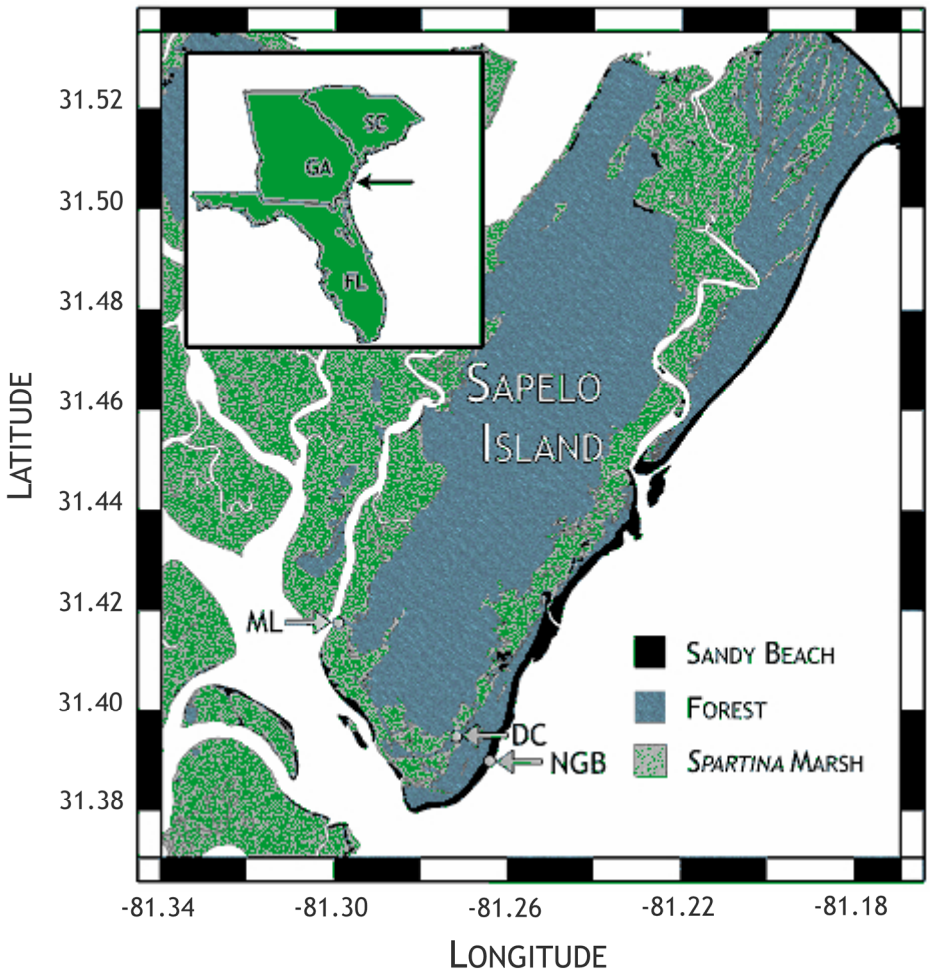
SC
GA
FL
SAPELO ISLAND
ML
DC
NGB
SANDY BEACH
FOREST
SPARTINA MARSH
31.52
31.50
31.48
31.46
31.44
31.42
31.40
31.38
LATITUDE
-81.34
-81.30
-81.26
-81.22
-81.18
LONGITUDE

# CHAPTER 2

## SPATIAL AND TEMPORAL VARIATIONS IN THE BENTHIC MICROBIAL FOOD WEB STRUCTURE IN SALT MARSH SEDIMENTS[1]

[1] M.R First and J.T. Hollibaugh
To be submitted to: *Microbial Ecology*

## ABSTRACT

We examined benthic microbial food web structure in three contrasting subtidal salt marsh sediments over the course of a year. Samples were collected monthly from a high energy, sandy beach (NB), a tidal creek bed (DC), and a *Spartina alternifora* marsh boarder (ML). The concentration and biomass of benthic microalgae (BMA), total and potentially active bacteria (measured by an enzyme-activated fluorogenic compound), heterotrophic protists and metazoan meiofauna were measured at each location. Sediment grain size and porewater pH explained most of the variability in biomass distributions; temperature did not correlate well with variations in benthic biomass. There was a general shift from BMA-dominated community in the spring/summer months to bacterial-dominated communities in the autumn at all locations. Bacteria and protist concentrations were significantly related to sediment porewater volume ($6.9\pm1.2 \times 10^9$ and $5.1\pm1.1 \times 10^3$ cells $ml^{-1}$, respectively). Relatively low numbers of bacterivorous protists and high bacterial biomass in the muddy sediments of ML and DC resulted in long bacterial turnover times. The stimulatory effects of protist grazing, such as nutrient regeneration, are therefore limited in muddy sediments. We hypothesize that both top-down pressure and low anaerobic growth efficiency led to relatively low biomass of bacterivorous protists (i.e. flagellates and small ciliates), which, in turn, led to high bacterial biomass and low cell-specific activity of sediment bacteria.

## INTRODUCTION

Salt marsh surficial sediments harbor high microbial biomass and are loci of substantial production by both benthic microalgae (BMA) and microheterotrophs. BMA production in sediments can account for over one-third of the annual primary production of salt marsh systems (Gallagher & Daiber 1974, Sullivan & Currin 2000). Sediments also receive carbon from burial of marsh grass and rhizomes and from particle settling from the water column. This carbon provides growth substrate for heterotrophic bacteria and fuels the microbial food web (e.g. Benner et al. 1984). The reservoir of organic carbon in salt marsh sediments supports an active benthic microbial food web. As a result, benthic microbes are major contributors to the overall flux of carbon through salt marshes and near-shore waters. For example, microbenthos (defined here to include bacteria and protists) and metazoan meiofauna are food sources for epibenthic invertebrates such as shrimp (Zimmerman et al. 2002) and fiddler crabs (Teal 1962). Resuspended BMA (De Jonge & Van Beusekom 1992, Thoresen 2004) and microheterotrophs (Kreeger & Newell 2002) are important components of the diet of filter-feeding bivalves.

The quantity of benthic production available to higher trophic levels depends on food web structure and trophic efficiency (i.e. the amount of fixed carbon respired relative to biomass production). Carbon fixed by BMA is rapidly transferred through the benthic food web. In isotope tracer studies, algal-derived carbon appeared in meiofauna within 1 h of addition of $^{13}C$ bicarbonate; bacteria incorporated the labeled carbon within several hours (Middelburg et al. 2000). These and other observations suggest that algal-derived carbon is channeled through two discrete pathways: 1) through herbivores to higher trophic levels, or 2) through bacteria to the microbial food web (van Oevelen et al. 2006). In some marine sediments, however, diatoms were ingested by flagellates and ciliates, as well as by meiofauna (Epstein 1997b). Likewise, ingestion

of bacteria by meiofauna and microinvertebrates has been observed (Kemp 1987). Additionally, the linkages between bacterivorous microbenthos and meiofauna (Epstein & Gallagher 1992, Hamels et al. 2001) indicate that the two major routes of carbon flow in the benthic environments, at least at times, intersect.

Bacteria in estuarine sediments are several orders of magnitude more concentrated than in the water column (reviewed by Rublee 1982). The relative constancy of total bacteria concentrations (when scaled to porewater volume) suggests that either bottom-up (resource supply) and/or top-down (predation) forces rigidly constrain the standing stock of benthic bacteria (Schmidt et al. 1998). Sediment bacteria play a major role in total benthic metabolism by transforming carbon, nitrogen, and sulfur compounds (reviewed by Nealson 1997). Bacterial production in sediments is linked to the supply of carbon and nutrients. The supply of growth substrate (e.g. dissolved organic carbon exuded from BMA) varies with solar irradiance (Smith & Underwood 1998), and therefore will vary over daily and seasonal cycles. Bacterial production resulting from these varying inputs must be tempered by loss processes, such as: bacterivory, advection out of the sediments, or viral lysis. Viral lysis rates in sediments are low (Glud & Middelboe 2004), therefore, the most likely internal loss factor is bacterial grazing by protists.

Bacterivorous protists are capable of high cell-specific ingestion rates, however, low abundance of these protists (relative to bacteria) prevents further utilization of benthic bacterial biomass (First and Hollibaugh, in press). The controls on the bacterivore biomass (and the subsequent higher grazing impact) are unclear. Physical and chemical characteristics of the sediments, such as oxygen penetration, constrain the abundance of some protists (Fenchel 1968, Fenchel & Bernard 1996, Böttcher et al. 2000). Top-down predation (e.g. Hamels et al. 2001)

and advection out of the system (e.g. Shimeta & Sisson 1999) also limit the abundance of heterotrophic protists in sediments.

Bacterivorous protists play a key role in overall benthic metabolism through regenerating nutrients (Sherr et al. 1982) and releasing labile organic carbon compounds (Biagini et al. 1998). Selective grazing by protists can impact the degradation of specific compounds. For instance, the degradation of naphthalene in sediments was accelerated by bacterivorous protists. Protists were able to control populations of bacteria that outcompeted naphthalene-degrading bacteria in the absence of high predation pressure (Tso & Taghon 2006). Bacterivorous protists are a food source for higher trophic levels (e.g. Hamels et al. 2001). Thus, the physical/chemical and biological controls on the abundances of heterotrophic protists have implications for overall benthic metabolism.

To understand the factors controlling the abundance of benthic heterotrophic protists, we measured the benthic microbial community structure (BMA, bacteria, metazoan meiofauna, and heterotrophic protists) at contrasting locations. Samples were collected monthly at each location throughout 2005 and the physical and chemical characteristics were measured at each site. Our goals were to test the hypotheses, that: 1) the food web structure (defined here as the relative biomass partitioning among microbenthos and meiofauna) will respond differently to seasonal patterns at contrasting locations, and 2) the concentration of benthic protists relates to the sediment porosity, as has been noted for bacteria (Schmidt et al. 1998). We found that concentrations of heterotrophic protists were significantly correlated with sediment porosity. However, heterotrophic protists were not more concentrated than in the water column and thus are rare relative to bacteria. In general, all locations showed a general trend of BMA dominance in the spring and early summer with bacteria becoming proportionately more abundant in the late

summer and fall. The shift from an algal to bacterial dominated community has implications for the efficiency in which benthic production is transferred to higher trophic levels.

## METHODS

**Sampling.** Samples were collected from three subtidal locations on Sapelo Island, Georgia, USA (Table 2.1). Nannygoat Beach (NB) is a high energy, sandy beach on the southeastern side of this barrier island. Dean Creek (DC) is a tidal creek on the southern end of the island. Samples were collected at a locations roughly 2 km from the mouth. Marsh Landing (ML) is a *Spartina alterniflora* marsh on the landward side of the island adjacent to a major tidal river. Sapelo Island has a mean daily tidal range of 2.3 m (NOAA). Air temperature and precipitation were recorded at a weather station at the University of Georgia Marine Institute, located within 3 km of the sample locations. Mean daily air temperature ranged from 2.2 to 31°C over the year and 160 cm of precipitation were recorded (Fig 2.1). Samples were collected monthly at low tide from the same locations throughout 2005 (sample dates denoted on Fig. 2.1). Sediments were collected during daylight at low tide and less than 0.5 m of water covered the sediment at the time of sampling. Although sampling occurred during both spring and neap tides, the sites were always covered with water at the time of sampling.

At each location, three samples (~ 200 g each) of the top 1 cm of sediment were collected with a plastic trowel. Sediments were kept at ambient water temperature in a water bath incubator until they were either chemically preserved or frozen (within 3 h of sampling). The sediment sample was mixed with a plastic spatula prior to subdividing and preserving samples. All samples were stored in the dark and frozen (chlorophyll *a* samples) or refrigerated (4 ± 2°C, all other samples) until analysis. Seawater was collected at each station and filtered through a

0.22 μm membrane (Poretics). This filtered seawater (FSW) was used to disperse bacteria in water that was isotonic to the sediment porewater (described below).

Sediment temperature was recorded immediately after sample collection. Approximately 2 g of wet sediment was centrifuged (10,000 x g for 10 min), and the salinity and pH determined of the supernatant were determined. Sediment density was determined by dispersing ~5 g of sediment in a graduated cylinder and measuring the weight and water displacement. Sediment porosity was determined by the weight lost after drying for 8 h at 60°C (when sediment weight stabilized). The sediment porosity (i.e. the volume of water per total sediment volume) in submerged sediments is equivalent to "fluid volume", a term used in other analyses (Schmidt et al. 1998). For comparisons with the water column, sediment water content is expressed as porewater volume (ml). Percent organic carbon was estimated as weight lost after combusting dried sediments at 550°C for 8 h. Grain size analysis was completed by sieving dried sediments through a series of standard mesh sizes. The mean grain size was determined from the sediment weight collected at each sieve size.

**Benthic Microalgae.** Three analytical replicate samples (approximately 5 g wet sediment) were placed in 15 ml centrifuge tubes with 0.5 ml of FSW saturated with $MgCO_3$. The samples were frozen (-20 ± 2 °C), and kept in the dark prior to and during extraction and analysis. Pigments were extracted from sediment samples for 24 h with a solution consisting of 45% acetone, 45% methanol and 10% water. Sample tubes were vortexed at high speed for 1 min every 8 - 10 h throughout the extraction period. Samples were then centrifuged (20 min at 5000 x *g*), absorbance spectra (485 – 750 nm) of the supernatants were recorded with a Shimadzu UV:Visible Spectrophotometer, then recorded again following acidification with HCl (final pH

2-3). Chlorophyll *a* (Chl *a*) and phaeopigment concentrations were calculated per g of wet sediment with standard spectrophotometric equations for microalgae (Lorenzen 1967). The efficiency of the first extraction was determined from the total pigment accumulated after three separate, serial extractions of the same sample. Concentration estimates for the remaining samples were adjusted based on one extraction using the average extraction efficiency for these sediments (40%, $n = 18$). Carbon biomass of BMA was estimated using a ratio of 40 μg C: μg Chl *a*, which is at the low end of the range of previous estimates for estuarine BMA (De Jonge & Colijn 1994).

**Bacteria.** Bacteria with intact cytosolic esterases were enumerated in replicate sediment samples (1 g) dispersed in 2 ml of FSW then stained with 50 μl of 0.5 mM of CellTracker Green Chloromethylfluorescein diacetate (CTG, Invitrogen). CTG is a non-fluorescent substance that freely diffuses into cells and becomes fluorescent and impermeant upon hydrolysis by cytosolic enzymes. Metabolically activated dyes have the advantages of high specificity for living cells and reduced non-specific labeling (Epstein & Rossel 1995). Dispersing the bacteria into a slurry oxygenates sediments and may stimulate bacterial activity. Therefore, the portion of bacteria that are CTG-positive are defined here as "potentially active bacteria". Cells were fixed after a 2 h incubation by adding 1 ml of 16% glutaraldehyde, then refrigerated (4 ± 2 °C) in the dark until analysis.

A subsample of this slurry (1 g) was dispersed in 1 ml of 0.04 M tetrasodium pyrophosphate and placed in a low energy sonic bath for 20 min. This suspension was vortexed, then serially diluted 1:10 in the tetrasodium pyrophosphate solution three times with sonication at each dilution (1:1000 final dilution) to separate bacteria from particles and to disperse colonies

(Weinbauer et al. 1998). One ml of the dilution was then filtered onto 0.2 μm Anodisc filters (Whatman). For these and all other slide preparations, 40 μl of 5:1 Citifluor:Vectashield was used as a mounting medium to reduce fluorochrome photobleaching. Potentially active bacteria were counted on a Leica DMX RA epifluorescence microscope using blue excitation (450 – 490 nm, dichromatic mirror 510 nm, longpass filter 515 nm) at 400-fold and 1000-fold magnification. All bacteria in the sample ("total bacteria") were enumerated as described above after staining the bacterial suspension with SYBR Green II (SYBR). At least 10 fields were counted per filter, usually resulting with >>300 cells per sample. Raw data were adjusted for dilutions, FSW and fixative additions and concentrations are reported as cells per g of wet sediment.

The size distribution of bacterial cells was determined by analyzing images of 12 – 15 fields for each replicate subsample, captured at 1000-fold magnification with a Hamamatsu CCD digital camera. Cells were automatically sized with image analysis software (Image-Pro Plus Version 4.1). A stage micrometer was used to calibrate the image analysis program and calibration was verified with 0.66 and 1.0 μm diameter fluorescent spheres. After manually excluding dividing cells, colonies and non-bacterial objects from the images, the average length and width of all remaining cells in images from each time point and replicate was determined. Bacterial biovolume ($V$, $\mu m^3$) was calculated as:

$$V = \frac{\pi}{4} W^2 \left( L - \frac{W}{3} \right) \quad (1)$$

where L and W are the average cell length and width in μm, respectively (Bratbak 1985). Cell volumes were converted into biomass ($M$, pg C) by the following allometric relationship (Norland 1993):

$$M = 0.09 V^{0.9} \quad (2)$$

Total and potentially active bacterial community biomass was the product of cell concentration and mean biomass of the bacterial cells at each time point.

**Protists and Meiofauna.** Benthic protists and meiofauna were extracted from preserved sediments using a density gradient created with a colloidal silica solution following published methods (Epstein 1995). Briefly, 6 ml of Percoll (density 1.13 g $ml^{-1}$; Amersham Biosciences) was placed in 10 ml tubes and centrifuged in a fixed angle rotor (30 min at 30,000 x *g*) to create a density gradient. Wet sediment slurry (~2 g) was added to the top of the gradient, then the tubes were centrifuged in a swinging bucket rotor (60 min at 2000 x *g*). The supernatant was removed and placed in a clean 15 ml centrifuge tube. The remaining sediment was resuspended in 1 ml of Percoll, centrifuged in the swinging bucket rotor again and the supernatant combined with the initial supernatant. A dual stain of 4',6-diamidino-2-phenylindole (DAPI) and fluorescein isothiocyanate (FITC) was added to the combined supernatant and the sample was incubated at 4 ± 2 °C for a minimum of 60 min. The dual stain was useful in identifying cells, as FITC labels cell proteins and DAPI labels nuclei (Sherr & Sherr 1993). The supernatant was centrifuged again to settle any sand grains remaining in suspension. The extraction efficiency of this method was determined by counting the total number of organisms extracted from a sample by three additional serial extractions ($n = 6$). On average >90% of the total biomass was obtained in the first extraction, so counts from the first extraction were used without correction.

The extract was filtered through a 5 μm pore size, black polycarbonate filter (Osmonics) and the organisms retained were counted using standard blue excitation for FITC and UV excitation filter sets (UV: 340-380 nm, dichromatic mirror 400 nm, longpass filter 425 nm) for DAPI. Because the biomass of autotrophic protists is included in the Chl *a* based estimates of

BMA biomass, only heterotrophic protists (cells lacking chloroplasts visible under green excitation; 515 – 560 nm, dichromatic mirror 580 nm, longpass filter 590) were enumerated. Large protists and meiofauna (mostly nematodes) were counted at 100-fold magnification by scanning the entire filter. Flagellates lacking chloroplasts were counted at 400-fold magnification along transects through the filter. Large (>20 μm in Equivalent Spherical Diameter, ESD) heterotrophic protists (mainly ciliates and testate amoebae) were grouped into 15 common morphotypes and the average size of each morphytope was determined from the length and width of >30 individuals using image analysis software (ImagePro Plus 4.1). Common ciliates were identified when possible using taxonomic guides (Carey 1992). Flagellates were grouped into two size ranges and the average dimensions for each size range were based measurements of >30 individuals. Nematodes were grouped into three size categories with the average dimensions based on measurements of 5 – 20 individuals at each location. Individual dimensions were used to calculate biovolume and, in turn, the biomass of protists (Putt & Stoecker 1989, Wetzel & Likens 1991) and nematodes (Baguley et al. 2004).

**Analysis.** The concentrations and total biomass of microbenthos and meiofauna are reported per grams of wet sediment examined (gws). These quantities can be converted to dry sediment weight (g DSW) or per unit area (of the top 1 cm of sediment) using the mean porosity and sediment density, respectively (Table 2.1). Correlations between the biomass of benthic organisms (BMA, bacteria, heterotrophic protists, and meiofauna) and environmental variables (grain size, water temperature, organic matter content, porewater pH, salinity and volume) were calculated using the BIO-ENV routine of Primer V5 (Plymouth Marine Laboratory). BIO-ENV determines a single abiotic variable (or combination of variables) that best explains the biomass

distribution patterns of the benthic organisms (Clarke & Warwick 2001). Data sets were normalized as described elsewhere (Clarke & Gorley 2001). Briefly, a similarity matrix of environmental conditions was normalized by Euclidean distance and the biomass matrix was normalized by Bray-Curtis similarity. An ordination of the matrices (multidimensional scaling) is performed and the Spearman rank correlation ($\rho$) was used to determine the environmental variable (or combination of up to three variables) best describing the biomass distributions at all locations.

## RESULTS

The BIO-ENV analysis relating environmental variables and microbenthos biomass revealed that sediment grain size and porewater pH explained the most of the variability in biomass ($\rho$ = 0.628). Water temperature (both surface and sediment) explained little of the variability in the benthic biomass ($\rho < -0.09$). Surface water or sediment salinity were not strongly correlated to biomass of microbenthos and meiofauna ($\rho$ = 0.186 and 0.293, respectively). The combination of multiple factors (including porosity and organic carbon content) did not improve the correlation between microbenthos biomass and environmental variables. These variables were also highly correlated to sediment grain size (data not shown). The top five variable combinations are shown in Table 2.2.

The concentration of BMA at DC increased throughout the year to a maximal value of 412 (±12 SE) μg C $gws^{-1}$ in June (Fig. 2.2A). Throughout the summer and fall, the BMA biomass was reduced to low concentrations (120 – 170 μg C $gws^{-1}$). During this period, bacterial biomass increased to a maximum of 253 (±16 SE) μg C $gws^{-1}$ in September, where the fraction of potentially active bacteria reached a minimum. Conversely, BMA biomass at NB was greatest

during winter and spring (Fig. 2B). The contribution of potentially active bacteria to total biomass was greatest in NB sediments, where greater than 70% of bacteria were CTG-positive in ten of 12 months. ML did not show a clear seasonal trend in BMA biomass (Fig. 2.2C). The highest BMA biomass concentrations at ML were observed in June and November, while in April and May the concentrations were one order of magnitude lower. Like DC and NB, bacterial concentrations were greatest in summer and fall at ML with the lowest contribution of potentially active bacteria occurring in September.

Heterotrophic protists were separated into two size classes. Small protists ranging from 5 to 20 μm in size included mostly heterotrophic flagellates and small Scuticociliates. Large heterotrophic protists (>20 μm) were dominated by ciliates, including representatives of the Classes Spirotrichea (e.g. *Aspidisca* sp.) and Karyorelictea (e.g *Tracheloraphis* sp.). Testate amoeba ranging in sizes from 50 to 300 μm were also common at the tidal creek site. At all locations, nematodes were the dominant group of meiofauna. Harpacticoid copepods and other unidentified microinvertebrates were included in the total meiofauna biomass. Protist biomass at DC followed the BMA trend, where total biomass generally increased from winter to summer (Fig. 2.3A). The highest biomass at DC was observed in May and July, when large protists were abundant. The ciliate, *Tracheloraphis* sp. (mean length, 230 μm), reached a concentration of 50 $gws^{-1}$ in May. Small protists dominated the biomass at both NB and ML during most of the year (Fig. 2.3).

The total benthic community biomass ranged over nearly two orders of magnitude at the locations sampled (Fig. 2.4). The general trend observed at all locations was a shift from BMA dominance in the early months of the year, to a bacteria-dominated community in the summer and fall months. The contribution of heterotrophic protists to total biomass was greatest at NB

(range, 1 to 6% of total) and lowest at ML (<2%). The greatest meiofaunal biomass was observed in DC in May (12% of total biomass). Meiofauna were less than 8% and 2% of total biomass at NB and ML, respectively.

The best fit relationship between bacterial biomass and porewater volume yielded a slope of 155 ± 40 μg C $ml^{-1}$ porewater (linear regression, mean ± SE, $r^2 = 0.30$, $p<0.05$, df = 35, in all cases) (Fig. 2.5). Bacteria concentrations (cells $gws^{-1}$) were also significantly related to porewater volume (slope = 6.9 ± 1.2 x $10^9$ cells $ml^{-1}$, df = 35, $p<0.05$, $r^2 = 0.49$). Protist biomass was not significantly related to porewater volume ($r^2 = 0.08$, $p>0.05$), however, there was a significant linear relationship between the protist abundance and porosity (slope = 5.1 ± 1.1 x $10^3$ cells $ml^{-1}$, $r^2 = 0.36$, $p<0.05$) (Fig. 2.6).

## DISCUSSION

**Seasonal Trends.** The total biomass range, organic-matter content, and grain-size distributions were highly different at all three locations. Nevertheless, we observed a similar trend at all locations where algal biomass dominated the total microbenthic in the spring and early summer followed by a bacterial dominated community in the late summer and fall. The difference between two stages was most pronounced at NB, where algal biomass was low throughout most of the year. The surface water at this location is highly turbid due to wave action, and reduced illumination is likely responsible for the relatively low algal biomass.

The progression from an algal to a bacterial dominated community was also apparent at ML, although the total community biomass varied widely throughout the year. The variable biomass in ML sediments is likely a result of variations in solar illumination at this location. Solar input was not recorded in this study, although the range of solar input varies widely in

these mesotidal sediments. For example, solar illumination in an intertidal mudflat at DC ranged from approximately 10 to 900 μE $m^{-2}$ $s^{-1}$ during daylight hours (First and Hollibaugh, in prep). Solar input to these shallow subtidal sediments will also vary over lunar and seasonal cycles. The low number of potential herbivores indicates predatory control of BMA unlikely. The combined biomass of potential herbivores (i.e. large protists and nematodes) were <3% of the total biomass throughout the year. Thus, BMA in ML sediments are likely controlled by resource supply (i.e. solar radiation) or metazoan herbivores (e.g Teal 1962).

The shift in dominance between benthic bacteria and algae has consequences for the magnitude of energy transferred through trophic pathways in coastal sediments. The relative importance of herbivory and bacterivory alternated throughout the year as result of the changes in production of bacteria and algae, and the predation by protists and meiofauna (Epstein 1997a). The herbivorous and bacterivorous food webs are predicted to have different trophic efficiencies. Herbivorous food webs are estimated to be more efficient and, thus, support more trophic levels (van Oevelen et al. 2006). Therefore, the shifting importance between these two pathways throughout the year suggests that the availability of benthic production to higher trophic levels will vary seasonally.

**Controls on Bacterivore Abundance.** Concentrations of heterotrophic protists are strongly related to porosity in these shallow-water sediments. Porewater protist concentrations were not several orders of magnitude greater than in the water column, as is the case with bacteria (Rublee 1982, Schmidt et al. 1998). Heterotrophic flagellates are the most abundant bacterivore in pelagic environments (Sherr & Sherr 2002, and references therein). Flagellates were also the most common of the heterotrophic protists found in these and other marine sediments (Lee &

Patterson 2002). In the water column, bacterial and heterotrophic flagellate concentrations are approximately $10^5 – 10^6$ $ml^{-1}$ and $10^2 – 10^4$ $ml^{-1}$, respectively (Calbet et al. 2001, Iriarte et al. 2003). Bacteria are proportionally more abundant than small heterotrophic protists in the salt marsh sediments observed in this study. The regulatory forces driving the high and constant biomass of benthic bacteria have been considered and discussed elsewhere (Schmidt et al. 1998). Here, we discuss the potential mechanisms that regulate the concentration of bacterivorous protists, and how these factors may control bacterial concentrations and overall sediment metabolism.

As in the water column, phagotrophic protists in sediment are grazed by both large carnivorous protists and microinvertebrates. For example, omnivorous ciliates depend on the ingestion of flagellates because bacterial ingestion alone cannot support high growth rates for these ciliates (Ohman & Snyder 1991). Also, copepods appear to prey selectively upon phagotrophic protists, even through protists are rare relative to phytoplankton (Calbet & Saiz 2005). Similar top-down controls operate in sediment microbial communities (Epstein & Gallagher 1992, Hamels et al. 2001). Large Karyorelictid ciliates were abundant throughout the spring and summer months at DC, reaching highest densities in May and June. Many of these ciliates are omnivorous and prey upon flagellates and small ciliates (Carey 1992). Grazing by these and other protists can limit the population of flagellates and small ciliates that are the major bacterivores.

Similarly, the abundance of nematodes impacts the population size of primary bacterivores (i.e. flagellates and small ciliates). Nematodes are typically considered deposit feeders. They ingest particulate organic matter and the resident microbial populations associated with these particles (Sikora & Sikora 1982). The abundance of nematodes (especially in DC

sediments) suggests that the portion of living and detrital biomass processed by nematodes is significant. It is unclear how important nematodes are to the diet of macrofauna. Methodological problems associated with measuring rates of nematode ingestion may have led to an underestimation of the importance of nematodes to macrofauna (Sikora & Sikora 1982). In this case, the flow of energy from bacterivorous protists through nematodes to higher trophic levels can be substantial.

The convergence of lower production rates (due to anaerobic metabolism) and high predation pressure on bacterivores (by large protists and meiofauna) result in situations where bacterial concentrations approach theoretical upper limits. In these situations, top-down controls on sediment bacteria are effectively non-existent. Schmidt et al (1998) suggested that the extraordinarily high abundance of bacteria in mangrove sediment as reported by Alongi (1988), may be due to the effective absence of loss processes. In other mangrove sediments, bacterivorous ciliates were too rare to obtain valid estimates of rates of bacteria ingestion (Kemp 1988). The low growth yield of anaerobic protists (e.g. Fenchel and Findlay 1990) may prevent higher protist growth rates and more complete use of the bacterial standing stock. Conversely, in sandy sediments the advection of oxygenated water stimulates high rates of respiration rates, which can limit the buildup of organic matter transported from the water column (de Beer et al. 2005).

**Implications of High Bacteria, Low Bacterivore Concentrations.** In general, bacterial concentrations were higher than those observed across a variety of marine sediments (Schmidt et al. 1998). This is mostly due to the higher bacterial standing stock in DC and ML. We applied a previously determined grazing rate to demonstrate how the food web structure impacts bacterial

turnover time. Bacterial ingestion rates were determined for intertidal sediment samples collected at a location near the DC sample site (roughly 1 km upstream) in July, 2005 (First and Hollibaugh, in press). The mean ingestion rate (bacterial cells ingested per protist biovolume) was calculated from eight samples collected over a diel period. This rate (0.5 bacteria $\mu m^{-3}$ $h^{-1}$) was multiplied by the total protist biovolume in each sample to yield an estimate of the potential bacterial grazing rate. The turnover time of bacteria was the bacterial standing stock divided by the grazing rate. The turnover time ranged between the sample dates and locations (Fig. 2.7). With the exception of DC in May, NB had the shortest turnover time for bacteria (6 – 21 d). Turnover times were as long as 600 days (DC, Feb). Estimated bacterial turnover times at ML were shortest in summer (<40 d) and in the winter months (<30 d).

Bacterivores play a major role in stimulating bacterial growth and the breakdown of organic matter via nutrient regenerations and selective grazing (Sherr et al. 1982). Protists also reshape the pool of dissolved organic carbon (Kujawinski et al. 2002). In coastal sediments, the low portion of active bacteria may be due in part to nutrient limitation (Luna et al. 2002). The suppression of primary predators by large omnivorous protists and meiofauna may set the relatively constant concentration of porewater bacteria and shift the bacterial community to a high biomass, low activity equilibrium. Highly active populations of bacterivorous protists drive short bacterial turnover times and higher rates of organic matter degradation (e.g. Curds 1982). Thus, the controls of protist bacterivores (i.e. low anaerobic growth efficiency, predation) lead to a high standing stock of relatively inactive bacteria.

## ACKNOWLEDGEMENTS

This work was supported by NSF Georgia Coastal Ecosystems LTER grant (OCE-9982133). We are grateful for the hospitality and logistical support of J. Garbish and M. Price at the University of Georgia Marine Institute (UGAMI). J. Bernhard, M. Farmer, S. Joye and C. Meile provided guidance on the design of this project and reviewed the manuscript. M. Moran and W. Ye generously allowed access to the Primer V5 software. M.R.F. was supported by a UGA Graduate School Assistantship. This is contribution no. 967 from UGAMI.

## REFERENCES


Alongi DM (1988) Bacterial productivity and microbial biomass in tropical mangrove sediments. Microb Ecol 15:59-79

Baguley JG, Hyde LJ, Montagna PA (2004) A semi-automated digital microphotographic approach to measure meiofaunal biomass. Limnol Oceanogr Methods 2:181-190

Benner R, Maccubbin AE, Hodson RE (1984) Anaerobic biodegradation of the lignin and polysaccharide components of lignocellulose and synthetic lignin by sediment microflora. Appl Environ Microbiol 47:998-1004

Biagini GA, Finlay BJ, Lloyd D (1998) Protozoan stimulation of anaerobic microbial activity: enhancement of the rate of terminal decomposition of organic matter. FEMS Microbiol Ecol 27:1-8

Böttcher ME, Hespenheide B, Llobet-Brossa E, Beardsley C, Larsen O, Schramm A, Wieland A, Böttcher G, Berninger UG, Amann R (2000) The biogeochemistry, stable isotope geochemistry, and microbial community structure of a temperate intertidal mudflat: an integrated study. Cont Shelf Res 20:1749-1769

Bratbak G (1985) Bacterial biovolume and biomass estimations. Appl Environ Microbiol 49:1488-1493

Calbet A, Landry MR, Nunnery S (2001) Bacteria-flagellate interactions in the microbial food web of the oligotrophic subtropical North Pacific. Aquat Microb Ecol 23:283-292

Calbet A, Saiz E (2005) The ciliate-copepod link in marine ecosystems. Aquat Microb Ecol 38:157-167

Carey PG (1992) Marine interstitial ciliates: an illustrated key, 2nd ed., Chapman and Hall, Norwell, MA

Clarke KR, Gorley RN (2001) Primer v5: User Manual/Tutorial, Primer-E, Ltd., Plymouth

Clarke KR, Warwick RM (2001) Change in Marine Communities: An Approach to Statistical Analysis and Interpretation, 2nd ed., Primer-E, Ltd., Plymouth

Curds CR (1982) The ecology and role of protozoa in aerobic sewage-treatment processes. Annu Rev Microbiol 36:27-46

de Beer D, Wenzhofer F, Ferdelman TG, Boehme SE, Huettel M, van Beusekom JEE, Böttcher ME, Musat N, Dubilier N (2005) Transport and mineralization rates in North Sea sandy intertidal sediments, Sylt-Romo Basin, Wadden Sea. Limnol Oceanogr 50:113-127

De Jonge VN, Colijn F (1994) Dynamics of microphytobenthos biomass in the Ems estuary. Mar Ecol Prog Ser 104:185-196

De Jonge VN, Van Beusekom JEE (1992) Contribution of resuspended microphytobenthos to total phytoplankton in the Ems estuary and its possible role for grazers. Netherlands J Sea Res 30:91-105

Epstein SS (1995) Simultaneous enumeration of protozoa and micrometazoa from marine sandy sediments. Aquat Microb Ecol 9:219-227

Epstein SS (1997a) Microbial food webs in marine sediments. 1.trophic interactions and grazing rates in two tidal flat communities. Microb Ecol 34:188-198

Epstein SS (1997b) Microbial food webs in marine sediments .2. Seasonal changes in trophic interactions in a sandy tidal flat community. Microb Ecol 34:199-209

Epstein SS, Gallagher ED (1992) Evidence for facilitation and inhibition of ciliate population-growth by meiofauna and macrofauna on a temperate zone sandflat. J Exp Mar Biol Ecol 155:27-39

Epstein SS, Rossel J (1995) Methodology of in situ grazing experiments: Evaluation of a new vital dye for preparation of fluorescently labeled bacteria. Mar Ecol Prog Ser 128:143-150

Fenchel T (1968) The ecology of marine microbenthos IV. Structure and function of the benthic ecosystem, its chemical and physical factors and the microfauna communities with special reference to ciliated protozoa. Ophelia 6:1-182

Fenchel T, Finlay B (1990) Anaerobic free-living protozoa: growth efficiencies and the structure of anaerobic communities. FEMS Microbiol Ecol 74:269-275

Fenchel T, Bernard C (1996) Behavioural responses in oxygen gradients of ciliates from microbial mats. Eur J Protistol 32:55-63

Gallagher JL, Daiber FC (1974) Primary pProduction of edaphic algalcommunities in a Delaware salt marsh. Limnol Oceanogr 19:390-395

Glud RN, Middelboe M (2004) Virus and bacteria dynamics of a coastal sediment: implication for benthic carbon cycling. Limnol Oceanogr 49:2073-2081

Hamels I, Moens T, Mutylaert K, Vyverman W (2001) Trophic interactions between ciliates and nematodes from an intertidal flat. Aquat Microb Ecol 26:61-72

Iriarte A, Madariaga I, Revilla M, Sarobe A (2003) Short-term variability in microbial food web dynamics in a shallow tidal estuary. Aquat Microb Ecol 31:145-161

Kemp PF (1987) Potential impact on bacteria of grazing by a macrofaunal deposit-feeder, and the fate of bacterial production. Mar Ecol Progr Ser 36:151-161

Kemp PF (1988) Bacterivory by benthic ciliates: significance as a carbon source and impact on sediment bacteria. Mar Ecol Progr Ser 49:163-169

Kreeger D, Newell R (2002) Trophic complexity between producers and invertebrate consumers in salt marshes. In: Concepts and controversies in tidal marsh ecology, p 187-220

Kujawinski EB, Farrington JW, Moffett JW (2002) Evidence for grazing-mediated production of dissolved surface-active material by marine protists. Mar Chem 77:133-142

Lee WJ, Patterson DJ (2002) Abundance and biomass of heterotrophic flagellates, and factors controlling their abundance and distribution in sediments of Botany Bay. Microb Ecol 43:467-481

Lorenzen CJ (1967) Determination of chlorophyll and pheo-pigments: spectrophotometric equations. Limnol Oceanogr 12:343-346

Luna GM, Manini E, Danovaro R (2002) Large fraction of dead and inactive bacteria in coastal marine sediments: comparison of protocols for determination and ecological significance. Appl Environ Microbiol 68:3509-3513

Middelburg JJ, Barranguet C, Boschker HTS, Herman PMJ, Moens T, Heip CHR (2000) The fate of intertidal microphytobenthos carbon: an in situ $^{13}$C-labeling study. Limnol Oceanogr 45:1224-1234

Nealson KH (1997) Sediment bacteria: Who's there, what are they doing, and what's new? Ann Rev Earth Planet Sci 25:403-434

Norland S (1993) The relationship between biomass and volume of bacteria. In: Kemp PF (ed) Handbook of methods in aquatic microbial ecology. Lewis Publishers, Boca Raton, p 303 - 307

Ohman MD, Snyder RA (1991) Growth-kinetics of the omnivorous oligotrich ciliate *Strombidium Sp*. Limnol Oceanogr 36:922-935

Putt M, Stoecker DK (1989) An experimentally determined carbon-volume ratio for marine oligotrichous ciliates from estuarine and coastal waters. Limnol Oceanogr 34:1097-1103

Rublee PA (1982) Bacteria and microbial distribution in estuarine sediments. In: Kennedy VS (ed) Estuarine comparisons. Academic Press, New York, p 159 - 182

Schmidt JL, Deming JW, Jumars PA, Keil RG (1998) Constancy of bacterial abundance in surficial marine sediments. Limnol Oceanogr 43:976-982

Sherr BF, Sherr EB, Berman T (1982) Decomposition of organic detritus - a selective role for microflagellate protozoa. Limnol Oceanogr 27:765-769

Sherr EB, Sherr BF (1993) Staining of heterotrophic protists for visualization by epifluorescence microscopy, In: Kemp PF (ed) Handbook of methods in aquatic microbial ecology. Lewis Publishers, Boca Raton

Sherr EB, Sherr BF (2002) Significance of predation by protists in aquatic microbial food webs. Antonie Van Leeuwenhoek Int J Gen Mol Microbiol 81:293-308

Shimeta J, Sisson JD (1999) Taxon-specific tidal resuspension of protists into the subtidal benthic boundary layer of a coastal embayment. Mar Ecol Prog Ser 177:51-62

Sikora WB, Sikora JP (1982) Ecological implications of the vertical distribution of meiofauna in salt marsh sediments. In: Kennedy VS (ed) Estuarine comparisons. Academic Press, New York, p 269 - 282

Smith DJ, Underwood GJC (1998) Exopolymer production by intertidal epipelic diatoms. Limnol Oceanogr 43:1578-1591

Sullivan MJ, Currin CA (2000) Community structure and functional dynamics of benthic microalgae in salt marshes. Concepts and controversies in tidalmarsh ecology. M. Weinstein and D. Kreeger (Eds.), Kluwer Publishing, pp. 81–106

Teal JM (1962) Energy flow in salt marsh ecosystem of Georgia. Ecology 43:614-&

Tso SF, Taghon GL (2006) Protozoan grazing increases mineralization of naphthalene in marine sediment. Microb Ecol 51:460-469

van Oevelen D, Soetaert K, Middelburg JJ, Herman PMJ, Moodley L, Hamels I, Moens T, Heip CHR (2006) Carbon flows through a benthic food web: Integrating biomass, isotope and tracer data. J Mar Res 64:453-482

Weinbauer MG, Beckmann C, Hofle MG (1998) Utility of green fluorescent nucleic acid dyes and aluminum oxide membrane filters for rapid epifluorescence enumeration of soil and sediment bacteria. Appl Environ Microbiol 64:5000-5003

Wetzel RG, Likens GE (1991) Limnological Analysis, 2nd ed., Springer Verlag, New York

Zimmerman R, Minello T, Rozas L (2002) Salt marsh linkages to productivity of penaeid shrimps and blue crabs in the northern Gulf of Mexico. In: Concepts and controversies in tidal marsh ecology, p 293-314

**Table 2.1** Sample site identifications, locations, and mean physical parameters of sediment at all sample dates.

| Location | ID | Longitude (W) | Latitude (N) | Mean Grain Size (μm) | Grain Size Skewedness | Sediment Density (g $ml^{-1}$) | Water content (% wet weight) | Organic matter (% dry weight) |
|---|---|---|---|---|---|---|---|---|
| Nannygoat Beach | NB | 81.264268° | 31.389762° | 276 | 2.27 | 1.8 | 23 ± 2 | 0.4 ± 0.1 |
| Dean Creek | DC | 81.269099° | 31.392425° | 199 | 2.67 | 1.1 | 52 ± 8 | 5.2 ± 1.7 |
| Marsh Landing | ML | 81.295823° | 31.392425° | 148 | 0.94 | 1.5 | 76 ± 6 | 13.1 ± 2.6 |

**Table 2.2.** The top five correlations between environmental conditions and the biomass distribution patterns of benthic organisms (shown by Spearman's correlation, ρ) as determined by the BIO-ENV routine.

| Variables | ρ |
|---|---|
| pH, Grain Size | 0.627 |
| Salinity, pH, Grain Size | 0.623 |
| Surface Salinity, pH, Grain Size | 0.593 |
| Surface and Sediment pH, Organic Matter | 0.565 |
| Surface and Sediment pH, porosity | 0.561 |

**Figure 2.1.** Air temperature and precipitation recorded at the University of Georgia Marine Science Institute during 2005. Dots show the mean daily air temperature with low and high temperatures denoted by the gray bars.

**Figure 2.1**

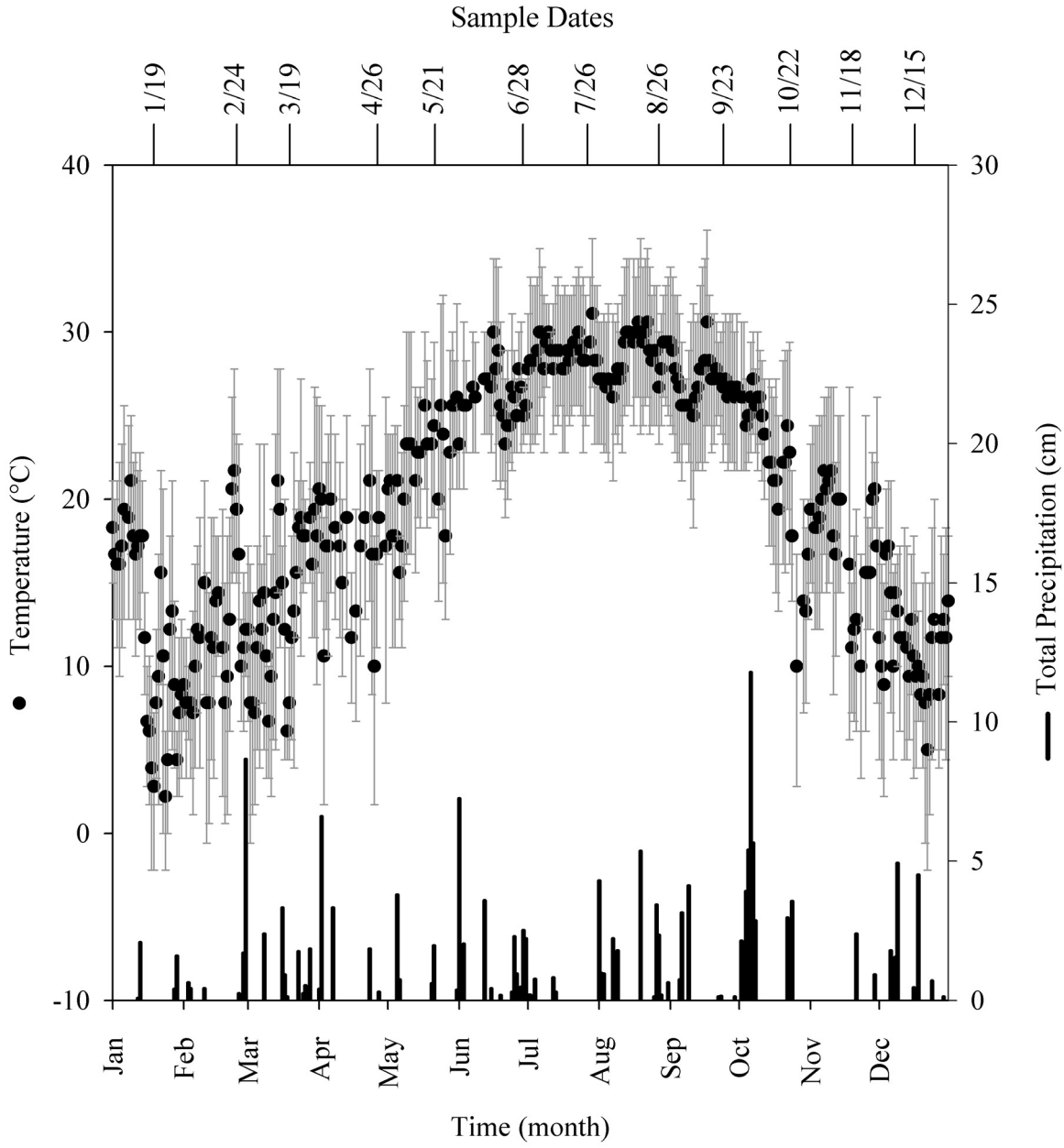
Sample Dates
1/19
2/24
3/19
4/26
5/21
6/28
7/26
8/26
9/23
10/22
11/18
12/15
40
30
20
10
0
-10
Temperature (°C)
30
25
20
15
10
5
0
Total Precipitation (cm)
Jan
Feb
Mar
Apr
May
Jun
Jul
Aug
Sep
Oct
Nov
Dec
Time (month)

**Figure 2.2.** Bacterial and algal biomass in sediments from A) Dean Creek, B) Nanny Goat Beach, and C) Marsh Landing. Bars show the mean biomass (n=3) of potentially active and total bacteria with standard error bars for the total biomass. The mean benthic microalgal (BMA) biomass is shown with standard error bars.

**Figure 2.2**

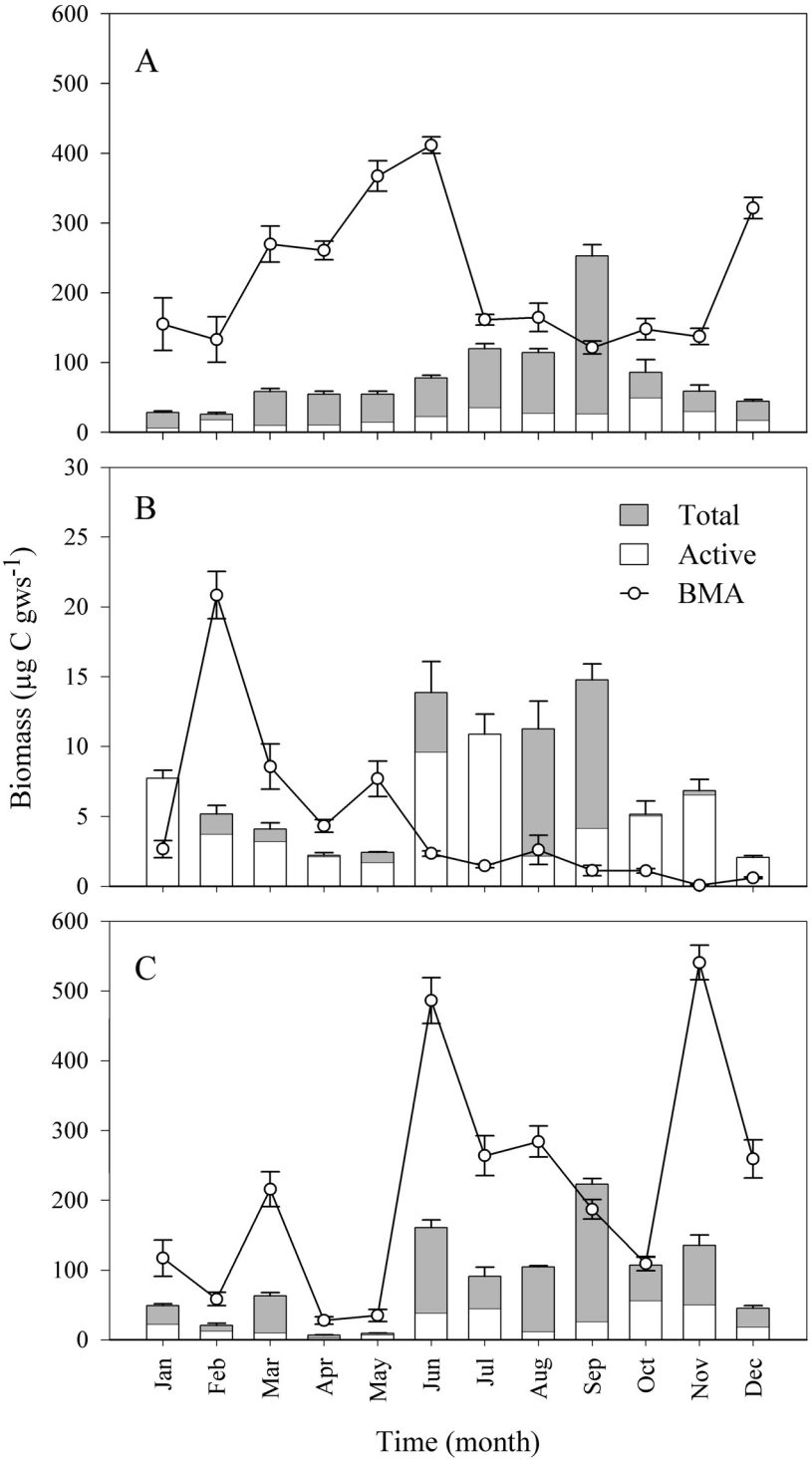
A
B
C
Total
Active
BMA
Biomass (µg C gws-1)
Time (month)
Jan
Feb
Mar
Apr
May
Jun
Jul
Aug
Sep
Oct
Nov
Dec

**Figure 2.3.** Protist biomass recorded in sediments from A) Dean Creek, B) Nannygoat Beach, and, C) Marsh Landing. Bars show the mean biomass (n=3) of small (<20 μm) and large (>20 μm) protists with standard error of the combined biomass shown.

**Figure 2.3**

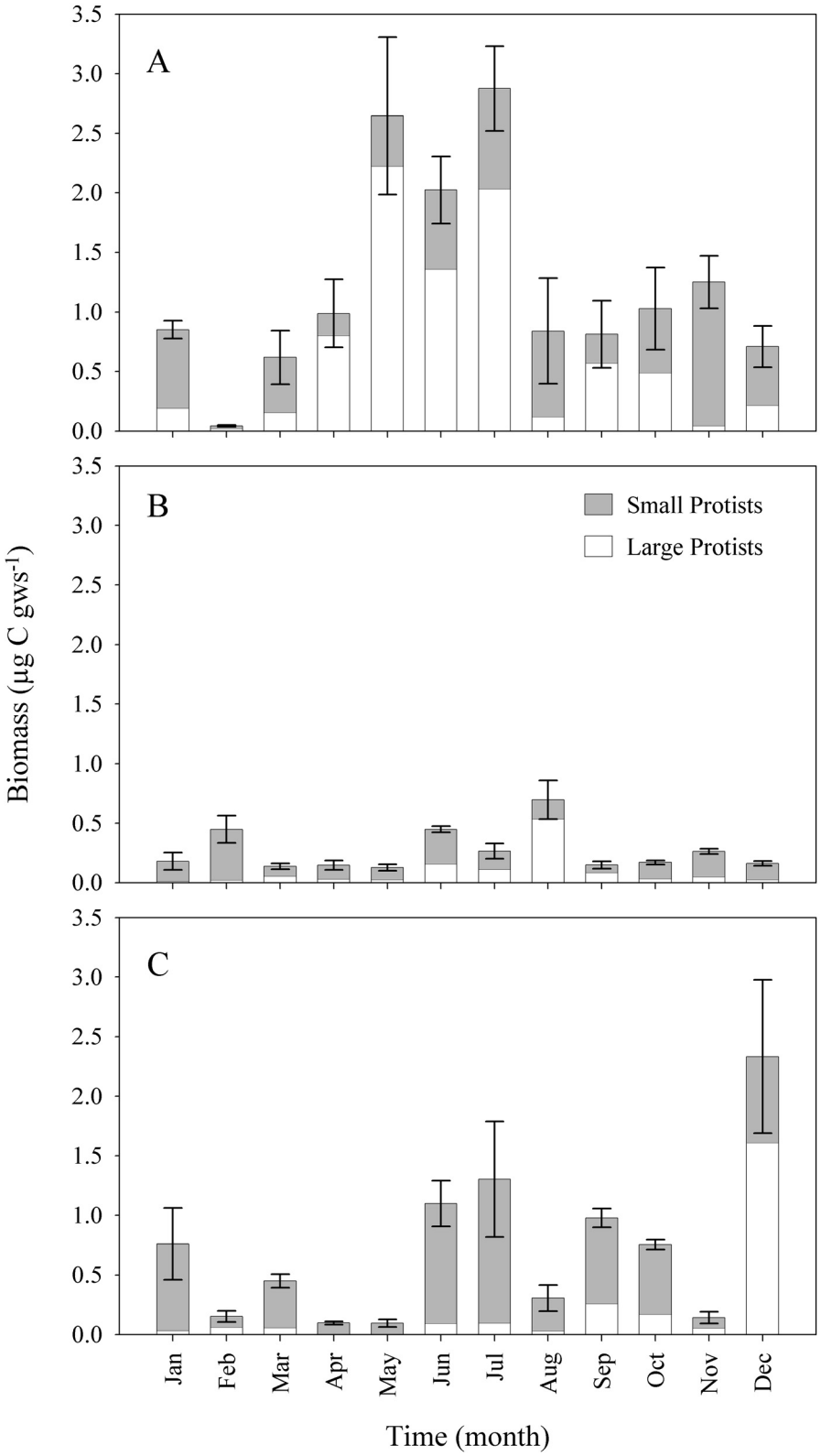
A
B
C
Small Protists
Large Protists
Biomass (µg C gws-1)
Time (month)
Jan
Feb
Mar
Apr
May
Jun
Jul
Aug
Sep
Oct
Nov
Dec
0.0
0.5
1.0
1.5
2.0
2.5
3.0
3.5

**Figure 2.4.** Total micro- and meiobenthos biomass in sediments from A) Dean Creek, B) Nannygoat Beach, and C) Marsh Landing. Top panels show the mean (n=3) total biomass of all groups with standard error bars (note the log scale). Bottom panels show the contribution of benthic microalgae (BMA), total bacteria, protists and meiofauna to the total biomass.

**Figure 2.4**

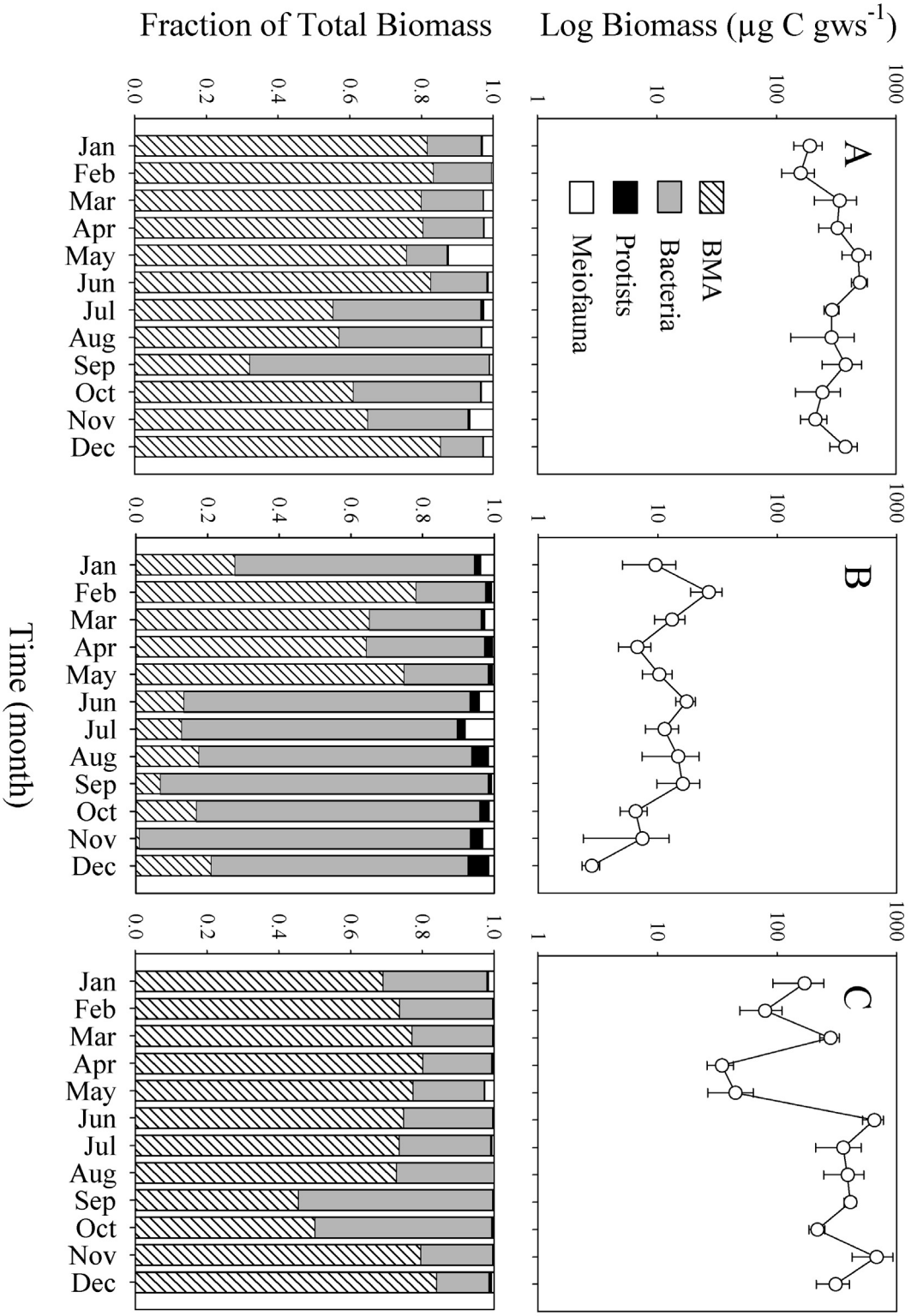
Fraction of Total Biomass
Log Biomass (µg C gws-1)
A
B
C
BMA
Bacteria
Protists
Meiofauna
Jan
Feb
Mar
Apr
May
Jun
Jul
Aug
Sep
Oct
Nov
Dec
Time (month)

**Figure 2.5.** The relationship between bacteria A) biomass, and B) concentration to sediment porosity (i.e. porewater volume) at all three locations over the year (See table 2.1 for site characteristics). The dotted line indicates a concentration of $10^9$ $ml^{-1}$; the solid lines show the linear regression best fit line. The slopes (± SE) are indicated in the plots.

**Figure 2.5**

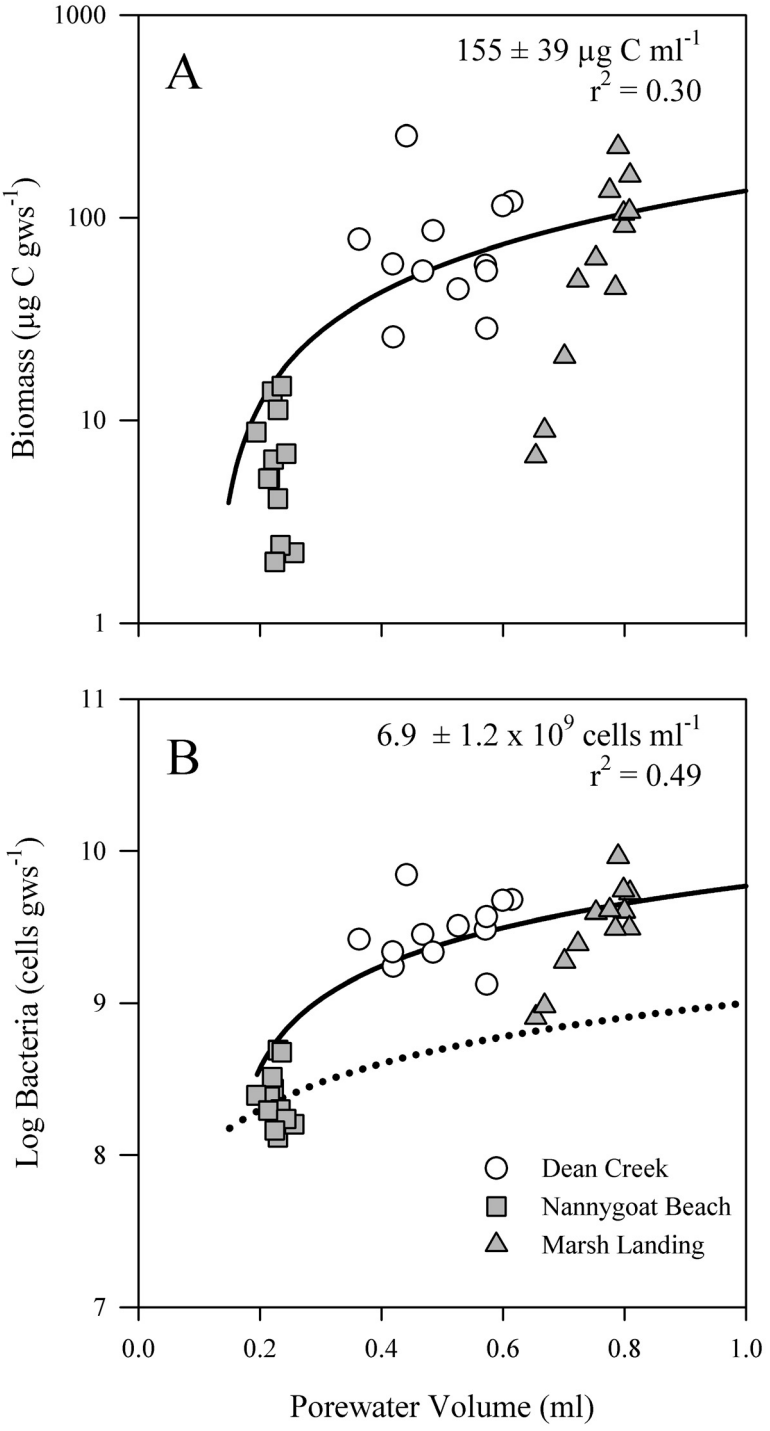
A
155 ± 39 µg C ml-1
r2 = 0.30
Biomass (µg C gws-1)
1000
100
10
1
B
6.9 ± 1.2 x 10^9 cells ml-1
r2 = 0.49
Log Bacteria (cells gws-1)
11
10
9
8
7
Dean Creek
Nannygoat Beach
Marsh Landing
0.0
0.2
0.4
0.6
0.8
1.0
Porewater Volume (ml)

**Figure 2.6.** The relationship between heterotrophic protist A) biomass, and B) concentration and sediment porosity (i.e. porewater volume) at all three locations over the year (See table 2.1 for site characteristics). The solid lines show the linear regression best fit line. The slopes (± SE) are indicated in the plots.

**Figure 2.6**

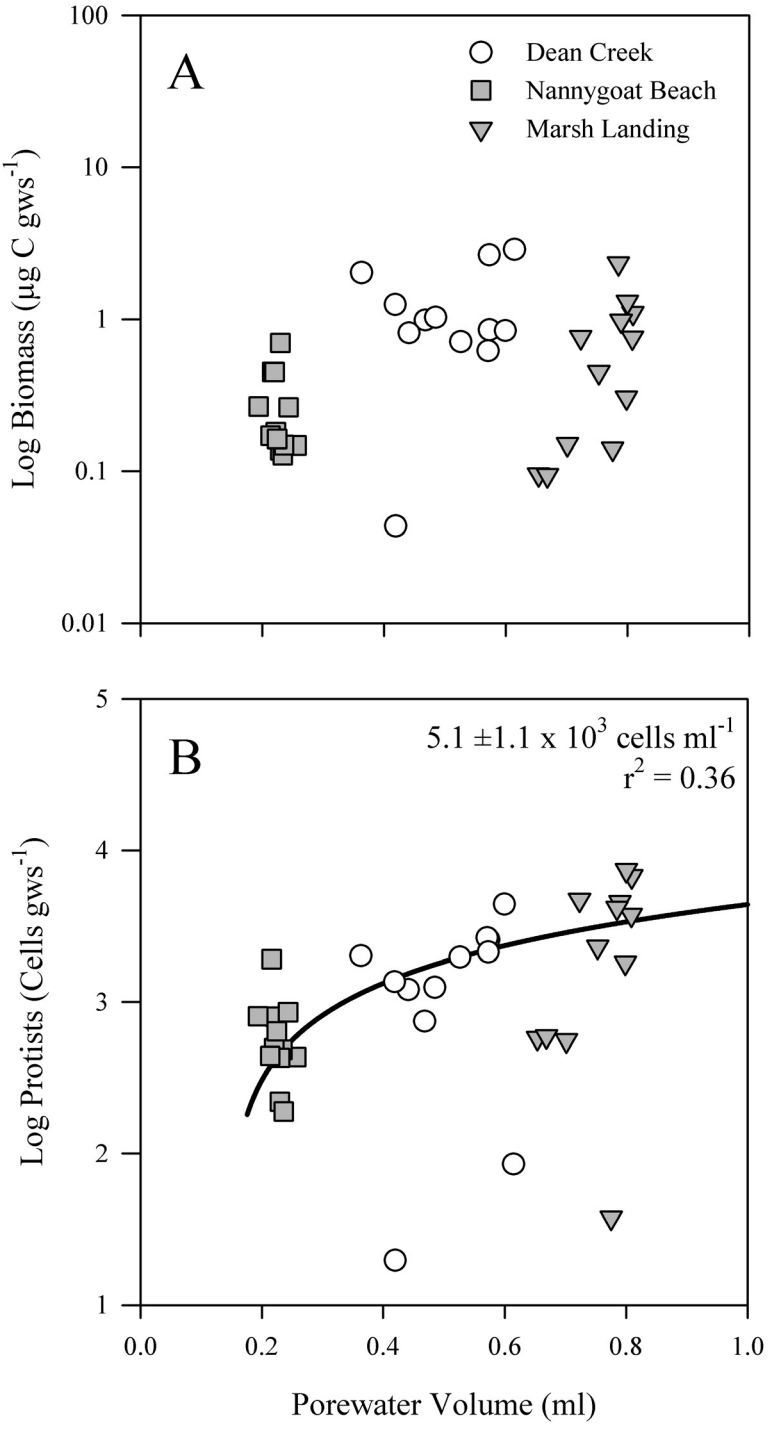
A
Dean Creek
Nannygoat Beach
Marsh Landing
Log Biomass (µg C gws-1)
100
10
1
0.1
0.01
B
5.1 ±1.1 x 10^3 cells ml-1
r2 = 0.36
Log Protists (Cells gws-1)
5
4
3
2
1
0.0
0.2
0.4
0.6
0.8
1.0
Porewater Volume (ml)

**Figure 2.7.** Mean turnover time (note the log scale) of bacteria at all three locations over the year.

**Figure 2.7**

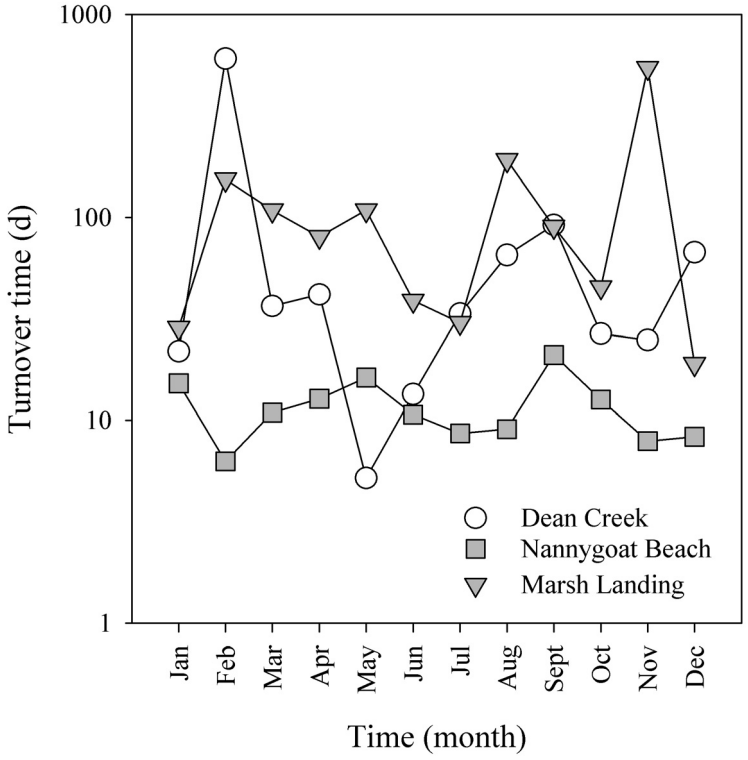
1000
100
10
1
Turnover time (d)
Dean Creek
Nannygoat Beach
Marsh Landing
Jan
Feb
Mar
Apr
May
Jun
Jul
Aug
Sept
Oct
Nov
Dec
Time (month)

# CHAPTER 3

## PROTISTAN BACTERIVORY AND BENTHIC MICROBIAL BIOMASS IN AN INTERTIDAL CREEK MUDFLAT[2]

[2] M.R First and J.T. Hollibaugh
In Press: Marine Ecology Progress Series. Reprinted with permission of the publisher.

## ABSTRACT

We examined eight sediment samples collected every three hours at Dean Creek (Sapelo Island, Georgia) to assess the impact of protist bacterivory on the standing crops of benthic bacterial biomass. The combined biomass of the benthic microalgae (BMA), bacteria, heterotrophic protists, and meiofauna ranged from 0.41 – 0.57 mg C (g wet sediment)$^{-1}$ in the samples examined. BMA represented >80% of total biomass and remained relatively stable throughout the study period. Bacterial biomass ranged from 28 to 91 μg C gws $^{-1}$ (5 – 16% of total biomass) in the samples. Heterotrophic protists (mainly ciliates, flagellates and testate amoeba) and meiofauna (mainly nematodes) each contributed small (<1% each) amounts to the total biomass. Protist grazing accounted for the loss of <1.1 and <4.7% h$^{-1}$ of the total and enzymatically active bacterial standing stock, respectively. Grazing rates were highest in the morning samples concurrent with the highest portion of potentially active bacteria. However, there was no statistically significant change in grazing impact throughout the day and in most cases bacterivory would not reduce the standing bacterial biomass. Food-web simulations demonstrate that the confluence of protist loss factors (such as meiofaunal predation) and reduced grazing at low bacterial concentrations can limit the production of bacterivorous protists and, in turn, their use of the large store of benthic bacterial biomass.

## INTRODUCTION

Marine sediments harbor both high abundance and high diversity of prokaryotes (Torsvik et al. 1996). Bacteria standing crop is several orders of magnitude greater in sediments than in the water column and (when scaled to porosity) remains relatively constant across a range of environments (Schmidt et al. 1998). This constancy suggests that there are strong controls on benthic bacterial biomass, either from the bottom-up (supply of growth substrate), top-down (predation), or self-regulation through quorum sensing (Schmidt et al. 1998). Because of the higher bacterial biomass in sediments, the flux of primary production passed to metazoans through bacteria and bacterivores may be substantial (Kemp 1990). The combined grazing of bacteria by benthic ciliates, flagellates, and meiofauna can account for a large portion of bacterial production (Epstein 1997). Yet bacterivory by ciliates (a major component of marine microbenthos - Fenchel 1967) has been estimated as only a small fraction of benthic bacterial production (Kemp 1988). When measured simultaneously, bacterial production often exceeds grazing loss (Epstein 1997, Hamels et al. 2001). The enigmatic co-occurrence of high production, low protistan grazing rates, and stable bacterial standing stock has also been observed in freshwater sediments (Wieltschnig et al. 2003).

One potential explanation is that other loss mechanisms, such as invertebrate deposit feeders or viral lysis, balance benthic bacterial production. Detritivorous meiofauna rely upon particle associated bacteria and protists for nutrition (Fenchel 1970). However, the abundance and production of invertebrate deposit feeders is low relative to benthic bacteria, effectively preventing the control of bacterial populations (Kemp 1987). Viral particles are present in high concentrations in the sediment but the rate of viral lysis is generally lower than observed in the

water column (e.g. Glud & Middelboe 2004) and in some benthic systems viral infection occurs in <0.1% of bacterial cells (Filippini et al. 2006).

Salt marsh sediments are subject to periodic tidal inundation. Tidal advection drives the resuspension of benthic microbes into the water column (Shimeta & Sisson 1999). These benthic microbes are an important component of the pelagic food web (De Jonge & Van Beusekom 1992). For example, benthic diatoms are approximately one-third of all diatoms ingested by oysters in the headwaters of tidal rivers (Thoresen 2004). Patterns of suspension and settling of intertidal bacterivores could lead to periods of the day when relatively higher abundances of bacterivorous protists significantly impact the benthic bacterial community.

The goal of this study was to test the hypothesis that protistan grazing impact on benthic bacteria varies significantly throughout the day. This variation could be due to either 1) change in the abundance of heterotrophic protists relative to bacteria, or 2) fluctuations in individual grazing rates throughout the day. To test these hypotheses, we recorded the biomass of benthic microbes (bacteria, protists, microalgae, meiofauna) in samples from an intertidal mudflat and measured grazing rates of protists on bacteria in each sample eight times throughout the day. A simple predator-prey model was used to interpret experimental results and to examine the potential role of bacterivory in controlling bacterial biomass and dynamics of protist bacterivores.

## METHODS

**Sampling**. The site selected for sampling was located beneath a foot-bridge crossing Dean Creek on Sapelo Island Georgia (USA). Sampling was conducted 28 – 29 July, 2005 by lowering a sediment grab sampler onto a 2 $m^2$ mudflat that was uniform in elevation and color and

contained no visible crab burrows. Sampling from the bridge allowed quick access to the site without disturbing the surrounding sediments. Sampling started at 0600 h and occurred at three hour intervals thereafter. Samples are identified by the time when the sample was collected (e.g. $T_{0600}$, $T_{0900}$, etc.). A complete description of the sediment sampling protocol is available elsewhere (First and Hollibaugh, submitted). Three replicate samples (~40 ml) were collected by scraping the top 1 cm off of the sediment from three areas roughly 10 cm apart in the grab sampler. This sediment was placed in plastic containers, mixed with a metal spatula and subsampled for analysis of photopigments, bacteria, protists and meiofauna, and grazing experiments.

Biomass content is reported per g of wet sediments (gws). Intertidal sediments can compact during tidal emersions due to dewatering; long periods of emersion (~ 2 – 3 h) can result in significantly different estimates of biomass density (Perkins et al. 2003). At the location sampled, sediments were emersed from 0925 to 1205 on 28 Jul 2005 and from 2340 to 0026 on 29 Jul 2005. Thus, the only sampling in which biomass density was likely to be affected by compaction was at 1200 h. We analyzed the porosity of Fluorescently Labeled Embedded Cores (FLEC; Bernhard et al 2003) collected from these grab samples to determine if there was a significant difference between the 1200 h and 1500 h (during tidal submersion) cores. These sediments were composed mostly of large sand grains (grain size 259 ± 113 μm, mean ± SD). FLEC profiles were analyzed via laser scanning confocal microscopy as described elsewhere (First and Hollibaugh, submitted). Sand grains had no fluorescence in contrast to the slight background fluorescence of the epoxy embedding media. Thus, porosity of these two different cores was determined by the relative portion of sand grain area to interstitial area.

**Benthic Microalgae**

[3]**.** Three analytical replicate samples (approximately 5 g wet sediment) were placed in 15 ml centrifuge tubes with 0.5 ml of Filtered (0.22 µm Nuclepore) Sea Water (FSW) saturated with $MgCO_3$. The samples were frozen (-20 ± 2 °C), and kept in the dark prior to and during extraction and analysis. Pigments were extracted from sediment samples for 24 h with a solution consisting of 45% acetone, 45% methanol and 10% water. Sample tubes were vortexed at high speed for 1 min every 8 - 10 h throughout the extraction period. Samples were then centrifuged (20 min at 5000 x *g*), absorbance spectra (485 – 750 nm) of the supernatants were recorded with a Shimadzu UV:Visible Spectrophotometer, then recorded again following acidification with HCl (final pH 2-3). Chlorophyll *a* (Chl *a*) and phaeopigment concentrations were calculated per g of wet sediment with standard spectrophotometric equations for microalgae (Lorenzen 1967). The efficiency of the first extraction was determined from the total pigment accumulated after three separate, serial extractions of the same sample. Concentration estimates for the remaining samples were adjusted based on one extraction using the average extraction efficiency for these sediments (40%, $n = 18$). Carbon biomass of BMA was estimated using a ratio of 40 µg C: µg Chl *a*, which is at the low end of the range of previous estimates for estuarine BMA (De Jonge & Colijn 1994).

**Bacteria**. Bacteria with intact cytosolic esterases were enumerated in replicate sediment samples (1 g) dispersed in 2 ml of FSW then stained with 50 µl of 0.5 mM of CellTracker Green Chloromethylfluorescein diacetate (CTG, Invitrogen). CTG is a non-fluorescent substance that

[3] The description of methods in the sections titled Benthic Microalgae, Bacteria, and Protists and Meiofauna, are the same as in Chapter 2. They are rewritten here as they are part of this accepted manuscript. The version of Chapter 2 that will be submitted will have only a truncated description of these methods, referring to this published manuscript based on Chapter 3.

freely diffuses into cells and becomes fluorescent and impermeant upon hydrolysis by cytosolic enzymes. Metabolically activated dyes have the advantages of high specificity for living cells and reduced non-specific labeling (Epstein & Rossel 1995). Dispersing the bacteria into a slurry oxygenates sediments and may stimulate bacterial activity. Therefore, the portion of bacteria that are CTG-positive are defined here as "potentially active bacteria". Cells were fixed after a 2 h incubation by adding 1 ml of 16% glutaraldehyde, then refrigerated (4 ± 2 °C) in the dark until analysis. These sediment samples were also used for counts of protists, meiofauna, and total bacteria.

A subsample of this slurry (1 g) was dispersed in 1 ml of 0.04 M tetrasodium pyrophosphate and placed in a low energy sonic bath for 20 min. This suspension was vortexed, then serially diluted 1:10 in the tetrasodium pyrophosphate solution three times with sonication at each dilution (1:1000 final dilution) to separate bacteria from particles and to disperse colonies (Weinbauer et al. 1998). One ml of the dilution was then filtered onto 0.2 µm Anodisc filters (Whatman). For these and all other slide preparations, 40 µl of 5:1 Citifluor:Vectashield was used as a mounting medium to reduce fluorochrome photobleaching. Potentially active bacteria were counted on a Leica DMX RA epifluorescence microscope using blue excitation (450 – 490 nm, dichromatic mirror 510 nm, longpass filter 515 nm) at 400-fold and 1000-fold magnification. All bacteria in the sample ("total bacteria") were enumerated as described above after staining the bacterial suspension with SYBR Green II (SYBR). At least 10 fields were counted per filter, usually resulting with >>300 cells per sample. Raw data were adjusted for dilutions, FSW and fixative additions and concentrations are reported as cells per g of wet sediment.

The size distribution of bacterial cells was determined by analyzing images of 12 – 15 fields for each replicate subsample, captured at 1000-fold magnification with a Hamamatsu CCD digital camera. Cells were automatically sized with image analysis software (Image Pro Plus 4.1). A stage micrometer was used to calibrate the image analysis program and calibration was verified with 0.66 and 1.0 μm diameter fluorescent spheres. After manually excluding dividing cells, colonies and non-bacterial objects from the images, the average length and width of all remaining cells in images from each time point and replicate was determined. Bacterial biovolume ($V$, $\mu m^3$) was calculated as:

$$V = \frac{\pi}{4} W^2 \left( L - \frac{W}{3} \right) \quad (1)$$

where L and W are the average cell length and width in μm, respectively (Bratbak 1985). Cell volumes were converted into biomass ($M$, pg C) by the following allometric relationship (Norland 1993):

$$M = 0.09 V^{0.9} \quad (2)$$

Total and potentially active bacterial community biomass was the product of cell concentration and mean biomass of the bacterial cells at each time point (average $n$=607; range: 369–825). The frequency of dividing cells (FDC) was determined by counting the number of dividing cells with a clear septum per 300 SYBR-stained cells (Hagström et al. 1979).

**Protists and Meiofauna.** Benthic protists and meiofauna were extracted from preserved sediments using a density gradient created with a colloidal silica solution following published methods (Epstein 1995). Briefly, 6 ml of Percoll (density 1.13 g $ml^{-1}$; Amersham Biosciences) was placed in 10 ml tubes and centrifuged in a fixed angle rotor (30 min at 30,000 x $g$) to create a density gradient. Wet sediment slurry (~2 g) was added to the top of the gradient, then the

tubes were centrifuged in a swinging bucket rotor (60 min at 2000 x *g*). The supernatant was removed and placed in a clean 15 ml centrifuge tube. The remaining sediment was resuspended in 1 ml of Percoll, centrifuged in the swinging bucket rotor again and the supernatant combined with the initial supernatant. A dual stain of 4',6-diamidino-2-phenylindole (DAPI) and fluorescein isothiocyanate (FITC) was added to the combined supernatant and the sample was incubated at 4 ± 2 °C for a minimum of 60 min. The dual stain was useful in identifying cells, as FITC labels cell proteins and DAPI labels nuclei (Sherr & Sherr 1993). The supernatant was centrifuged again to settle any sand grains remaining in suspension. The extraction efficiency of this method was determined by counting the total number of organisms extracted from a sample by three additional serial extractions ($n = 6$). On average >90% of the total biomass was obtained in the first extraction, so counts from the first extraction were used without correction.

The extract was filtered through a 5 μm pore size, black polycarbonate filter (Osmonics) and the organisms retained were counted using standard blue excitation for FITC and UV excitation filter sets (UV: 340-380 nm, dichromatic mirror 400 nm, longpass filter 425 nm) for DAPI. Because the biomass of autotrophic protists is included in the Chl *a* based estimates of BMA biomass, only heterotrophic protists (cells lacking chloroplasts visible under green excitation; 515 – 560 nm, dichromatic mirror 580 nm, longpass filter 590) were enumerated. Large protists and meiofauna (mostly nematodes) were counted at 100-fold magnification by scanning the entire filter. Flagellates lacking chloroplasts were counted at 400-fold magnification along transects through the filter. Large (>20 μm in Equivalent Spherical Diameter, ESD) heterotrophic protists (mainly ciliates and testate amoebae) were grouped into 15 common morphotypes and the average size of each morphytope was determined from the length and width of >30 individuals using image analysis software (ImagePro Plus 4.1). Common ciliates were

identified when possible using taxonomic guides (Carey 1992). Flagellates were grouped into 3 size ranges and the average dimensions for each size range were based on >30 individuals. Nematodes were grouped into 4 size categories with the average dimensions based upon 60 individuals. Individual dimensions were used to calculate biovolume and biomass of protists (Putt & Stoecker 1989, Wetzel & Likens 1991) and nematodes (Baguley et al. 2004).

**Bacterial Grazing Experiments.** Grazing by sediment protists on bacteria was measured by the Fluorescently Stained Sediment (FSS) method (Starink et al. 1994). In this method, sediment bacteria are labeled by adding a fluorescent stain directly to the sediment. Excess stain is removed by repeated rinsing. Sediment containing stained cells is mixed with an unstained sample of sediment and the quantity of stained bacterial cells ingested is determined by enumerating cells in protist food vacuoles. Grazing rate is calculated from ingestion and the ratio of FSS bacteria to total bacteria. The advantage of this method is that FSS contains a natural assemblage of living bacterial prey (including both free-living and particle-associated bacteria). Therefore, potential artefacts arising from selective grazing (e.g. preferences for cell-size, motility, etc.) are reduced. To avoid non-specific labeling, CTG was used as the label and the ratio of labeled cells to total cells in FSS is determined as described above.

To produce FSS, sediments were collected from the study site 1 d prior to the start of the observation period. Approximately 20 g of sediment from of the top 1 cm of a grab sample was placed in a 50 ml conical centrifuge tube. The sediment was dispersed with 1 ml of FSW then 50 µl of 0.5 mM CTG was added to the slurry. The sample was incubated in creek water for >10 h then the slurry was centrifuged (20 min at 2000 x *g*). The supernatant was discarded, then the FSS was dispersed in ~20 ml of FSW and centrifuged again. This process was repeated for a

total of three FSW washes. Washed FSS was incubated in creek water prior to use. For each replicate sample, 10 g of sediment was added to a 50 ml centrifuge tube and dispersed in 5 ml of FSW. Roughly 2.5 g of FSS was weighed on the tube cap. The experiment was started by placing the cap on the centrifuge tube and thoroughly mixing the sediment by inverting the tube. A control consisting of non-stained sediment was run at each time point to determine if naturally fluorescent materials occur in food vacuoles or if artefacts of fixation can mimic prey ingestion. Samples were incubated at the ambient creek water temperature for 15 min, as digestion can reduce the apparent number of ingested cells if incubation times are >15 min (Sherr et al. 1988). Incubations were stopped by adding 1 ml of 16% glutaraldehyde then samples were stored in the dark and refrigerated (4 ± 2°C) until analysis.

The rate of bacterivory was determined by enumerating bacteria in the food vacuoles of at least 30 protists per replicate sample (except at 11:00 h, when one replicate was lost). Protists were extracted from sediments and collected on filters as described above. Protists were located by transmitted light microscopy (100-fold magnification) as the 5 μm pore size filters were relatively translucent. Fluorescent, bacteria-sized particles inside protists were counted by epifluorescence microscopy under blue excitation as described above for CTG-stained, potentially active bacteria. Grazing was determined as both the average number of bacteria per protist examined (per capita grazing) and as the overall potential grazing impact determined by the average number of bacterial cells per unit of protist biovolume, multiplied by the total biovolume of protists (including flagellates, ciliates, and amoeba) at each time point. Because there was no relationship between cell size and ingestion (data not shown), this method allows for the extrapolation of the per capita grazing rate to the entire size range of protists. Fluorescent

food vacuoles with an indistinct number of labeled bacteria were scored conservatively as containing one bacterium.

**Food Web Model.** The interactions between bacteria (*B*) and bacterivorous protists (*P*) were modeled with the Lotka-Volterra equations:

$$\frac{dB}{dt} = \mu B - FP(B - T)$$
$$\frac{dP}{dt} = eFP(B - T) - dP \quad (3)$$

Variables are described in Table 3.1. The initial biomass values for total bacteria, bacterivorous protists, and meiofauna were the average of all eight observations, set to: 51, 2.8, and 2.4 μgC $gws^{-1}$, respectively. We performed three simulations to investigate the roles of feeding thresholds (*T*) and predation pressure on bacterivorous protists. In these simulations, protist mortality is attributed to meiofauna ($d = M \cdot F_M$, see Table 3.1); meiofauna concentration was assumed to remain constant over the simulation time span. Each simulation was performed 1000 times with parameter values randomly chosen from a normal distribution within 10% of the mean value. For all of these simulations, mean protist clearance rate was set to the mean of all eight field observations (0.037 gws $d^{-1}$), growth efficiency was 0.3, and initial biomass values were as specified above. The mean and standard deviations of bacterial and protist biomass were generated from 1000 model runs with a total incubation time of 5 d sampled at 0.2 d intervals. We assumed the system was closed (i.e. no imports or exports from the system) and that bacterial growth rate was exponential. In Simulation I, the threshold bacterial biomass (*T*) was set to 10 or 20 μgC $gws^{-1}$. Bacterial biomass available for protist ingestion is equal to the biomass minus *T* and no bacterivory occurs when the bacterial biomass is less than *T*. In Simulation II, *T* was set to zero and the clearance rate of meiofauna ingesting protists was set to either 0.05 or 0.1 gws

μgC $d^{-1}$. Finally, in Simulation III, both predation and threshold feeding occur in concert with runs initialized using mean values as listed above.

## RESULTS

**Biomass.** The physical conditions during sampling, including temperature, salinity, photosynthetically active radiation (PAR) and granulometry are reported elsewhere (First and Hollibaugh, submitted). There was no significant difference between porosity of cores taken during tidal emersion and immersion (t-test, df = 4, $p > 0.05$); therefore, we assume that compaction of these sediments during emersion does not lead to significant changes in biomass density over a tidal cycle (sensu Perkins et al. 2003). Chl *a* ranged from 8.9 (± 0.9 SD) to 12 (± 1.0) μg $gws^{-1}$ in the top 1 cm, corresponding to BMA biomass of 0.36 to 0.48 mg $gws^{-1}$ (Fig. 3.1). Phaeopigment concentrations were less than 14 % of Chl *a* concentrations and were not significantly different from zero in several samples.

Total bacteria concentrations ranged from 1.4 to 3.6 x $10^9$ cells $gws^{-1}$; bacterial biomass, ranged from 27.5 to 91.3 μgC $gws^{-1}$ (Fig. 3.2A). Two samples (09:00 and 21:00 h) contained anomalously high bacterial biomass; in one of theses samples (21:00 h), the abundance and biomass were greater than twice the mean of the other time points. Potentially active bacteria were roughly 10% of total bacteria (0.2 – 0.4 x $10^9$ cells $gws^{-1}$, 4.9 – 15.7 μgC $gws^{-1}$) and contributed the most to total bacterial biomass at the 8:00 and 11:00 h samples. The mean bacteria cellular biovolume varied from 0.20 to 0.37 $\mu m^3$ with the largest cells observed at 11:00 h (Fig. 3.2B), followed by a reduction in mean cell volume corresponding to an increase in the FDC (Fig. 3.2C).

Ciliates were the major group of large (>20 μm ESD) heterotrophic protists found in our samples, with *Uronema marinum*, and *Geleia* sp. accounting for a large portion of total abundance and biomass, respectively. Testate amoeba were also common among large protists (19 ± 10 cells $gws^{-1}$, mean ± SD). Foraminifera tests, however, were rarely found. Total abundance of large protists ranged from 67 – 245 cells $gws^{-1}$ (Fig. 3.3A), corresponding to 1.3 – 3.4 μg C $gws^{-1}$. Small protists (< 20 μm ESD), mostly flagellates, were always abundant (Fig. 3.3B). Despite high concentrations ranging from 2,200 to 4,900 individuals $gws^{-1}$, the biomass of small protists (0.33 – 0.73 μgC $gws^{-1}$) was a minor component of total microbenthic biomass. Nematodes were the dominant metazoan found at the study location and along with a few harpacticoid copepods comprised almost the entire meiofauna biomass. The concentration and biomass of meiofauna ranged from 17 – 65 individuals $gws^{-1}$ (Fig. 3.3C), corresponding to a biomass contribution of 1.2 to 4.5 μgC $gws^{-1}$.

Overall, the combined microbenthic biomass (including bacteria) ranged from 0.4 – 0.6 mg C $gws^{-1}$ (Fig. 3.4). This accounts for 2 – 3% of total organic matter in the sediment. BMA was >80% of the total microbenthic biomass while bacteria ranged from 5 – 16 % of the total biomass. The contributions of heterotrophic protists and meiofauna ranged from 0.3 – 0.8 % (mean 0.6 %) and 0.2 – 0.8 % (mean 0.5 %) of total microbenthic biomass, respectively. The ratio of protist to bacterial biomass ranged from 0.03 to 0.12 for large protists; for small protists, the protist:bacteria biomass ratio was always <0.02 (Fig. 3.5A). Likewise, meiofauna were only a small portion of bacterial biomass (0.02 to 0.08). However, the ratio of meiofauna to total protists was often >1 and, in one case ($T_{2100}$), was equal to 1.9 (Fig. 3.5B).

**Bacterial Grazing.** Both the individual (mean per capita grazing rate) and the total protist community grazing rate (hereafter, "grazing impact") were highest in morning samples (09:00 and 12:00 h, Fig. 3.6). However, there were no significant differences between protist grazing impacts measured at different times throughout the day (ANOVA, $F_{(7,15)} = 1.78$, $p > 0.05$). The per capita grazing rate declined steadily to a minimum at 21:00 h. In all cases, only a small fraction of the available bacterial biomass was lost to protist grazing: 0.1 – 1.1 % $h^{-1}$ (mean 0.4 % $h^{-1}$) of the total standing stock of bacteria or 0.6 – 4.7 % $h^{-1}$ of the potentially active bacteria (mean 2.4 % $h^{-1}$). Grazing impact did not co-vary significantly with total or potentially active bacteria concentration (linear regressions, 7 df =, $R^2<0.44$, $p>0.05$ in both cases). The turnover time (total bacterial concentration / grazing impact) ranges from 3.8 to 75 d in these samples.

**Food Web Model**. Simulation I demonstrated that setting a threshold bacterial concentration ($T$) limited the final protist:bacteria ratio to <0.65 and <0.35 when $T$ was set to 10 or 20 μgC $gws^{-1}$, respectively (Fig. 3.7). Similarly, the protist:bacteria ratio was <0.66 and <0.32 when the clearance rate of meiofauna was set to 0.05 and 0.10 gws $\mu gC^{-1}$ $d^{-1}$, respectively. With both threshold feeding ($T = 20$ μgC $gws^{-1}$) and predation loss ($F_M = 0.10$ gws $d^{-1}$), the final protists:bacteria ratio ranged from the initial value of 0.05 to 0.10 over the 5 d time span (Fig. 3.7).

## DISCUSSION

Intertidal sediments are dynamic environments; the benthic microbial community is closely coupled to the pelagic through patterns of settling and resuspension driven by tidal flow (e.g. Shimeta & Sisson 1999). We hypothesized that the protist grazing impact varies over a diel

period, and that high grazing during portions of the day could reduce the standing stock of bacteria. The grazing impact of protists could drive down the standing stock of bacteria in some samples. For example, at $T_{0600}$ the bacterial growth rate necessary to balance loss to grazing would be 0.26 $d^{-1}$. While active subpopulations of sediment bacteria can have growth rates much higher than this value, total bacterial community growth rates in coastal sediments are <0.1 $d^{-1}$ (Luna et al. 2002). However, throughout most of the day the grazing impact would not be sufficient to balance even low bacterial growth rates. The per capita ingestion rates of bacteria by protists measured in this study are at the high end of values reported for benthic (Kemp 1988) and pelagic (Sherr et al. 1988) bacterivorous protists. Therefore, the low abundance of protists (relative to bacteria) is more likely to be the cause of the persistent high bacterial standing stocks in these sediments. Potential factors limiting the accumulation of bacterivorous protist biomass and, in turn, more complete utilization of benthic bacteria, are considered below.

First, benthic protists may have low growth efficiencies and the high per-capita ingestion rates observed do not translate into high protist production rates. Aerobic protists in oxic environments have high growth efficiencies (e.g Ohman & Snyder 1991) and high intrinsic growth rates (Banse 1982). At the mean clearance rates observed, the potential production of these bacterivores should be high, even at low or moderate growth efficiencies. However, the majority of these sediments were anoxic (First and Hollibaugh, In Prep.) and growth efficiencies of anaerobic benthic bacterivores is likely much lower – roughly 25% that of aerobic metabolism (Fenchel & Finlay 1990).

Second, a majority of bacteria in sediments may be effectively unavailable for ingestion by protists. The high standing crops of benthic bacteria may result from refuge in microhabitats, which protect bacteria from viral infection and bacterivores. Grain size distributions explain the

majority of bacterial biomass variability in sediments (Dale 1974). Bacterial adhesion to particles provides a refuge from protist grazing, allowing for a higher standing stock of prokaryotic biomass. In laboratory experiments, feeding rates on unattached, interstitial bacteria were double the rates on particle-bound bacteria (Eisenmann et al. 1998). Solitary and unattached bacteria may encounter the heaviest predation pressure from interstitial grazers, which could have consequences for the overall structure of the bacterial community and, in turn, sediment metabolism. For example, bacteria attached to inorganic particles may be protected from grazers but may also have reduced access to substrate, nutrients and the electron acceptors necessary for growth (Murray & Jumars 2002). Conversely, free-living bacteria have increased access to solutes but are more likely consumed by bacterivorous protists. The most favorable strategy may vary between these two extremes throughout the day. For instance, unattached cells could more readily access labile DOC and oxygen produced when the sediments are illuminated in the late morning. The greatest portion of potentially active bacteria occurred concurrently with the greatest grazing impact at this time, suggesting that unattached cells susceptible to grazing were more abundant than at other times throughout the day. Both occurred during the late morning when the production of labile DOC was likely greatest due to algal production (Smith and Underwood 1998).

Third, factors such as predation or export into the water column may limit the abundance of protists and, consequently, their grazing impact on the bacteria. The abundance of bacterivorous protists (relative to bacteria) was roughly constant in model simulations when both predation pressure on protists and grazing thresholds were included. If bacterivorous protists are rapidly consumed by meiofauna, the cycling of energy through the microbial loop in sediments could be substantial. Benthic protists may also be advected into the water column due to tidal

flow (Shimeta & Sisson 1999), where they are assimilated into the pelagic food web. For instance, ciliates are efficiently captured and retained by oysters (LeGall et al. 1997). Also, microheterotrophs (including both protists and bacteria) supply a large portion of the carbon and nitrogen necessary for the growth of the ribbed mussel, *Geukensia demissa* (Kreeger & Newell 2000).

Protist grazing varies throughout the day and, in some periods, may be sufficient to reduce bacterial standing stock. The high per capita grazing rates of protists in the morning samples indicates bacterial prey were relatively abundant at these times. In contrast, reduced grazing rates over the day suggest that labile bacteria may become less available for protists. Regardless of these diel variations in per capita grazing, the amount of bacterial carbon consumed does appear to translate into a high standing stock of bacterivorous protists. The relative biomasses of protists and bacteria may oscillate on time scales greater than observed in this study. However, assuming the biomass of these two groups remain constant over long periods, the factors limiting the abundance of benthic protists (e.g. low growth efficiencies, predation pressure) will illuminate the causes and consequences of high benthic bacterial biomass.

## ACKNOWLEDGEMENTS

This work was supported by NSF Georgia Coastal Ecosystems LTER grant (OCE-9982133). M.R.F. was also supported by a UGA Graduate School Assistantship. H.L. Miller III assisted with the design and coding of the food web model. C. Meile critically reviewed an earlier version of this manuscript. We are grateful for the hospitality and logistical support of J. Garbisch and M. Price at the University of Georgia Marine Institute. J. Bernhard, M. Farmer, S. Joye and C.

Meile provided guidance on the design of this project. M.A. Moran and W. Ye kindly provided access to their ultracentrifuge. The comments of two anonymous reviewers greatly improved this manuscript. This is contribution no. 952 the University of Georgia Marine Science Institute.

## REFERENCES


Baguley JG, Hyde LJ, Montagna PA (2004) A semi-automated digital microphotographic approach to measure meiofaunal biomass. Limnol Oceanogr Methods 2:181-190

Banse K (1982) Cell volumes, maximal growth-rates of unicellular algae and ciliates, and the role of ciliates in the marine pelagial. Limnol Oceanogr 27:1059-1071

Bernhard JM, Visscher PT, Bowser SS (2003) Submillimeter life positions of bacteria, protists, and metazoans in laminated sediments of the Santa Barbara Basin. Limnol Oceanogr 48:813-828

Bratbak G (1985) Bacterial biovolume and biomass estimations. Appl Environ Microbiol 49:1488-1493

Carey PG (1992) Marine interstitial ciliates: an illustrated key. Chapman and Hall, Norwell, MA

Dale NG (1974) Bacteria in intertidal sediments: factors related to their distribution. Limnol Oceanogr 19:509-518

De Jonge VN, Colijn F (1994) Dynamics of microphytobenthos biomass in the Ems estuary. Mar Ecol Progr Ser 104:185-196

De Jonge VN, Van Beusekom JEE (1992) Contribution of resuspended microphytobenthos to total phytoplankton in the Ems estuary and its possible role for grazers. Netherlands J Sea Res 30:91-105

Eisenmann H, Harms H, Meckenstock R, Meyer EI, Zehnder AJB (1998) Grazing of a *Tetrahymena* sp. on adhered bacteria in percolated columns monitored by in situ hybridization with fluorescent oligonucleotide probes. Appl Environ Microbiol 64:1264-1269

Epstein SS (1995) Simultaneous enumeration of protozoa and micrometazoa from marine sandy sediments. Aquat Microb Ecol 9:219-227

Epstein SS (1997) Microbial food webs in marine sediments. I. trophic interactions and grazing rates in two tidal flat communities. Microb Ecol 34:188-198

Epstein SS, Rossel J (1995) Methodology of in situ grazing experiments: evaluation of a new vital dye for preparation of fluorescently labeled bacteria. Mar Ecol Prog Ser 128:143-150

Fenchel T (1967) The ecology of marine microbenthos I. the quantitative importance of ciliates as compared with metazoans in various types of sediments. Ophelia 4:121-137

Fenchel T (1970) Studies on decomposition of organic detritus derived from turtle grass *Thalassia testudinum*. Limnol Oceanogr 15:14-&

Fenchel T, Finlay BJ (1990) Anaerobic free-living protozoa: growth efficiencies and the structure of anaerobic communities. FEMS Microbiol Ecol 74:269-275

Filippini M, Buesing N, Bettarel Y, Sime-Ngando T, Gessner MO (2006) Infection paradox: high abundance but low impact of freshwater benthic viruses. Appl Environ Microbiol 72:4893-4898

Glud RN, Middelboe M (2004) Virus and bacteria dynamics of a coastal sediment: implication for benthic carbon cycling. Limnol Oceanogr 49:2073-2081

Hagström A, Larsson U, Hörstedt P, Normark S (1979) Frequency of dividing cells, a new approach to the determination of bacterial growth rates in aquatic environments. Appl Environ Microbiol 37:805-812

Hamels I, Muylaert K, Casteleyn G, Vyverman W (2001) Uncoupling of bacterial production and flagellate grazing in aquatic sediments: a case study from an intertidal flat. Aquat Microb Ecol 25:31-42

Kemp PF (1987) Potential impact on bacteria of grazing by a macrofaunal deposit-feeder, and the fate of bacterial production. Mar Ecol Prog Ser 36:151-161

Kemp PF (1988) Bacterivory by benthic ciliates: significance as a carbon source and impact on sediment bacteria. Mar Ecol Prog Ser 49:163-169

Kemp PF (1990) The fate of benthic bacterial production. Rev Aquat Sci 2:109-124

Kreeger DA, Newell RIE (2000) Trophic complexity between producers and invertebrate consumers in salt marshes. In: Weinstein MP, Kreeger DA (eds) Concepts and controversies in tidal marsh ecology. Kluwer, Dordrecht, Netherlands, p 187-220

LeGall S, Hassen MB, LeGall P (1997) Ingestion of a bacterivorous ciliate by the oyster *Crassostrea gigas*: protozoa as a trophic link between picoplankton and benthic suspension-feeders. Mar Ecol Progr Ser 152:301-306

Lorenzen CJ (1967) Determination of chlorophyll and pheo-pigments: spectrophotometric equations. Limnol Oceanogr 12:343-346

Luna GM, Manini E, Danovaro R (2002) Large fraction of dead and inactive bacteria in coastal marine sediments: comparison of protocols for determination and ecological significance. Appl Environ Microbiol 68:3509-3513

Murray JLS, Jumars PA (2002) Clonal fitness of attached bacteria predicted by analog modeling. Bioscience 52:343-355

Norland S (1993) The relationship between biomass and volume of bacteria. In: Kemp PF (ed) Handbook of methods in aquatic microbial ecology. Lewis Publishers, Boca Raton, p 303-308

Ohman MD, Snyder RA (1991) Growth-kinetics of the omnivorous oligotrich ciliate *Strombidium* sp. Limnol Oceanogr 36:922-935

Perkins RG, Honeywill C, Consalvey M, Austin HA, Tolhurst TJ, Paterson DM (2003) Changes in microphytobenthic chlorophyll *a* and EPS resulting from sediment compaction due to de-watering: opposing patterns in concentration and content. Cont Shelf Res 23:575-586

Putt M, Stoecker DK (1989) An experimentally determined carbon - volume ratio for marine oligotrichous ciliates from estuarine and coastal waters. Limnol Oceanogr 34:1097-1103

Schmidt JL, Deming JW, Jumars PA, Keil RG (1998) Constancy of bacterial abundance in surficial marine sediments. Limnol Oceanogr 43:976-982

Sherr BF, Sherr EB, Rassoulzadegan F (1988) Rates of digestion of bacteria by marine phagotrophic protozoa: temperature dependence. Appl Environ Microbiol 54:1091-1095

Sherr EB, Sherr BF (1993) Staining of heterotrophic protists for visualization by epifluorescence microscopy, In: Kemp PF (ed) Handbook of methods in aquatic microbial ecology. Lewis Publishers, Boca Raton

Shimeta J, Sisson JD (1999) Taxon-specific tidal resuspension of protists into the subtidal benthic boundary layer of a coastal embayment. Mar Ecol Prog Ser 177:51-62

Smith DJ, Underwood GJC (1998) Exopolymer production by intertidal epipelic diatoms. Limnol Oceanogr 43:1578-1591

Starink M, Krylova IN, Bär-Gilissen MJ, Bak RPM, Cappenberg TE (1994) Rates of benthic protozoan grazing on free and attached sediment bacteria measured with fluorescently stained sediment. Appl Environ Microbiol 60:2259-2264

Thoresen M (2004) Temporal and spatial variation in seston available to oysters and the contribution of benthic diatoms to their diet in the Duplin River, Georgia. PhD Dissertation, University of Georgia, Athens, GA

Torsvik V, Sorheim R, Goksoyr J (1996) Total bacterial diversity in soil and sediment communities - a review. J Ind Microbiol 17:170-178

Weinbauer MG, Beckmann C, Hofle MG (1998) Utility of green fluorescent nucleic acid dyes and aluminum oxide membrane filters for rapid epifluorescence enumeration of soil and sediment bacteria. Appl Environ Microbiol 64:5000-5003

Wetzel RG, Likens GE (1991) Limnological Analysis. Springer-Verlag, New York

Wieltschnig C, Fischer UR, Kirschner AKT, Velimirov B (2003) Benthic bacterial production and protozoan predation in a silty freshwater environment. Microb Ecol 46:62-72

**Table 3.1** Variables and units in the food web model. Sediment weight (gws) refers to g of wet sediment. Values used in the simulations are reported in the text.

| Variable | Description | Units |
|---|---|---|
| | **Biomass** | |
| $B$ | Bacteria | $\mu gC\ gws^{-1}$ |
| $P$ | Bacterivorous protists | $\mu gC\ gws^{-1}$ |
| $M$ | Meiofauna | $\mu gC\ gws^{-1}$ |
| | **Parameters** | |
| $\mu$ | Bacterial growth rate | $d^{-1}$ |
| $F$ | Protist clearance rate | $gws\ \mu gC^{-1}\ d^{-1}$ |
| $F_M$ | Meiofauna clearance rate | $gws\ \mu gC^{-1}\ d^{-1}$ |
| $d = M \cdot F_M$ | Protist mortality rate | $d^{-1}$ |
| $e$ | Protist growth efficiency | $\mu gC\ \mu g\ C^{-1}$ |

**Figure 3.1.** Chlorophyll *a* (Chl *a*) and phaeopigment concentrations (μg $gws^{-1}$) over the study period. Bars show the standard deviation of the mean (n=3). Negative values are set to zero and denoted by an asterisk.

**Figure 3.1**

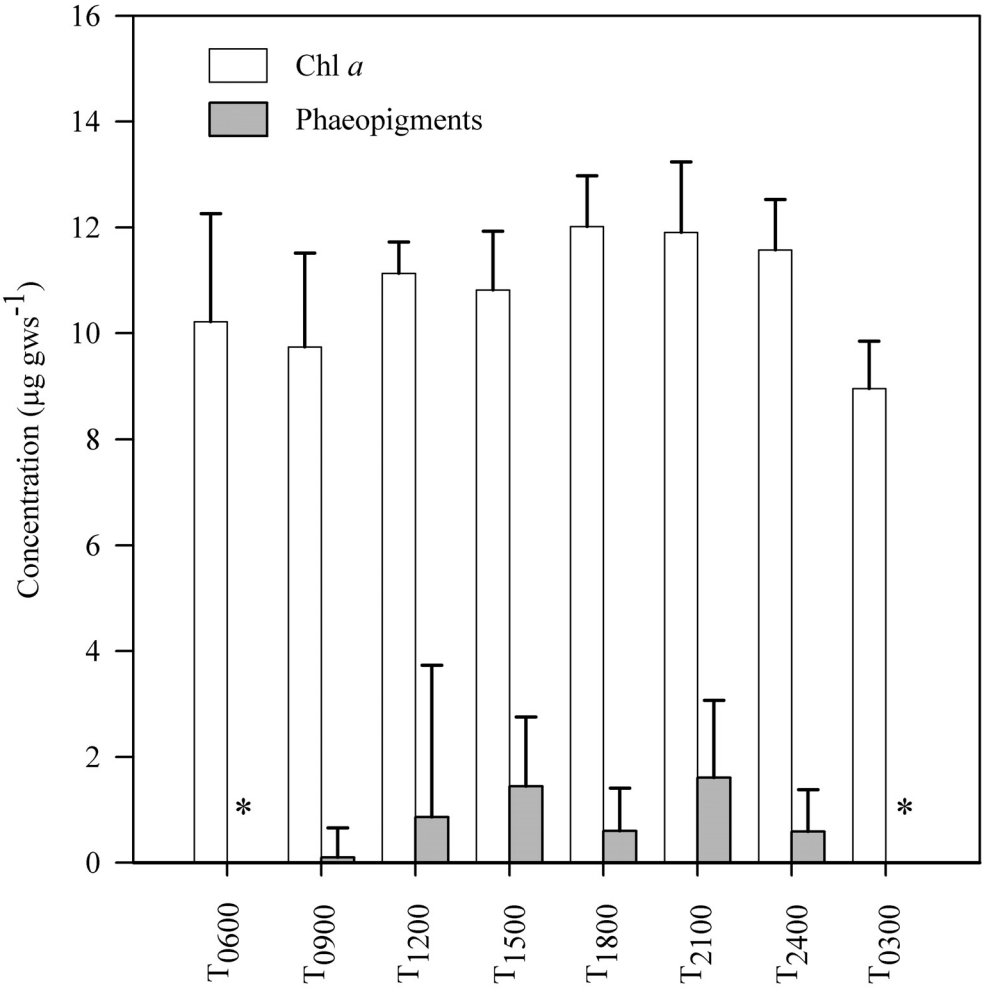
Chl *a*
Phaeopigments
Concentration (µg gws$^{-1}$)
16
14
12
10
8
6
4
2
0
*
*
$T_{0600}$
$T_{0900}$
$T_{1200}$
$T_{1500}$
$T_{1800}$
$T_{2100}$
$T_{2400}$
$T_{0300}$

**Figure 3.2.** A) Mean concentration of total and potentially active ("active") bacteria in the top 1 cm of sediment. Bars show the standard deviation of the mean (n=3). B) Biovolume distributions of total bacteria; dots and bars represent the upper and lower 5% and 10% percentiles, respectively; the box indicates 25%, 50%, and 75% of the data; mean values are indicated with a white diamond, n = 369–825. C) Mean frequency of dividing cells (FDC). Bars show the standard deviation of the mean (n=3).

**Figure 3.2**

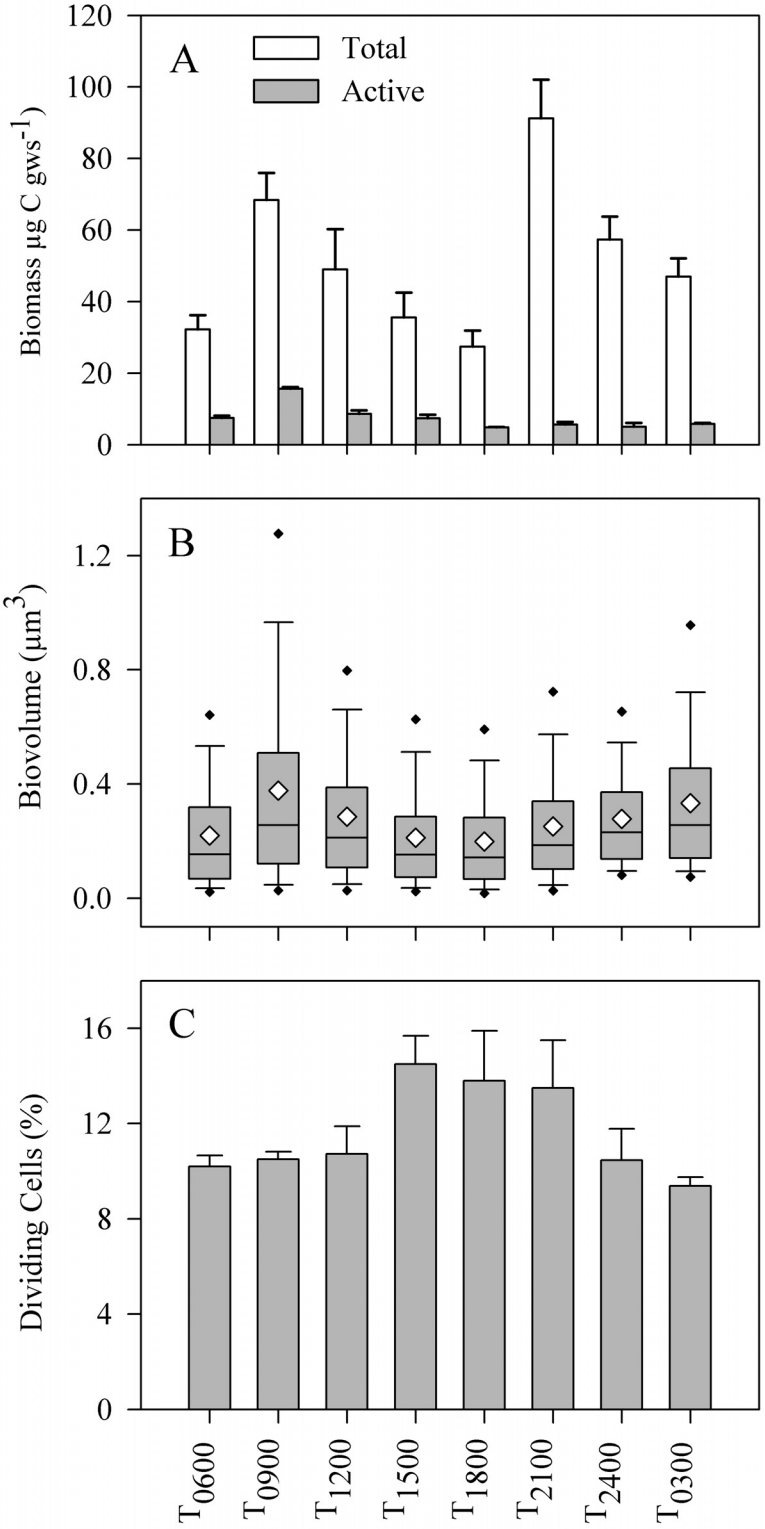
A
Total
Active
Biomass µg C gws-1)
120
100
80
60
40
20
0
B
Biovolume (µm3)
1.2
0.8
0.4
0.0
C
Dividing Cells (%)
16
12
8
4
0
T0600
T0900
T1200
T1500
T1800
T2100
T2400
T0300

**Figure 3.3.** Total concentration of A) large heterotrophic protists (>20 μm ESD); B) small heterotrophic protists (<20 μm ESD); and C) meiofauna in the top 1 cm of sediment throughout the study period. Bars show the standard deviation of the mean (n=3).

**Figure 3.3**

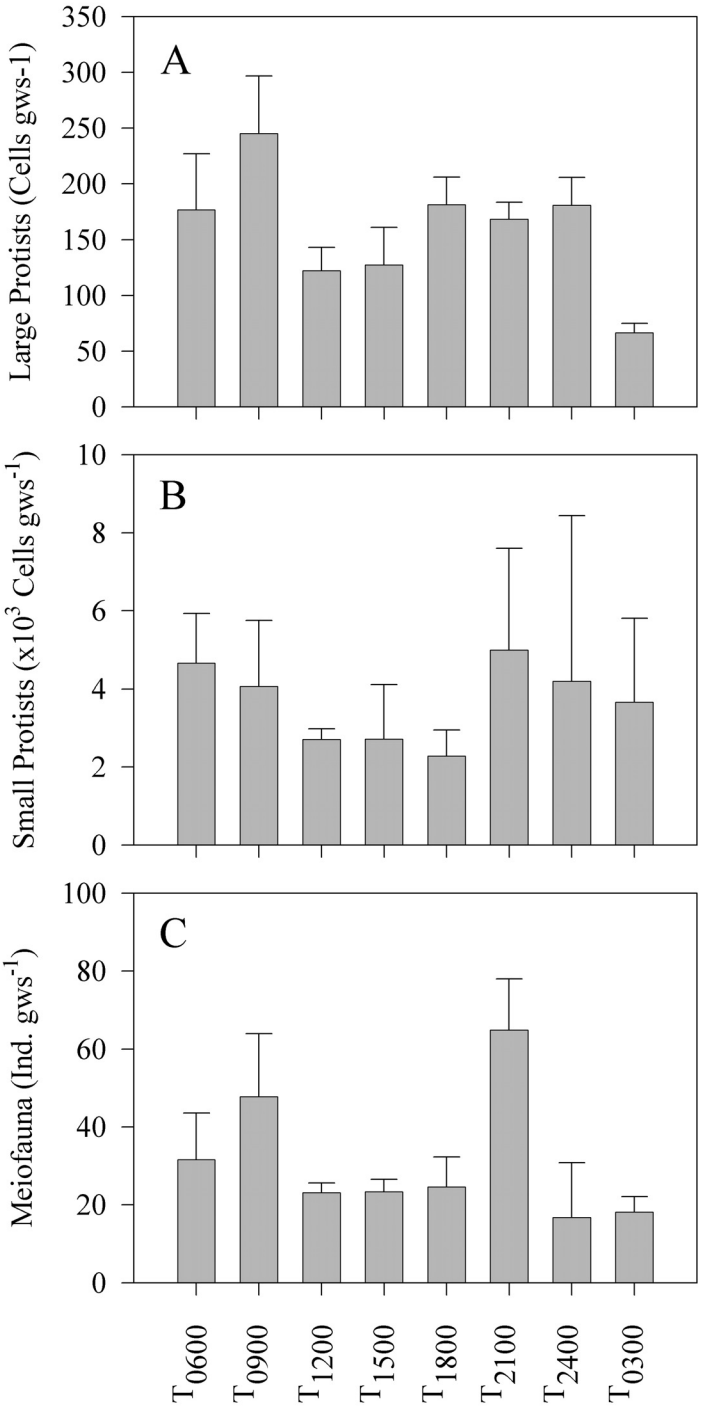
A
B
C
Large Protists (Cells gws-1)
Small Protists (x10$^3$ Cells gws$^{-1}$)
Meiofauna (Ind. gws$^{-1}$)
0
50
100
150
200
250
300
350
2
4
6
8
10
20
40
60
80
100
T$_{0600}$
T$_{0900}$
T$_{1200}$
T$_{1500}$
T$_{1800}$
T$_{2100}$
T$_{2400}$
T$_{0300}$

**Figure 3.4.** Total benthic biomass (top) at all sample times; bars show the standard error of the mean (n=3). The relative distribution of biomass between the major groups is shown (bottom).

**Figure 3.4**

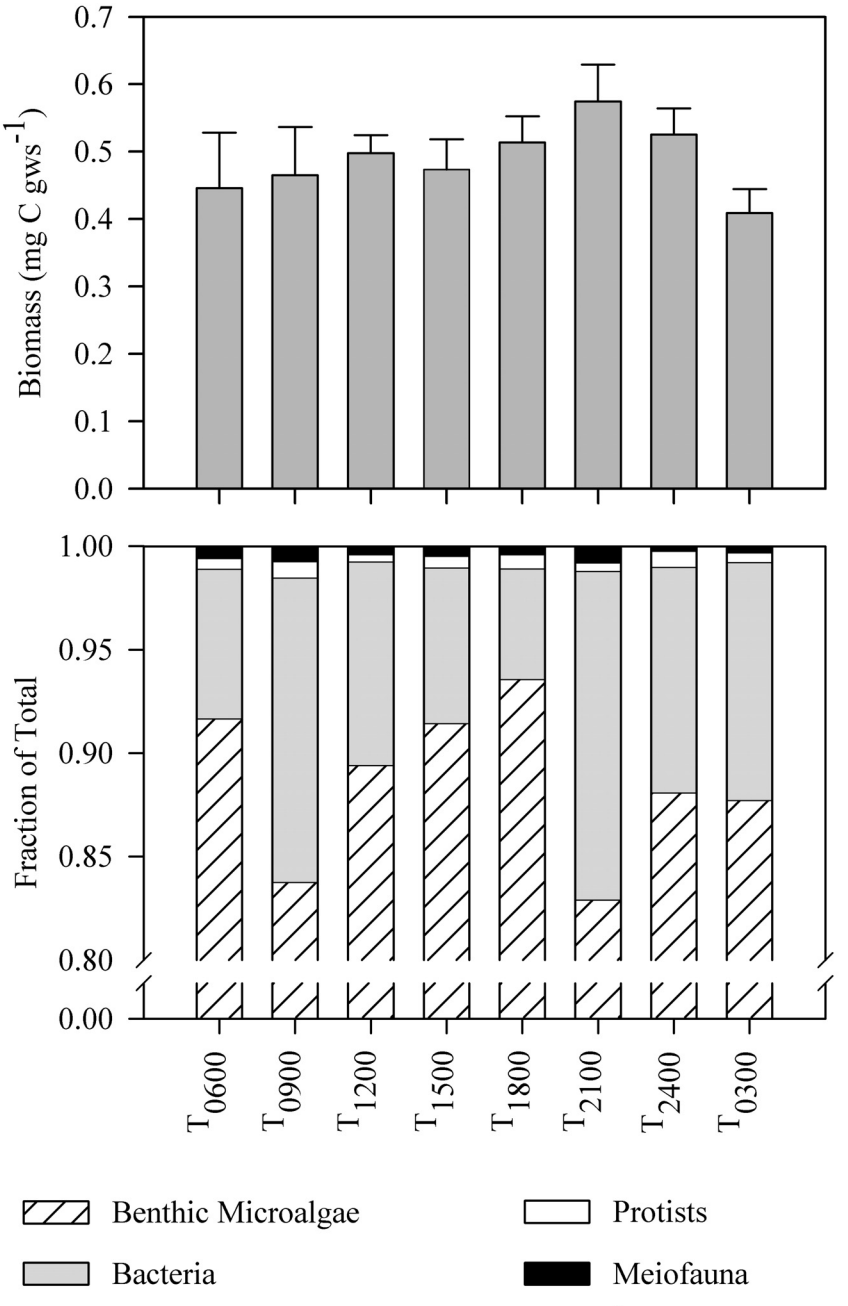
Biomass (mg C gws-1)
0.7
0.6
0.5
0.4
0.3
0.2
0.1
0.0
Fraction of Total
1.00
0.95
0.90
0.85
0.80
0.00
T0600
T0900
T1200
T1500
T1800
T2100
T2400
T0300
Benthic Microalgae
Protists
Bacteria
Meiofauna

**Figure 3.5.** Biomass ratios of: A) small and large protists to total bacteria; and B) Meiofauna to protists and to bacteria. Bars show the standard deviation of the mean (n=3).

**Figure 3.5**

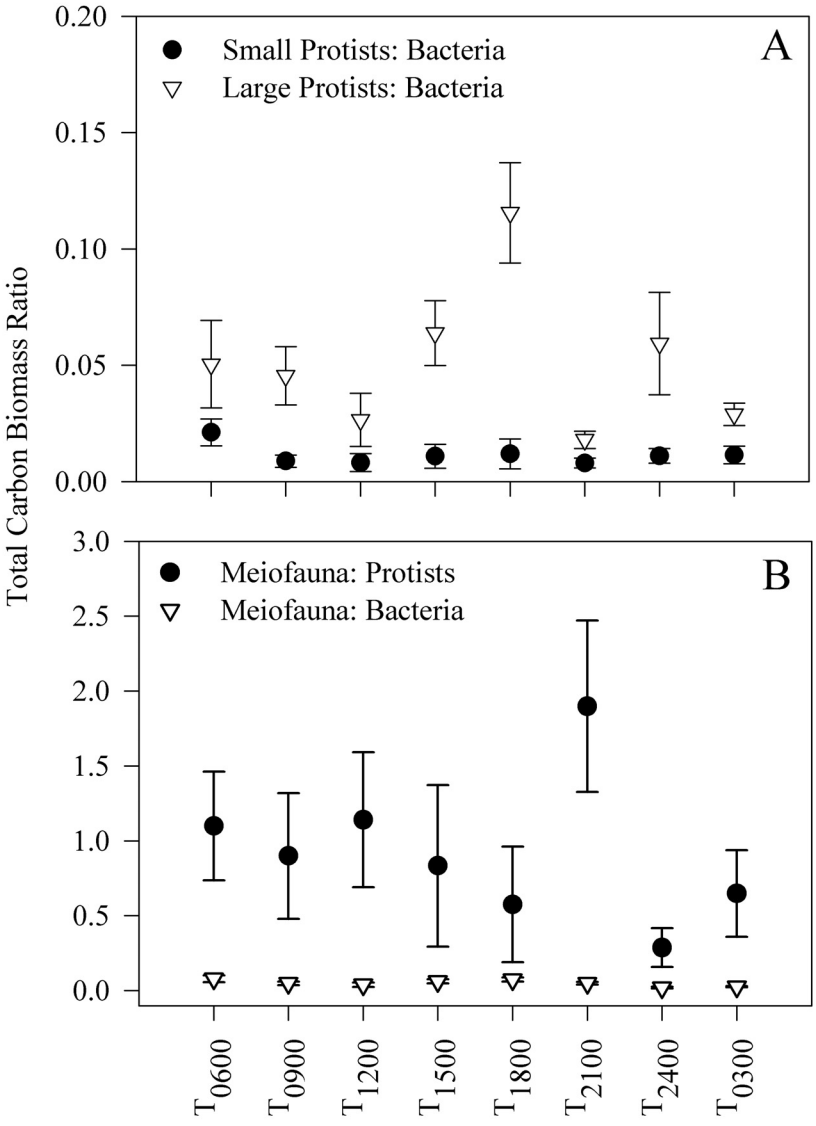
Total Carbon Biomass Ratio
0.20
0.15
0.10
0.05
0.00
Small Protists: Bacteria
Large Protists: Bacteria
A
3.0
2.5
2.0
1.5
1.0
0.5
0.0
Meiofauna: Protists
Meiofauna: Bacteria
B
T0600
T0900
T1200
T1500
T1800
T2100
T2400
T0300

**Figure 3.6.** A) Mean per capita bacterial ingestion rates and B) potential grazing impact on bacteria of the total heterotrophic protist community. Bars show the standard deviation of the mean (n=3).

**Figure 3.6**

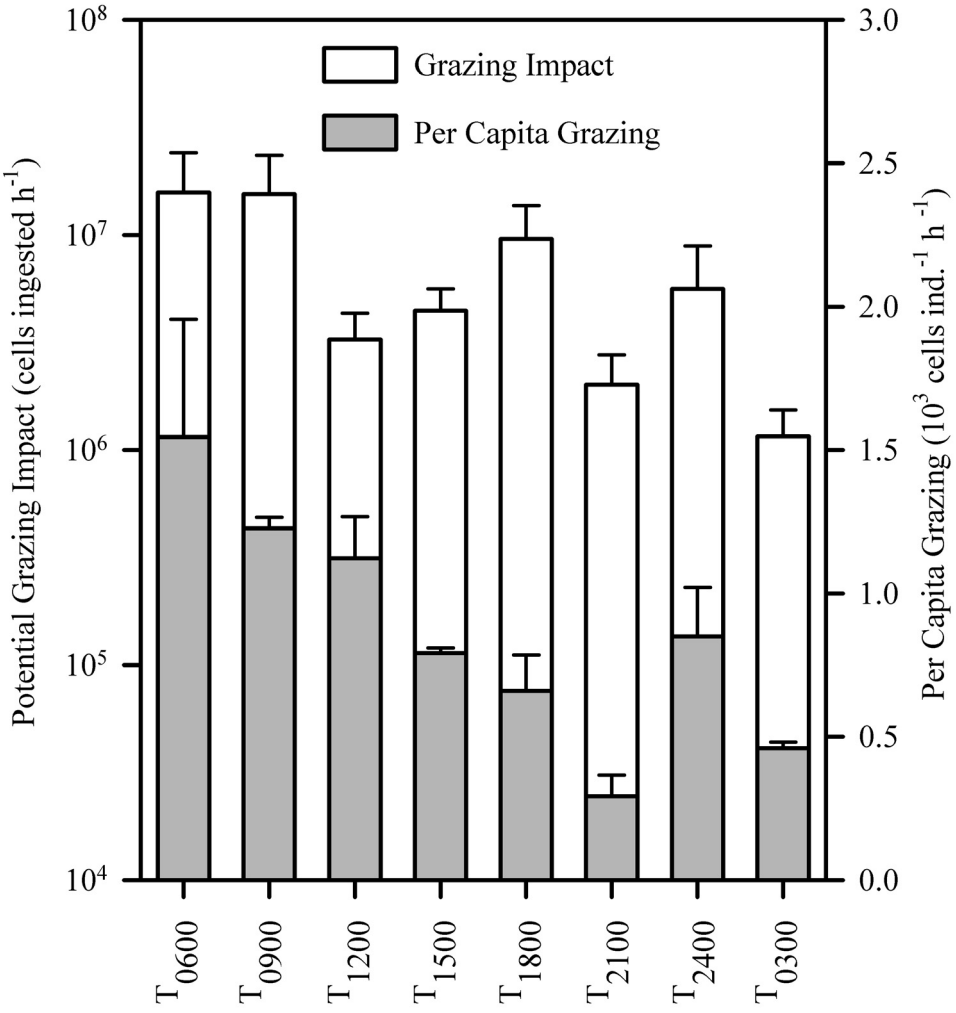
Grazing Impact
Per Capita Grazing
Potential Grazing Impact (cells ingested h-1)
Per Capita Grazing (10^3 cells ind.-1 h-1)
10^8
10^7
10^6
10^5
10^4
3.0
2.5
2.0
1.5
1.0
0.5
0.0
T0600
T0900
T1200
T1500
T1800
T2100
T2400
T0300

**Figure 3.7.** Results of model Simulation I - III indicating the protist:bacteria biomass ratio over 5 days. The threshold bacterial concentration ($T$) is set to 10 (top panel) and 20 μgC $gws^{-1}$ (bottom panel) in simulation I. In simulation II, the clearance rate of meiofauna consuming protists ($F_M$) in set at 0.05 (top panel) and 0.1 gws $\mu gC^{-1}$ $d^{-1}$ (bottom panel). Simulation III combines the smaller (top panel) and larger (bottom panel) $T$ and $F_M$ values. Simulations were conducted using both low (0.01 $d^{-1}$) and high (0.1 $d^{-1}$) bacterial growth rates. Bars indicate the standard deviation of the mean value of 1000 model runs.

**Figure 3.7**

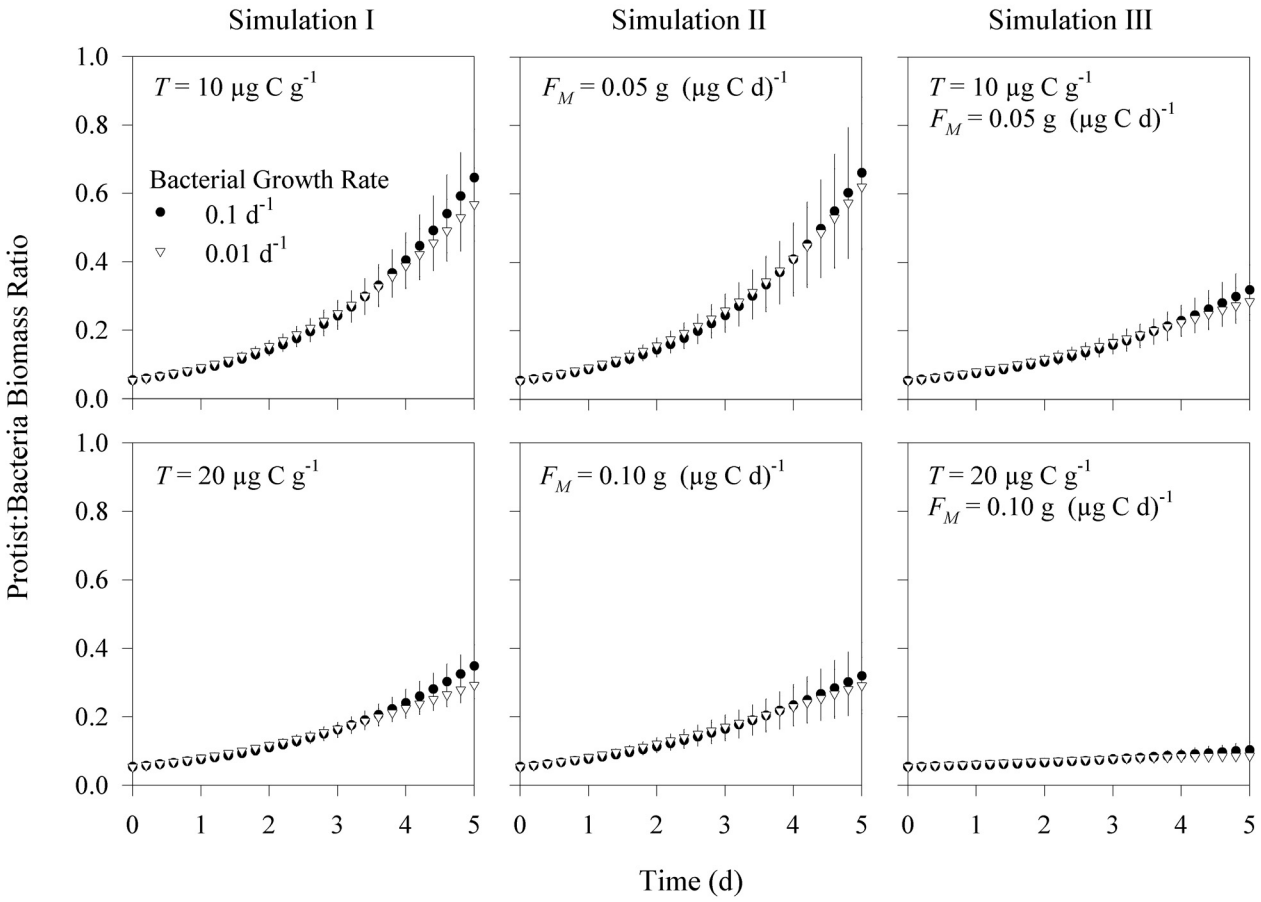
Simulation I
Simulation II
Simulation III
Protist:Bacteria Biomass Ratio
Time (d)
T = 10 µg C g-1
Bacterial Growth Rate
0.1 d-1
0.01 d-1
FM = 0.05 g (µg C d)-1
T = 10 µg C g-1
FM = 0.05 g (µg C d)-1
T = 20 µg C g-1
FM = 0.10 g (µg C d)-1
T = 20 µg C g-1
FM = 0.10 g (µg C d)-1
0.0
0.2
0.4
0.6
0.8
1.0
0
1
2
3
4
5

# CHAPTER 4

## DIEL DEPTH DISTRIBUTIONS OF MICROBENTHOS IN A TIDAL CREEK MUDFLAT: HIGH RESOLUTION MAPPING IN FLUORESCENTLY LABELED EMBEDDED CORES (FLEC)[4]

[4] M.R First and J.T. Hollibaugh
To be submitted to: *Hydrobiologia*

## ABSTRACT

We applied the Fluorescently Labeled Embedded Core (FLEC) technique to map distribution patterns of microbenthos in tidal creek sediments. Our aims were to determine if micro-scale distributions varied with environmental conditions and to test the null hypothesis that microbenthos are randomly distributed. Eight samples were collected at three hour intervals from an intertidal mudflat on Sapelo Island, Georgia, USA. Cores were incubated with CellTracker Green (CTG), a substrate that facilitates detection of cells that were metabolically active during incubation. Cores were embedded with epoxy and examined with laser scanning confocal microscopy. Image analysis was used to map the vertical locations of active microbenthos, which in these sediments consisted of benthic microalgae (BMA), ciliates, and flagellates. Microbenthos were abundant over the entire depth profiled (2 cm), although $O_2$ microelectrode profiles indicate that only the top 3 mm of sediment was oxygenated during high light (1000 μE $m^{-2}$ $s^{-1}$). More than 91% of organisms mapped were <22 μm in diameter and, based upon size and cell appearance, were BMA. Microbenthos accumulated in the top 1 mm at 0800 and 1100 h, corresponding to both low tide and high solar irradiation. This pattern conforms to BMA migratory rhythms determined by other methods. The standardized Morisita's Index of dispersion determined that CTG-positive objects were significantly clumped at all time points and at each of the 3 spatial scales examined. This clumping pattern likely results from the heterogeneous distribution of resources, such as prey items for phagotrophs and dissolved nutrients or growth substrates for autotrophs or heterotrophs.

## INTRODUCTION

Shallow-water sediments support high rates of primary production by benthic microalgae (BMA) that, in turn, are important to the sustenance and growth of both epibenthic and pelagic invertebrates (MacIntyre et al. 1996, Miller et al. 1996). Benthic production in creek sediments is several times higher than in other intertidal zones (e.g. vegetated marshes) and creek bed algae show little photoinhibition, even at high irradiance (Whitney & Darley 1983). Furthermore, creek bed algae appear to be less nitrogen-limited than BMA in other marsh habitats (Darley et al. 1981). However, creek-bed BMA experience significant short-term variability in many physical and chemical properties. As tidal creeks are emptied and filled, large fluctuations of insolation, temperature, and salinity occur over short time periods. These changes drive diel cycles of photosynthesis and vertical migrations of BMA (Pomeroy 1959, Gallagher & Daiber 1973, Easley et al. 2005). Daily feeding patterns of algivorous meiofauna are, consequently, linked to the location and density of their diatom prey and constrained by factors such as tolerance to high irradiance (Buffan-Dubau & Carman 2000). Variable production throughout the day also leads to a shifting depth of dissolved oxygen availability, restructuring the fine scale distributions of benthic protists (Fenchel & Jansson 1966, Böttcher et al. 2000, Gücker & Fischer 2003). Tidal flow and processes related to emersion-immersion cycles can drive the resuspension (Shimeta & Sisson 1999) and vertical migration patterns (Saburova et al. 2004) of benthic ciliates.

Diel vertical migration patterns of benthic diatoms are closely linked to tidal cycles. For example, benthic diatoms typically migrate to the sediment surface during the low tide emersion period (Pomeroy 1959). It is also during these periods that the herbivorous deposit-feeding crabs can have a substantial impact on BMA biomass (Teal 1962). While large portions of BMA

migrate to the illuminated sediment surface, some of the photosynthetic component remains below the sediment photic zone (Pinckney & Zingmark 1993). The activity of subsurface BMA is unclear. BMA in aphotic sediments may employ osmotrophy and use dissolved organic carbon to meet energy requirements (Saks 1983). Several techniques have been used to examine vertical migrations and distributions of BMA, including: microelectrode oxygen production profiles (Revsbech & Jørgensen 1983); sub-sectioning sediment cores; and capturing the vertically-migrating BMA on a porous tissue placed on the sediment surface (Williams 1963). Sectioning cores can yield highly-resolved depth distributions of benthic microorganisms (e.g. MacIntyre & Cullen 1995). The Cryolander technique (in which cores are frozen in liquid nitrogen and sectioned on a microtome) can obtain sections with a 0.2 mm vertical resolution (Kelly et al. 2001). However, determining spatial distribution patterns of microbenthos on a micrometer scale remains a challenge. Micro-scale associations of benthic organisms can provide insight into their ecology and physiology that may be overlooked or obscured by core sectioning.

The Fluorescently Labeled Embedded Core (FLEC) technique was developed to detect the life positions of protists and meiofauna in sediment with high spatial resolution (Bernhard et al. 2003). First, a sediment core is incubated with a non-fluorescent reagent that diffuses freely into cells. Upon reaction with non-specific cytosolic esterases, the reagent fluoresces and becomes non-diffusible across the cell membrane. Thus, cells with active enzymes and intact membranes will accumulate the fluorescent stain. Then, the core is chemically-fixed, serially dehydrated in ethanol, and finally embedded with low-viscosity epoxy. Horizontal or vertical sections can be cut and analyzed via laser scanning confocal microscopy to reveal the life-positions of benthic organisms. The FLEC technique also has the potential to resolve the

distributions of sediment organisms in both experimental manipulations and time-series observations.

We used the FLEC technique to examine the micro-scale changes in the distribution and associations of microbenthos (here, eukaryotes <200 μm, typically BMA, ciliates, and flagellates) in a tidal creek mudflat over a diel cycle. Nematodes were also occasionally encountered and were included in this analysis. The goal of this study was to observe the distribution of microbenthos over the course of a day and 1) determine if distributions vary with environmental conditions over the day; 2) determine if diel variation in the distributions of active microbenthos are consistent with typical migratory patterns of intertidal BMA; and 3) test the null hypothesis that active microbenthos are randomly distributed throughout the core.

## METHODS

**Sampling**. We sampled an area of mudflat in the bed of a tidal creek (Dean Creek) on Sapelo Island, a 67 $km^2$ barrier island on the Georgia coast, during 28 – 29 July, 2005. Dean Creek is a major tidal creek at the southern end of the island. The sampling location was a 2 $m^2$ area of intertidal mudflat adjacent to and immediately downstream of the Dean Creek Nature Trail bridge (31.3946° N, 81.2700° W), roughly 2 km from the mouth of the creek.

The plot was flat and level with no crab burrows and the sediment surface was uniform in color. Sediment was collected at 3 h intervals starting at 0600 h using an Ekman grab sampler (15 $cm^2$) lowered from the bridge (Fig. 4.1). Resampling the same area was avoided by marking the location where the grabs were taken on the bridge deck. Care was taken to deploy and retrieve the grab smoothly and slowly so that the sediment in the grab was minimally disturbed during the sampling. The sediment surface was not visibly disturbed and no cracks or folding

were observed. The sediment adjacent to the grab sampler walls (which was likely disrupted during the sampling) was not used in this experiment.

During the two weeks preceding the sampling, the average daily water temperature measured near the mouth of Dean Creek was 30.4 °C (range 29 – 32 °C) and no rainfall was recorded (http://gce-lter.marsci.uga.edu/lter). A Seabird CTD (SBE-19) was placed in the creek about 1 m away from the mudflat with its sensors at roughly the same depth as the sample plot. Water temperature, salinity, depth and Photosynthetically Active Radiation (PAR) were recorded every 60 s during the course of the sampling series. PAR was recorded with a 4π sensor, and detects light reflected from the sandy sediment surface. Thus, these measurements do not represent the absolute incident PAR on the surface. Rather, these measurement indicate the timing and relative intensity of incident PAR. Upon retrieval, the unopened sampler was carefully placed in a bucket filled with creek water (except during low tide when sediments were exposed) and transported to the lab at the University of Georgia Marine Institute within 10 min. As soon as the Ekman grab was opened, small sub-cores were collected for FLEC analysis and chlorophyll measurements as described below. Then samples for sediment porosity (~30 ml of the top 1 cm of sediment in the grab sampler, scraped with a plastic trowel) were taken. Porosity was determined as loss of water upon drying (24 h at 60°C) and converting water and sediment weight to volume based on density. Sediment grain size was determined by sieving the dried sediment and organic matter content was determined as weight loss after combustion of dried sediments at 550°C for 8 h. Chlorophyll *a* (Chl *a*) concentrations of the top 1 cm of sediment were determined by spectrophotometric analysis of acetone: methanol extracted pigments (Lorenzen 1967). A completed description of this procedure is available elsewhere (First and Hollibaugh, in press).

**Fluorescently Labeled Embedded Cores (FLEC).** Four sub-cores roughly 3 cm long were collected from each grab sample using 10 ml plastic syringes with the tips removed and beveled to reduce compaction upon coring. These cores were collected roughly 10 cm apart, then treated and analyzed separately. The 10 cm distance between cores is between 3 and 4 orders of magnitude greater than the size of organisms being investigated. Thus, we treat these cores as independent replicates that capture the small-scale variability within the mudflat examined (Heffner et al. 1996). Cotton was added to the syringe to support the sediment and rubber stoppers with holes capped the syringe and allowed for fluid movement. Filtered (0.22 μm) seawater (FSW, 0.5 ml) was added to the surface of samples taken when the site was flooded; no FSW was added when sediments were exposed at low tide. Microbenthos were labeled by adding of 25 μl of 1 mM of CellTracker Green chloromethylfluorescein diacetate (CTG – Invitrogen) solution to the top of the core. Syringes were placed upright in 100 ml containers filled with FSW to roughly 75% of the sediment height (allowing for movement of the CTG through the top 2 cm of sediment) and incubated for 2 h. Note that sample identifiers are based on the time that incubations were stopped, rather than when the core was collected. Cores collected during daylight hours were exposed to indirect sunlight through south-facing windows during the incubation and samples collected at night were covered to exclude light. CTG concentrations and the incubation duration were determined in preliminary experiments to be adequate for the CTG to permeate into the sediment, be taken up and transformed under the conditions encountered during this study. Cores were then fixed with 8% electron microscopy grade glutaraldehyde and kept upright in the dark at 4 ± 2 °C until further processing.

Fixed cores were progressively dehydrated with FSW: ethanol (10%, 30%, 50%, 80%, and three rinses of 100% ethanol) by allowing a volume roughly 3X the sediment volume to pass through the core. Anhydrous cupric sulfate was used to dehydrate the 100% ethanol used for the final rinses. Care was taken to always keep sediments submerged. Equal weights of a two-part, low viscosity epoxy resin (Embed-It™, Polysciences) were mixed with 100% dehydrated ethanol and used for one rinse. Finally, two rinses of 100% epoxy (each equal to the volume of the sediment) were passed through the sediment core. Flow was stopped before all of the second rinse had passed though sediments, then the epoxy was polymerized at 50°C for 72 h. The solidified cores were stored at room temperature away from light. At least three of the four sub-cores from each grab sample survived the embedding process and polymerized.

Embedded cores were cut along the long axis with a thin-blade diamond saw. Both halves of the split core were polished with progressively finer grit (up to 600 grit) to produce a flat, uniform surface. The polished surface was examined at 100X magnification using a Leica Laser Scanning Confocal Microscope (LSCM) with excitation at 488 nm by an argon/krypton laser (dichroic mirror: 500 nm, range: 510 – 525 nm, pinhole: 1.6X airy). The high sand content of the sediment cores restricted laser light penetration to ~20 μm into the exposed face. Infrared multiphoton illumination did not allow for deeper penetration into the core, so we did not adopt this alternative method. The location of the maximum pixel value encountered in 14 to 16 images taken along the axis of penetration was used to determine the position of active cells. Image editing software (Adobe Photoshop) was used to adjust the brightness and contrast of images to equalize minor differences in display range. The three dimensional images were flattened along the axis of laser light penetration to yield a two dimensional map. This third axis contained much less spatial information (~20 μm) and flattening did not cause significant overlapping or

obscuring of objects. The map images were then assembled to form a 1.5 x 20 mm profile along the core. The top of the sediment core was often uneven. Therefore, we defined the position of the $10^{th}$ fluorescent object encountered along a vertical scan from the highest point of the sediment surface as zero depth and discarded the objects above this depth. One vertical profile was assembled for each core. The dimensions, area and vertical position of fluorescent objects >12 $\mu m^2$ (~3.8 μm equivalent circular diameter – ECD) were measured with image analysis software (ImagePro Plus 4.1). This size range included larger organisms, such as nematodes. Thus, the term "microbenthos" as used here includes nematodes, even though they are generally referred to as meiofauna.

**Analysis.** Microbenthos distributions were analyzed by two methods. First, the two-dimensional dispersion of microbenthos was evaluated via Morisita's standardized index of dispersion ($I_M$) (Krebs 1989). This index indicates whether the population is randomly, uniformly, or unevenly (clumped or patchily) dispersed. When $1>I_M>0.5$, the population is significantly under-dispersed (clumped) according to a $\chi^2$ distribution (alpha = 0.025, *df* = number of quadrats – 1). Likewise, when $-1<I_M<-0.5$, the population distribution is significantly over-dispersed (uniform); and when $0.5> I_M>-0.5$ the population is randomly dispersed (Krebs 1989). Each profile was trimmed by 0.25 mm on each side to account for the slight lateral drift of the microscope as images were collected along the long axis of the core, yielding a 1 x 20 mm profile. Morisita's index was calculated for each profile using quadrat sizes of 0.25 x 0.25 mm, 0.5 x 0.5 mm, and 1.0 x 1.0 mm, yielding 80, 40, or 20 quadrats for the entire profile, respectively. A computer algorithm to sort objects to quadrants and to perform calculations and statistical analyses was written in

MatLab 6.1. The average $I_M$ was calculated from the three profiles at each time point for each quadrat size.

Second, the relative inequality of the depth distribution was calculated by the Gini Coefficient of Inequality (*G*), which is a non-parametric measure of distribution unevenness (Dixon et al. 1987, Dixon 1988):

$$G = \frac{1}{\overline{X}\, n(n-1)} \sum_{i=1}^{n} (2i - n - 1) X_i$$

Where *X* is the number of objects in depth bin *i* (sorted from the most populated to least populated bin), and *n* is the sample size. The Gini Coefficient is 0 for a perfectly even distribution and approaches perfect inequality at 1. The degree of unevenness in depth distribution was based upon the mean percent difference between the observed number of microbenthos in each depth interval and the expected number in each interval assuming an even distribution with depth. Unlike Morisita's index of dispersion, the Gini coefficient only measures the distribution along one dimension (depth); therefore, there was no need to trim the profiles as was done for the two dimensional analysis described above. All data from each time point were pooled and objects were binned into 50 equal depth intervals. Bootstrapping analysis (2000 replicates) was used to calculate the standard error of the bias-corrected Gini Coefficient (Stats Direct 2.5). The mean depth of the population was calculated from the positions of all microbenthos observed in each profile.

**Oxygen Profiles.** A second set of sediment cores (1.5 cm diameter syringe, ~3 cm depth) was collected from the site at low tide on 30 July, 2005. These cores were stored at 24 ± 3 °C under a natural light regime and transported to Athens, GA for analysis. Oxygen concentration profiles in the cores were determined 2 d later. A microelectrode with a 50 μm tip (Revsbech & Jørgensen

1983) was lowered through the sediment at 100 μm intervals after the sediment was equilibrated in the light (~1000 μE $m^{-2}$ $s^{-1}$) or darkness for at least 10 min. The electrode was calibrated at $O_2$ saturation and at anoxia by measuring the stable voltage reached after bubbling FSW with air, or at ~3 cm sediment depth in a core, respectively. Estimates of $O_2$ concentration (μM) were calculated as linear interpolations between the voltage at zero $O_2$ and at calculated $O_2$ saturation at the salinity and temperature of FSW.

## RESULTS

Salinity at the study site fluctuated between 19 and 24 and temperature ranged from 29.0 to 34.6°C over the study period (Fig. 4.1A); the water depth over the sampling site ranged from 0 to 1.2 m (Fig. 4.1B). Sediments were exposed once during daylight hours (0925 to 1204 h) and again during the night (2340 to 0026 h). The top 1 cm of sediment had a density of 1.46 g $cm^{-3}$, mean grain size of 0.26 mm (± 0.11 SD), porosity of 0.41 (± 0.12 SD), and an organic matter content of 2.0 % (± 0.4 SD). Microelectrode profiles revealed supersaturating $O_2$ concentrations at about 1 mm depth during high illumination (Fig. 4.2). However, no $O_2$ was detected below 3 mm depth at high light and at low light, $O_2$ at 1 mm was < 7% of saturation and was not detectable below 2 mm.

The FLEC technique yielded high contrast images of CTG-positive cells in all cores examined (Fig. 4.3). At all time points, the majority of microbenthos (>90 % of total) mapped in FLEC depth profiles were smaller than 22 μm ECD (Fig. 4.4). This size range of organisms is mostly composed of small diatoms, flagellates and small ciliates (First and Hollibaugh, in press). Mean Chl *a* concentration ranged from 13.1 (±1.3 SD) to 17.5 (±1.4 SD) μg $cm^{-3}$, whereas the concentration of microbenthos per profile volume (1 cm x 1.5 mm x 20 μm) varied from 0.44 (±

0.03 SD) to 2.4 (±0.35 SD) x $10^6$ individuals $cm^{-3}$ in the top 1 cm of FLEC profiles (Fig. 4.5). The ratio of Chl *a* to total cells ranged from 6.7 to 38 pg Chl *a* $cell^{-1}$, with a mean of 19 pg Chl *a* $cell^{-1}$. Chl *a* varied <17% from the mean of all time points; whereas, CTG-positive cell concentrations varied >100% from the mean of all time points. There was no significant linear correlation between the two measurements (linear regression; adjusted $R^2 = 0.07$, $F_{(1,7)} = 1.5$, $p = 0.264$).

Although there was no measurable $O_2$ at depths >3 mm, active cells were found over the entire 20 mm profile (Fig. 4.6). Microbenthos were non-randomly and unevenly dispersed at all time points in all replicate cores at all spatial scales examined. The mean Morisita index ($I_M$) was >0.5 at all time points, indicating that microbenthos were significantly clumped. Also, $I_M$ was >0.5 for all quadrat sizes examined and increased with increasing quadrat size (Fig. 4.7). The only exception to this trend was in one profile from the 0800 h sample, where the population was determined to be randomly distributed when analyzed at 1.0 $mm^2$ quadrat size. This point was omitted when calculating the average $I_M$ for this time point.

Data from the three cores for each sample were pooled for analysis of depth distributions of microbenthos (average *n*=2301, range: 772–5043). Microbenthos were most abundant near the surface at 0800 h and 1100 h, corresponding to a pattern of migration to the sediment surface during tidal emersion and high light. A subsurface maximum between 12 – 14 mm depth was also present at 1100 h. Microbenthos were depleted from the top 3 mm during the afternoon and into the evening, with subsurface maxima deeper in the sediment (Fig. 4.8). At 0200 h, microbenthos were most abundant at the sediment surface. At 0500 h microbenthos were depleted from the top 6 mm of sediment.

The relative unevenness (Gini coefficient) ranged from 0.15 (± 0.01 SE) to 0.31 (± 0.03) throughout the sampling period, with organisms most equally distributed at 1700 and 2300 h (Fig. 4.9). Usually, as the mean depth of the microbenthos population increases, organisms become more equally distributed. The higher Gini coefficient with lower mean depth indicates that sediment populations are unevenly concentrated near the sediment surface. However, the 0500 h profiles do not follow this trend as microbenthos are unevenly distributed with accumulations in deeper sediment horizons.

## DISCUSSION

Despite the shallow depth of oxygen penetration, active microbenthos were found throughout the entire depth examined at all time points. Because the fluorescent stain used in this study only detects enzymatically active microbenthos, the accumulation in deeper sediment horizons cannot be explained as the burial of dead or inactive cells. The presence of CTG-positive cells throughout the depth examined also indicates that CTG was able to permeate completely through at least the upper 20 mm of the core and react within the incubation time.

The Chl *a* concentration encountered in this study were slightly higher than other intertidal creek beds in subtropical salt marshes (Pinckney & Zingmark 1993, Velasquez 2005). We found that BMA biomass, as determined by Chl *a* extraction or microscopy accounted for >80% of total microbenthic biomass (First and Hollibaugh, in press). The FLEC images are consistent with this, as most CTG-labeled cells could be identified as pennate diatoms (See Fig. 3). Microbenthos accumulated at the surface during the morning (0800 and 1100 h), consistent with previous reports indicating that BMA migrate to the sediment surface during high illumination (Pomeroy 1959). The surface layers were relatively depleted of BMA during

afternoon sampling when tidal flooding resulted in lower irradiance at the sediment surface. Thus, the vertical distribution patterns of BMA observed in these cores conformed to typical migratory patterns in tidal creek sediments.

Overall, microbenthos showed a clumped distribution in all sample profiles. In sandy salt marsh sediments, the aggregation of microbenthos in interstitial spaces might contribute to the clumped dispersion patterns. However, the quadrat sizes used in this analysis were equal to or larger than the mean grain size. The index of dispersion increased with increasing quadrat size (see Fig. 7), indicating that microbenthos were more unevenly dispersed at larger spatial scales. If the dispersion patterns were solely defined by interstitial spaces, then the dispersion would become more uniform with larger quadrats. Instead, the observed distribution of microbenthos is likely driven by aggregation near favorable microhabitats. Sediments are heterogeneous environments with sharp resource gradients; the uneven distribution of the microbenthic community is likely a response to these resource gradients. Symbiotic associations between organisms also result in a clumping of microbial populations. For example, benthic eukaryotes aggregate near sulfide-oxidizing bacteria, perhaps as a refuge from high sulfide concentrations (Bernhard et al. 2003). Also, microbial mats and consortia can lead to highly localized zones of sediment microbial biomass (Boetius et al. 2000, Stal 2001).

Heterogeneous microbial distributions are observed even in less structured environments than sediments, for example the pelagic ocean. Colonies of phytoplankton can support high production of heterotrophic bacteria; abundance of bactivorous protists and microinvertebrates in these aggregates are several orders of magnitude greater than the surrounding environment (Alldredge & Silver 1988, Alldredge & Gotschalk 1990, Sheridan et al. 2002). These particulates are also enriched in nutrients (Shanks & Trent 1979). In particulate “hot spots”, the combined

impact of bacterial exoenzymes speeds the degradation of particulate matter and all cells in the proximity that can take up labile dissolved organic carbon benefit (Kiorboe & Jackson 2001).

The presence of high densities of BMA in subsurface sediments as we found here is counterintuitive, yet commonly observed (see Pinckney & Zingmark 1993, and references therein). Because of the high light attenuation, BMA found below the top 1 – 2 mm of sediment are unable to obtain light for photosynthesis, and are described functionally as 'photosynthetically inactive biomass' (Kelly et al. 2001). Diel vertical migrations of BMA are commonly observed in intertidal sediments. The migratory rhythms may function to deter resuspension by tidal flow or predation by surface grazers (MacIntyre et al. 1996). BMA might also migrate into the sediments to access inorganic nutrients (Kingston 2002). Regardless, subsurface BMA may comprise a large portion of total chlorophyll, and explain the constancy of total chlorophyll amid large variations in the photosynthetically active surface BMA (Kelly et al. 2001). Chl *a* concentrations were much more stable than the concentration of CTG-positive cells, which varied greater than 100% of the mean value. The poor correlation between CTG positive cells and Chl *a* observed here could be a result of a high concentration of inactive BMA. The high Chl *a* cell$^{-1}$ ratio, relative to other diatoms (e.g. Eker-Develi et al. 2006), also suggests that much of the Chl *a* from these sediments is from inactive cells.

The abundance of BMA and other microorganisms found at depth in sediments suggests that most microbenthos can tolerate anoxic and sulfidic sediments. However, $O_2$ concentrations measured in cores in the lab may not reflect the availability of $O_2$ to subsurface aerobic microbes in the field. For example, tidal forcing may increase the depth of $O_2$ penetration (Rusch et al. 2001) and the $O_2$ concentrations determined in sediment cores may be lower than available in the field during tidal flow. Likewise, bioturbation by microbenthos can extend the depth of $O_2$

penetration (Glud & Fenchel 1999, Pike et al. 2001) and allow aerobic respiration. Alternatively, the abundance of aerobic organisms in anoxic sediments may demonstrate spatial heterogeneity of chemical gradients in sediments that is not captured by microelectrode profiling (Bernhard et al. 2003). For example, the movement of meiofauna through anoxic sediments can allow for the highly localized transport of solutes (Pike et al. 2001).

The mean depth of microbenthos varied throughout the day. In general, when the depth was greater than 10 mm (half of the core depth), the vertical distribution became more even. Restated, microbenthos were generally unevenly distributed towards the upper half of the core at most time points. However, one exception to this was at 0500 h, when microbenthos were unevenly distributed towards the bottom half of the core. This sampling time occurred several hours into flood tide. Therefore, tidal advection may have resuspended microbenthos into the water column, causing a depletion of microbenthos from the surface sediments. The timing and magnitude of microbenthos advection into the water column can be critically important for water column filter feeders (Thoresen 2004).

The FLEC technique was originally designed and applied to deep sea microbial mats in fine sediments (Bernhard and Bowser 1996, Bernhard et al. 2003). The application of this technique to salt marsh sediments presented several challenges. First, the dehydration series necessary for embedding cores in epoxy also extracts Chl *a* and, therefore, autofluorescence could not be used to identify CTG positive cells as BMA. Second, sandy sediments limit the depth of optical penetration into the sediment core. This limits the ability to identify and categorize CTG-positive organisms in the FLEC profiles. Many of the organisms could be identified as pennate diatoms by their morphology; other eukaryotes such as ciliates can also be roughly identified by shape. However, there is a potential for misidentifying objects, especially

for organisms longer or wider than 20 μm, as cell orientation relative to the plane of observation can disguise true shape. Therefore, we only used the two-dimensional size to categorize objects. More detailed morphological examinations should be possible in fine-grained sediments where the depth of laser light penetration into the core is extended. Nematodes could be identified by size, even when they were sectioned along a transverse plane (See Fig. 3D). The embedded cores can also be sectioned horizontally to reveal the planar distribution of organisms at a chosen depth.

The spatial distribution of organisms is a fundamental parameter of many ecological processes. The relative distance between individuals reveals competitive and synergistic associations, as well as affecting resource partitioning. Thus analysis of the micro-scale distributions of microbenthos can provide insight into the physiology and ecology of sediment microbial communities.

## ACKNOWLEDGEMENTS

This work was supported by NSF Georgia Coastal Ecosystems LTER grant (OCE-9982133). J. Bernhard critically reviewed an earlier draft of this manuscript. S. Joye was generous with the use of her microelectrode probes and provided guidance for this work. We are grateful for the hospitality and logistical support of J. Garbisch and M. Price at the University of Georgia Marine Institute (UGAMI). J. Bernhard, M. Farmer, S. Joye and C. Meile provided guidance on the design of this project. D. Di Iorio and P. McKay (Dept. Marine Sci., UGA) assisted with the CTD. C. Fleisher (Geology Dept., UGA) advised and assisted on the diamond saw operation. C. Keith and J. Shields (Center for Ultrastructural Research, UGA) assisted with confocal

microscope operation. M.R.F. was supported by a UGA Graduate School Assistantship. This is contribution no. 957 from UGAMI.

## REFERENCES


Alldredge AL, Gotschalk CC (1990) The relative contribution of marine snow of different origins to biological processes in coastal waters. Cont Shelf Res 10:41-58

Alldredge AL, Silver MW (1988) Characteristics, dynamics and significance of marine snow. Progr Oceanogr 20:41-82

Bernhard JM, Bowser SS (1996) Novel epifluorescence microscopy method to determine life position of foraminifera in sediments. J Micropalaeont 15:68-68

Bernhard JM, Visscher PT, Bowser SS (2003) Submillimeter life positions of bacteria, protists, and metazoans in laminated sediments of the Santa Barbara Basin. Limnol Oceanogr 48:813-828

Boetius A, Ravenschlag K, Schubert CJ, Rickert D, Widdel F, Gieseke A, Amann R, Jørgensen BB, Witte U, Pfannkuche O (2000) A marine microbial consortium apparently mediating anaerobic oxidation of methane. Nature 407:623-626

Böttcher ME, Hespenheide B, Llobet-Brossa E, Beardsley C, Larsen O, Schramm A, Wieland A, Böttcher G, Berninger UG, Amann R (2000) The biogeochemistry, stable isotope geochemistry, and microbial community structure of a temperate intertidal mudflat: an integrated study. Cont Shelf Res 20:1749-1769

Buffan-Dubau E, Carman KR (2000) Diel feeding behavior of meiofauna and their relationships with microalgal resources. Limnol Oceanogr 45:381-395

Darley WM, Montague CL, Plumley FG, Sage WW, Psalidas AT (1981) Factors limiting edaphic algal biomass and productivity in a Georgia salt marsh. J Phycol 17:122-128

Dixon P (1988) Correction. Ecology 69:1307-1307

Dixon PM, Weiner J, Mitchell-Olds T, Woodley R (1987) Bootstrapping the Gini coefficient of inequality. Ecology 68:1548-1551

Easley JT, Hymel SN, Plante CJ (2005) Temporal patterns of benthic microalgal migration on a semi-protected beach. Estuar Coast Shelf Sci 64:486-496

Eker-Develi E, Kideys AE, Tugrul S (2006) Effect of nutrients on culture dynamics of marine phytoplankton. Aquat Sci 68:28-39

Fenchel T, Jansson B-O (1966) On the vertical distribution of the microfauna in the sediments of a brackish-water beach. Ophelia 3:161-177

Gallagher JL, Daiber FC (1973) Diel rhythms in edaphic community metabolism in a Delaware salt marsh. Ecology 54:1160-1163

Glud RN, Fenchel T (1999) The importance of ciliates for interstitial solute transport in benthic communities. Mar Ecol Prog Ser 186:87-93

Gücker B, Fischer H (2003) Flagellate and ciliate distribution in sediments of a lowland river: relationships with environmental gradients and bacteria. Aquat Microb Ecol 31:67-76

Heffner RA, Butler MJ, Reilly CK (1996) Pseudoreplication revisited. Ecology 77:2558-2562

Kelly JA, Honeywill C, Paterson DM (2001) Microscale analysis of chlorophyll-*a* in cohesive, intertidal sediments: the implications of microphytobenthos distribution. J Mar Biol Assoc U K 81:151-162

Kingston MB (2002) Effect of subsurface nutrient supplies on the vertical migration of *Euglena proxima* (Euglenophyta). J Phycol 38:872-880

Kiørboe T, Jackson GA (2001) Marine snow, organic solute plumes, and optimal chemosensory behavior of bacteria. Limnol Oceanogr 46:1309-1318

Krebs CJ (1989) Ecological methodology. Harper & Row, New York

Lorenzen CJ (1967) Determination of chlorophyll and pheo-pigments: spectrophotometric equations. Limnol Oceanogr 12:343-346

MacIntyre HL, Cullen JJ (1995) Fine-scale vertical resolution of chlorophyll and photosynthetic parameters in shallow-water benthos. Mar Ecol Progr Ser 122:227-237

MacIntyre HL, Geider RJ, Miller DC (1996) Microphytobenthos: the ecological role of the "secret garden" of unvegetated, shallow-water marine habitats. I. distribution, abundance and primary production. Estuaries 19:186-201

Miller DC, Geider RJ, MacIntyre HL (1996) Microphytobenthos: The ecological role of the "secret garden" of unvegetated, shallow-water marine habitats. II. role in sediment stability and shallow-water food webs. Estuaries 19:202-212

Pike J, Bernhard JM, Moreton SG, Butler IB (2001) Microbioirrigation of marine sediments in dysoxic environments: implications for early sediment fabric formation and diagenetic processes. Geology 29:923-926

Pinckney J, Zingmark RG (1993) Biomass and production of benthic microalgal communities in estuarine habitats. Estuaries 16:887-897

Pomeroy LR (1959) Algal productivity in salt marshes of Georgia. Limnol Oceanogr 4:386-397

Revsbech NP, Jørgensen BB (1983) Photosynthesis of benthic microflora measured with high spatial resolution by the oxygen microprofile method: capabilities and limitations of the method. Limnol Oceanogr 28:749-756

Rusch A, Forster S, Huettel M (2001) Bacteria, diatoms and detritus in an intertidal sandflat subject to advective transport across the water-sediment interface. Biogeochemistry 55:1-27

Saburova MA, Azovskii AI, Polikarpov IG (2004) A comparative analysis of the vertical migrations of interstitial ciliates in different types of sediments. Oceanology 44:535-547

Saks NM (1983) Primary production and heterotrophy of a pennate and a centric salt-marsh diatom. Mar Biol 76:241-246

Shanks AL, Trent JD (1979) Marine snow: microscale nutrient patches. Limnol Oceanogr 24:850-854

Sheridan CC, Steinberg DK, Kling GW (2002) The microbial and metazoan community associated with colonies of *Trichodesmiu*m spp,.: a quantitative survey. J Plankton Res 24:913-922

Shimeta J, Sisson JD (1999) Taxon-specific tidal resuspension of protists into the subtidal benthic boundary layer of a coastal embayment. Mar Ecol Prog Ser 177:51-62

Stal LJ (2001) Coastal microbial mats: the physiology of a small-scale ecosystem. S Afr J Bot 67:399-410

Teal JM (1962) Energy flow in salt marsh ecosystem of Georgia. Ecology 43:614-624

Thoresen M (2004) Temporal and spatial variation in seston available to oysters and the contribution of benthic diatoms to their diet in the Duplin River, Georgia. PhD dissertation, University of Georgia, Athens, GA

Velasquez LE (2005) Benthic primary production in coastal salt marsh systems. MS Thesis, University of Georgia, Athens, GA

Whitney DE, Darley WM (1983) Effect of light intensity upon salt marsh benthic microalgal photosynthesis. Mar Biol 75:249-252

Williams RB (1963) Use of netting to collect motile benthic algae. Limnol Oceanogr 8:360-361

**Figure 4.1.** (A) Temperature, salinity, (B) water depth and Photosynthetically Active Radiation (PAR) in Dean Creek, Sapelo Island, Georgia between 28 – 29 Jul 2005. Timeline bars show CTG incubation durations.

**Figure 4.1**

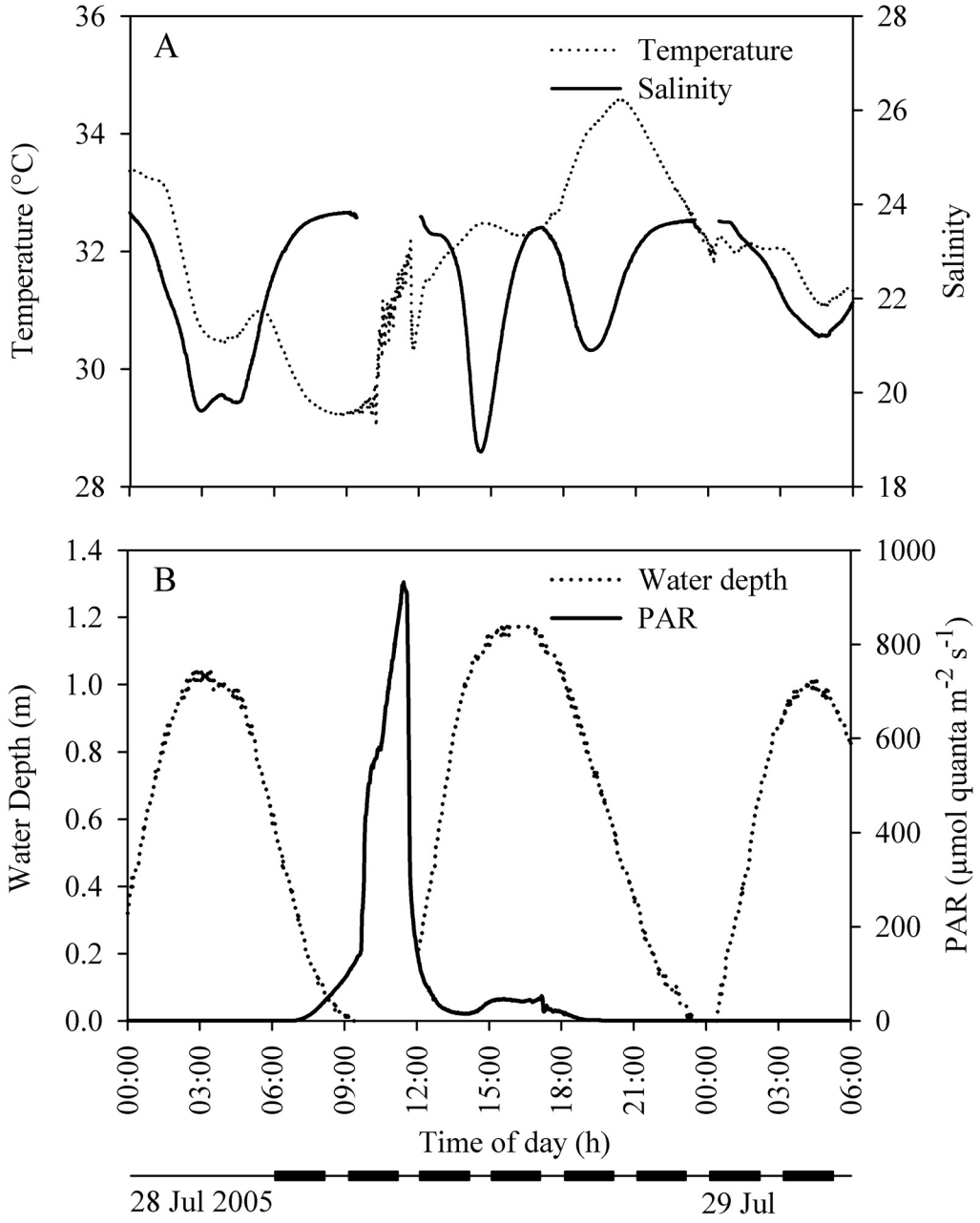
A
Temperature
Salinity
Temperature (°C)
Salinity
36
34
32
30
28
28
26
24
22
20
18
B
Water depth
PAR
Water Depth (m)
PAR (µmol quanta m-2 s-1)
1.4
1.2
1.0
0.8
0.6
0.4
0.2
0.0
1000
800
600
400
200
0
00:00
03:00
06:00
09:00
12:00
15:00
18:00
21:00
00:00
03:00
06:00
Time of day (h)
28 Jul 2005
29 Jul

**Figure 4.2.** Oxygen concentration profiles in light and dark-adapted Dean Creek sediment cores. The vertical line indicates the dissolved $O_2$ saturation at *in situ* salinity and temperature. Mean (line and points) and standard error (bars) are based on a total of 8 profiles from 2 cores.

**Figure 4.2**

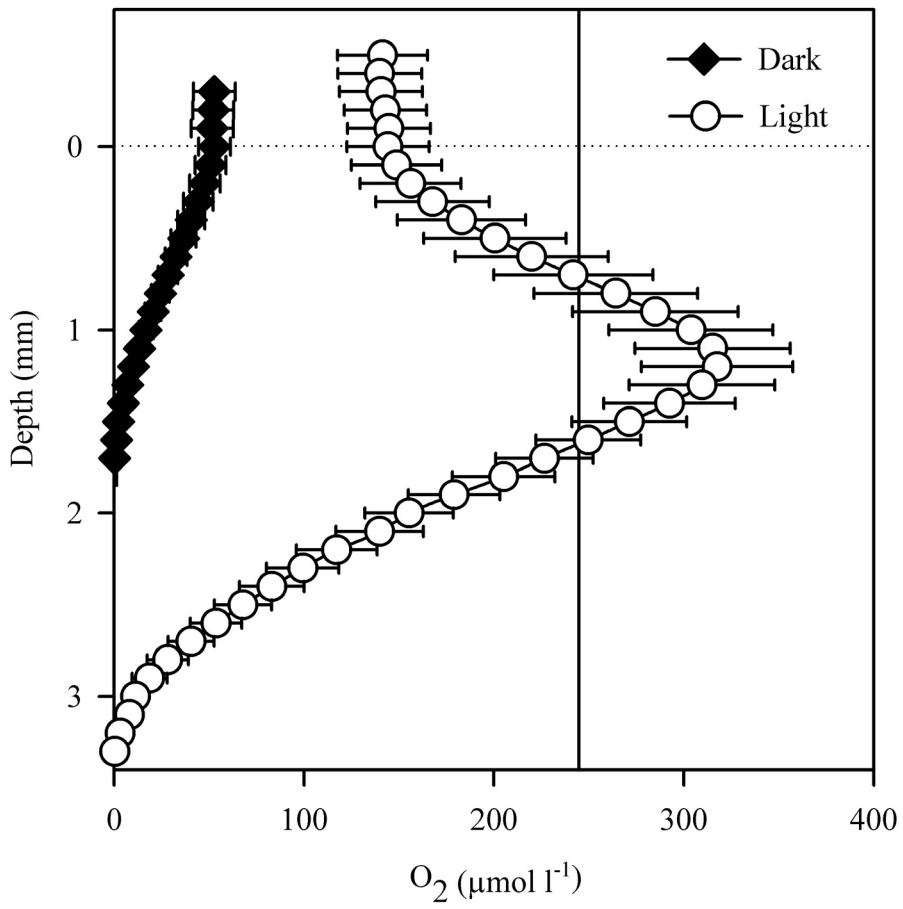

**Figure 4.3.** Images of microbenthos in FLEC cores. (A) Microbenthos clustered at the sediment surface, denoted by a dotted line, scale bar = 300 μm. Examples of microbenthos: (B) a pennate diatom, (C) a ciliate, and (D) a portion of a nematode. Scale bars = 100 μm. Images were inverted for clarity (i.e. dark objects were fluorescent).

**Figure 4.3**

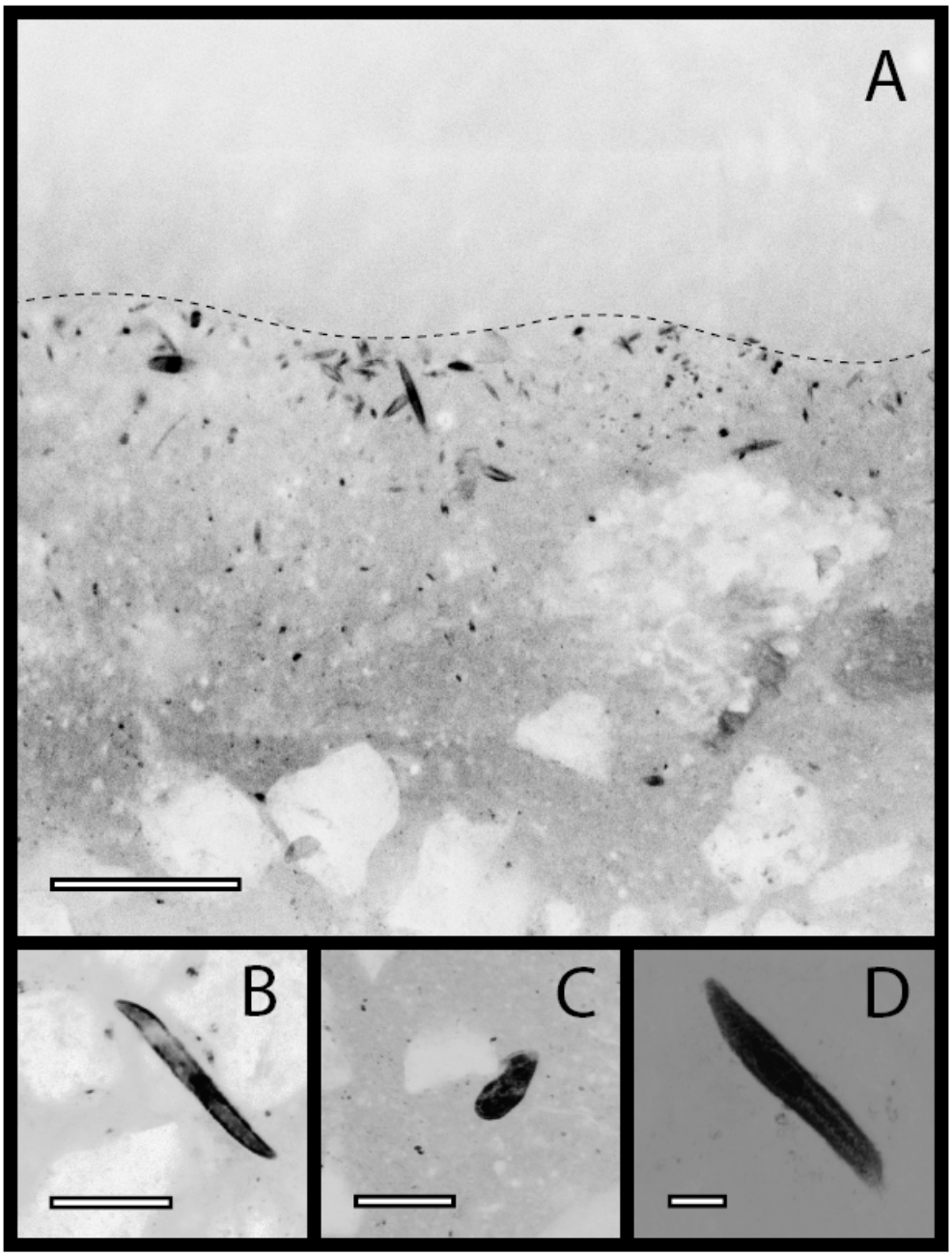

**Figure 4.4.** Size distribution (Equivalent Circular Diameter, ECD) of CTG-positive microbenthos in pooled FLEC core profiles.

**Figure 4.4**

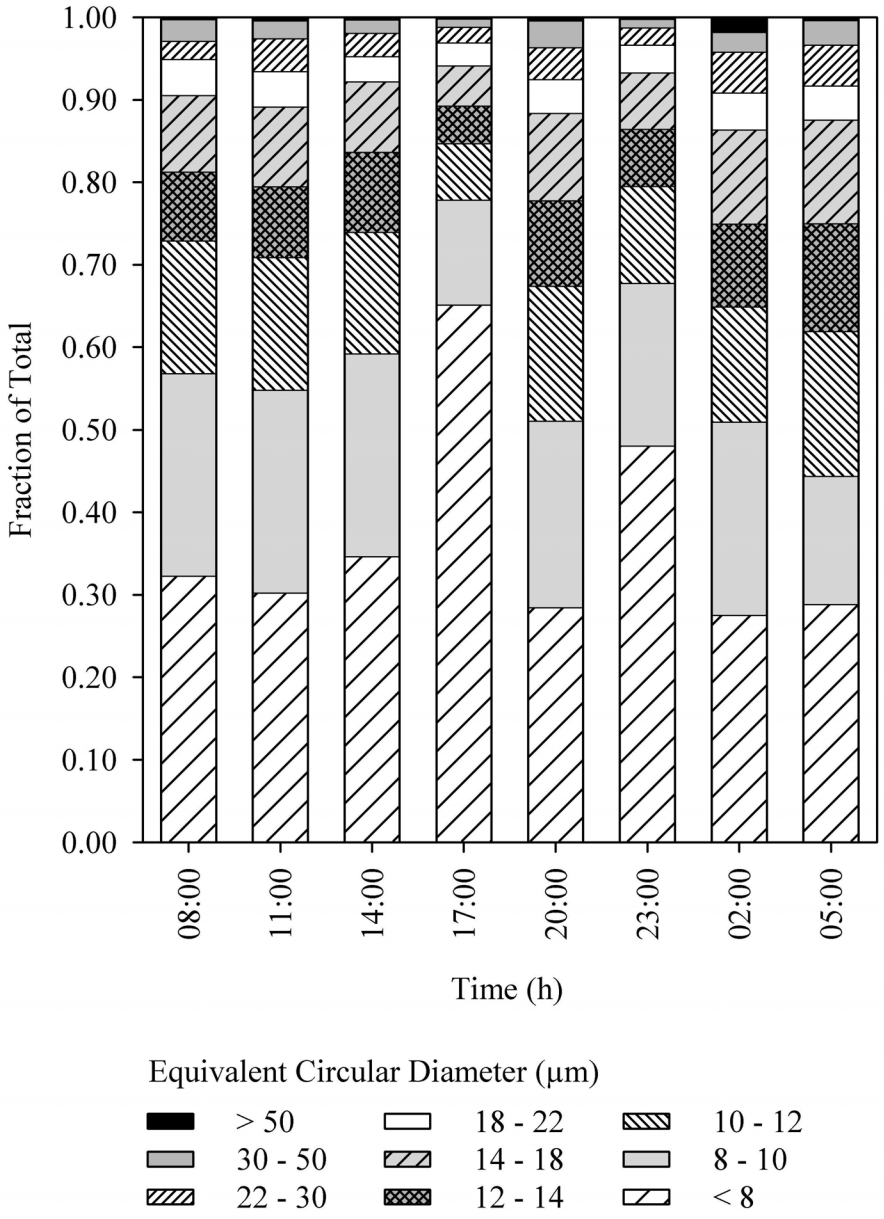
1.00
0.90
0.80
0.70
0.60
0.50
0.40
0.30
0.20
0.10
0.00
Fraction of Total
08:00
11:00
14:00
17:00
20:00
23:00
02:00
05:00
Time (h)
Equivalent Circular Diameter (μm)
> 50
30 - 50
22 - 30
18 - 22
14 - 18
12 - 14
10 - 12
8 - 10
< 8

**Figure 4.5.** Comparison of microbenthos concentration (x $10^6$ individuals $cm^{-3}$) determined by FLEC versus Chl *a* concentration (μg $cm^{-3}$). Points show mean ± SD (n = 3).

**Figure 4.5**

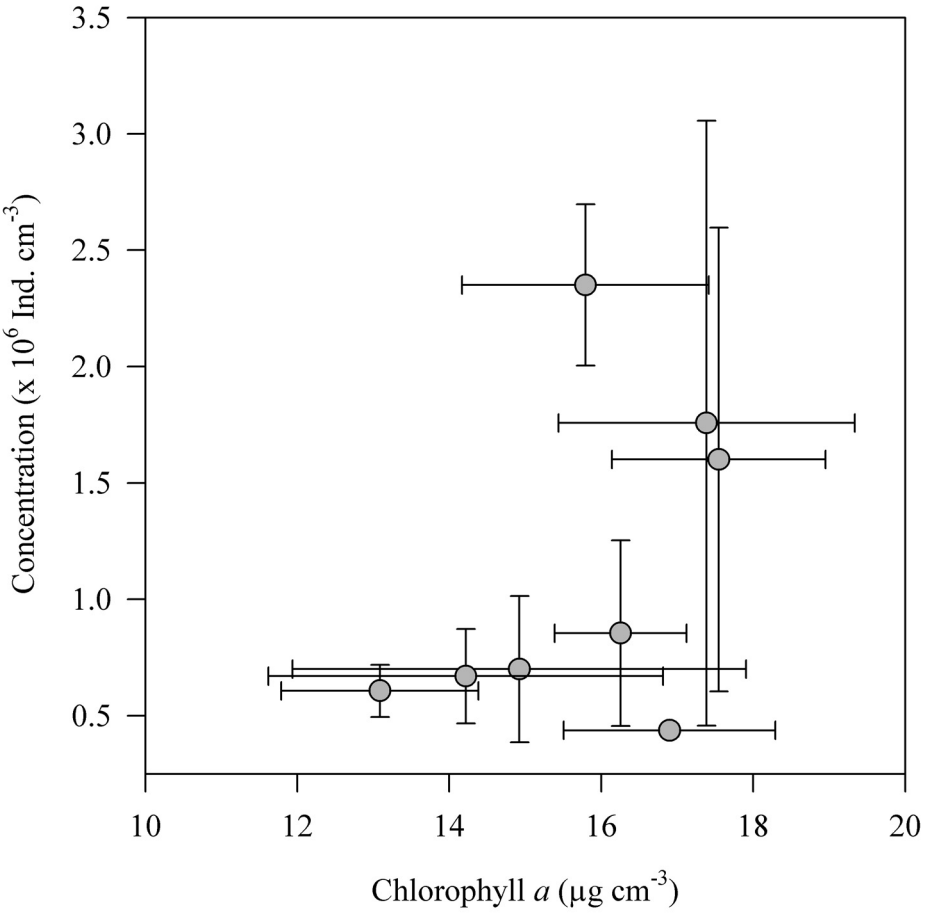
3.5
3.0
2.5
2.0
1.5
1.0
0.5
Concentration (x 10^6 Ind. cm^-3)
10
12
14
16
18
20
Chlorophyll a (µg cm^-3)

**Figure 4.6.** Example of the spatial distribution of microbenthos as determined by the FLEC method (shown here is a profile taken at 1700 h). The sizes of points on the map are scaled to the ECD of the fluorescent object at each point.

**Figure 4.6**

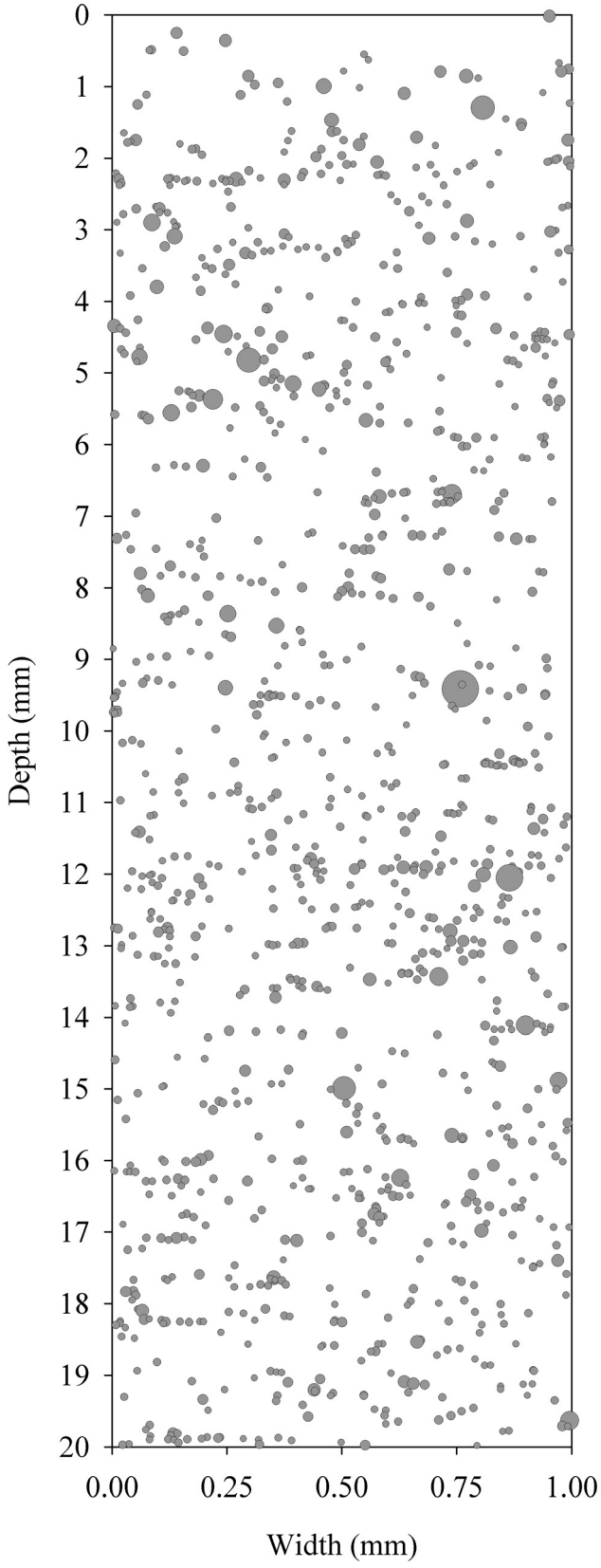
0
1
2
3
4
5
6
7
8
9
10
11
12
13
14
15
16
17
18
19
20
Depth (mm)
0.00
0.25
0.50
0.75
1.00
Width (mm)

**Figure 4.7.** Dispersion of microbenthos in sediment cores calculated by Morisita's Index ($I_M$). The spatial scale is defined by the quadrat size (0.25 x 0.25, 0.5 x 0.5 or 1.0 x 1.0 mm). Points show the mean $I_M$ value (n=3, except for 0800 h, where n =2); SD bars are only shown for 0.25 x 0.25 mm, error bars for other quadrat sizes are omitted for clarity, but SD <0.1% of the mean In these cases.

**Figure 4.7**

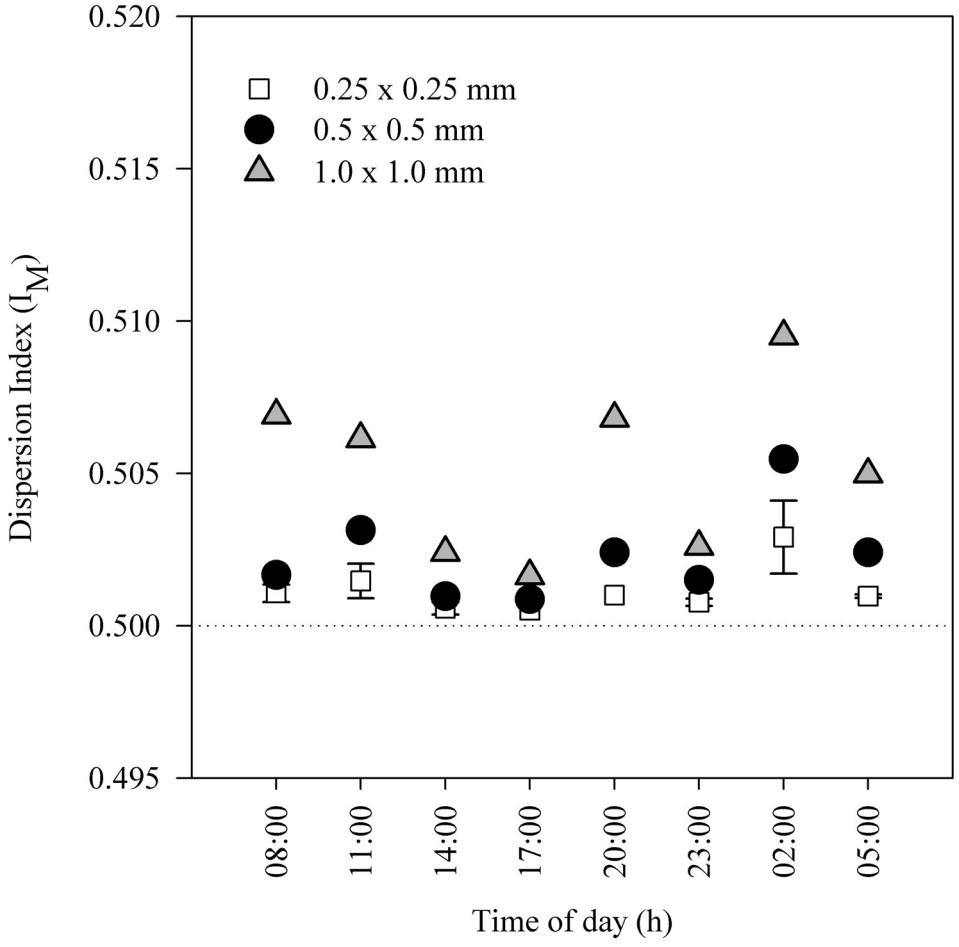
0.520
0.515
0.510
0.505
0.500
0.495
Dispersion Index ($I_M$)
0.25 x 0.25 mm
0.5 x 0.5 mm
1.0 x 1.0 mm
08:00
11:00
14:00
17:00
20:00
23:00
02:00
05:00
Time of day (h)

**Figure 4.8.** Vertical distribution of CTG-positive microbenthos in profiles at all time points. Bars indicate the percent deviation from the abundance expected in the depth interval if cells were evenly distributed along the profile. Deviations greater than 5% from expected are indicated with arrows (at 0800 and 0200 h). Line plots indicate the accumulated abundance of cells with depth compared with an even distribution (dotted line).

**Figure 4.8**

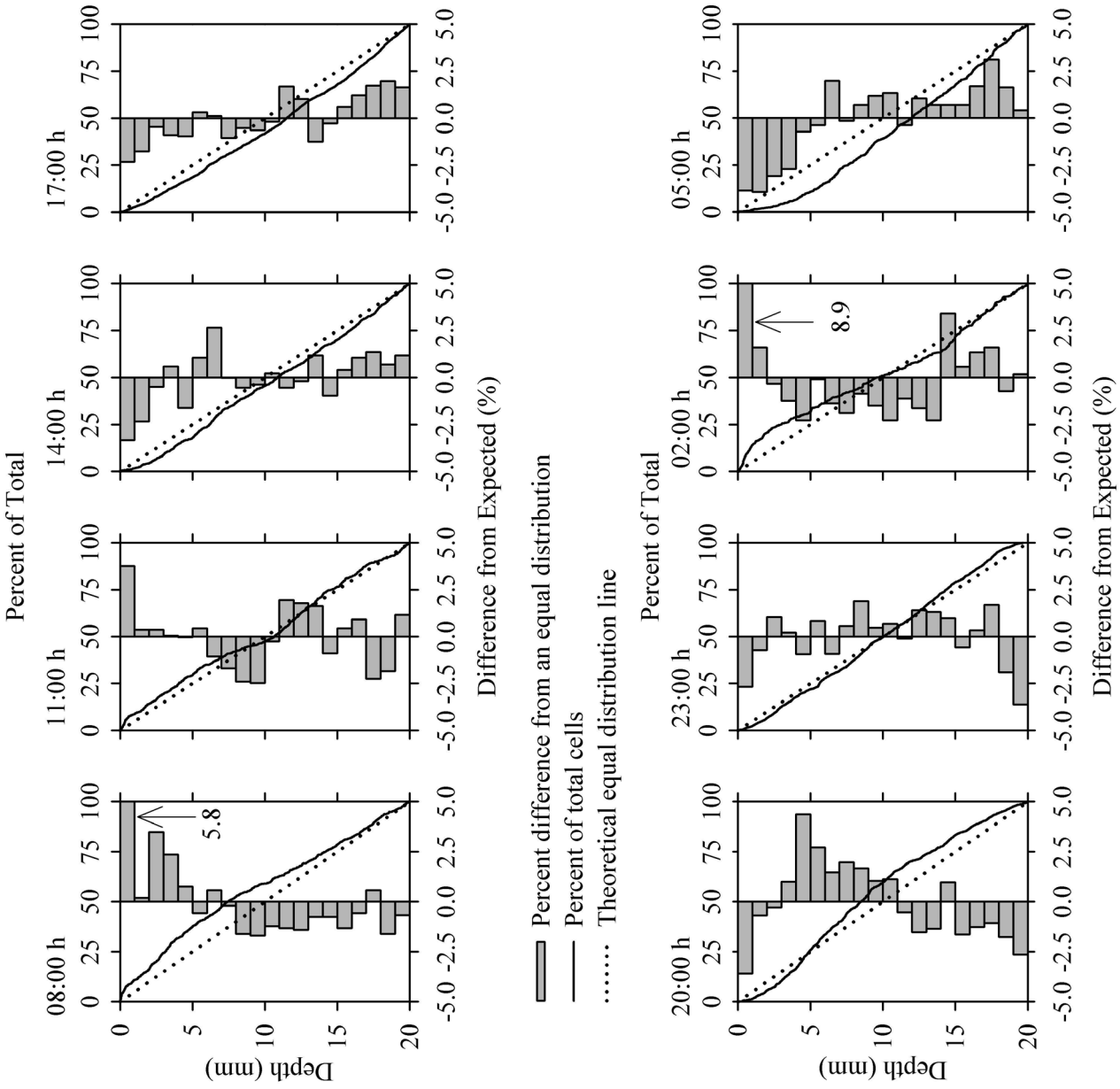
Percent of Total
Depth (mm)
Difference from Expected (%)
08:00 h
11:00 h
14:00 h
17:00 h
23:00 h
02:00 h
05:00 h
20:00 h
5.8
8.9
Percent difference from an equal distribution
Percent of total cells
Theoretical equal distribution line

**Figure 4.9.** Mean population depth and Gini coefficient of inequality of FLEC profiles at all sample times. Bars show standard error of mean depth or the bootstrap standard error.

**Figure 4.9**

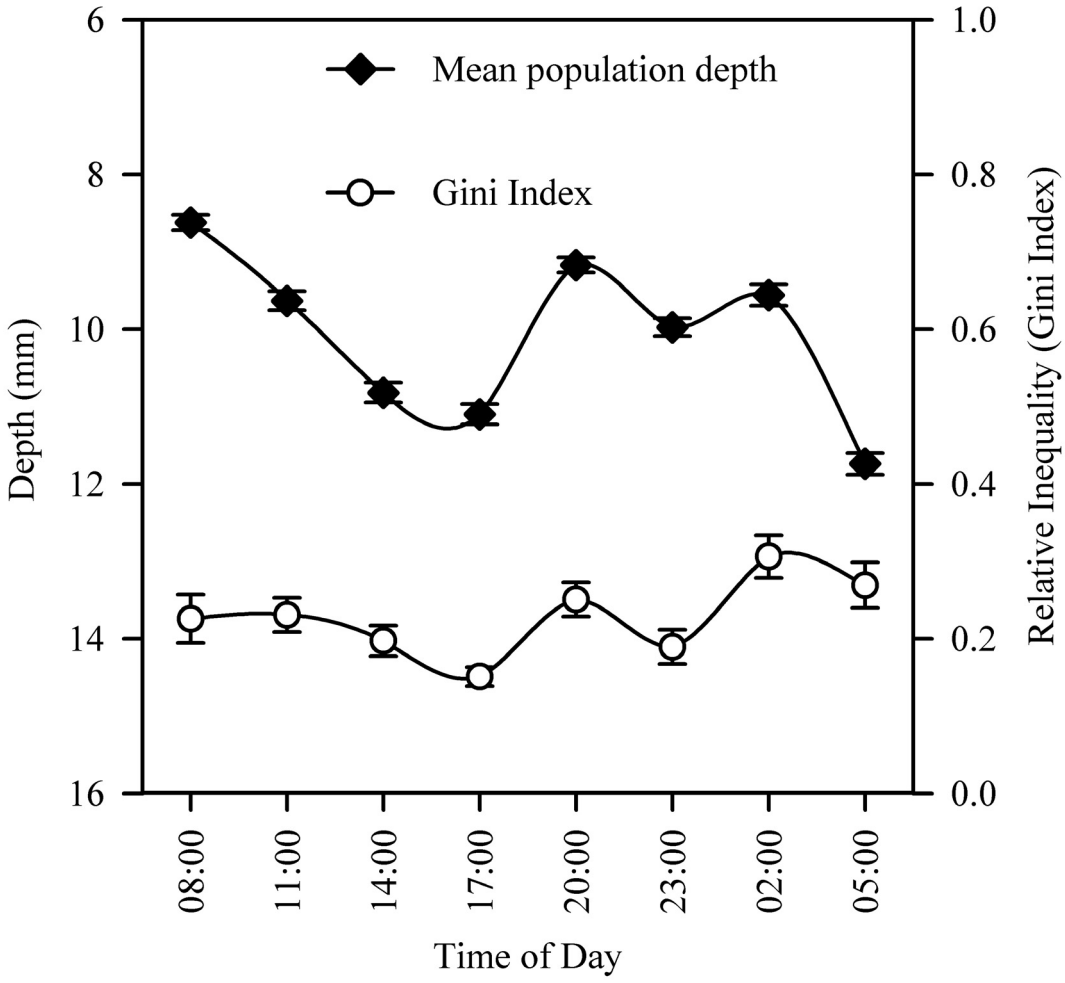
Mean population depth
Gini Index
Depth (mm)
Relative Inequality (Gini Index)
6
8
10
12
14
16
1.0
0.8
0.6
0.4
0.2
0.0
08:00
11:00
14:00
17:00
20:00
23:00
02:00
05:00
Time of Day

# CHAPTER 5

## INGESTION OF HIGH MOLECULAR WEIGHT DISSOLVED ORGANIC CARBON BY THE BENTHIC CILIATE, *URONEMA MARINUM*[5]

[5] M.R First and J.T. Hollibaugh
To be submitted to: *Applied and Environmental Microbiology*

## ABSTRACT

We investigated the ability of the marine benthic ciliate, *Uronema marinum*, to ingest dextran at concentrations typical for coastal salt marsh sediments as an analog for high molecular weight dissolved organic carbon (HWM-DOC). Ingestion was measured by incubating ciliates with fluorescein-labeled dextran (2,000 kDa) and measuring the fluorescent signal of the labeled compound in cells via flow cytometry. Ciliates accumulated dextran (relative to formalin-killed controls) at concentrations as low as 0.1 mg $l^{-1}$ (3 μM DOC). Labeled dextran accumulated in food vacuoles and near the buccal cavity, thus, the ingestion of HMW-DOC appears to be a consequence of feeding activities rather than transport across the cell membrane via parasomal sac formation. Dextran accumulation rate did not increase with increased ingestion of bacteria; uptake of dextran was greatest at intermediate grazing rates and bacteria concentrations. Ciliate biomass production rates were measured in treatments amended with model carbon compounds – soluble starch, acetate, and glucose (3mM DOC). There was no significant increase in ciliate biomass production with these compounds in bacteria-enriched or bacteria-free treatments. Although the addition of DOC did not significantly increase ciliate growth or production rates, the uptake and transformation of HMW-DOC may increase the reactivity and bioavailability of recalcitrant carbon compounds.

## INTRODUCTION

Phagotrophic ciliates rely upon the ingestion of particulates (e.g. bacteria, algae) to satisfy their cellular metabolic requirements. Some of these ciliates are capable of growth in carbon-rich, axenic media by taking up dissolved materials (Soldo & Van Wagtendonk 1969, Orias et al. 2000). The uptake of dissolved compounds can occur across the cell membrane (osmotrophy), or through the formation of vacuoles at locations along the cell body (pinocytosis) (Radek & Hausmann 1996). Amino acids and low molecular weight sugars are transported rapidly across the cell membrane (Seaman 1961, Aomine 1974), while complex macromolecules enter the cell via the formation and invagination of parasomal sacs (Radek & Hausmann 1996). Macromolecules can also enter the cell via food vacuoles formed at the buccal cavity where phagocytosis of particles occurs (Seaman 1961). Ciliates in carbon-rich environments, such as the rumen of cattle, use soluble carbohydrates but must also ingest bacteria for growth (Gutierrez & Hungate 1957). These bacteria supply the nitrogen-rich biomolecules, such as amino acids and purines, required for ciliate growth (Soldo & Van Wagtendonk 1969). The acidity of and digestive enzymes in food vacuoles are likely essential for the breakdown of complex molecules, regardless of whether they originate from dissolved or particulate sources (Seaman 1961, Tiedtke et al. 1988).

Direct uptake of DOC also occurs in free-living aquatic protists. Planktonic estuarine flagellates exhibited increased growth when incubated with high molecular weight dissolved organic carbon (HMW-DOC) in the form of dextran, a linear carbohydrate composed of dextrose subunits with molecular weight approximately 2,000 kDa (Sherr 1988). The phototrophic dinoflagellate, *Alexandrium catenella*, can take up 2,000 kDa dextran in the absence of any detectable bacterial ingestion (Legrand & Carlsson 1998). Pelagic choreotrichous ciliates did not

appear to directly assimilate macromolecules (Tranvik et al. 1993). Ciliates are capable of taking up low concentrations of dissolved sugars and amino acids (Glaser 1988), although the significance of this process to both ciliate growth or food web structure is not clear. Direct uptake by protists may play a more important role in sediments, where HMW-DOC is released from the breakdown of plant matter and the production of exopolymeric substances by benthic microalgae (e.g. Wheeler 1976, Smith & Underwood 1998). The ingestion of DOC by benthic ciliates has been suggested as an energy source for benthic ciliates when the rate of particle ingestion appears lower than required for cell maintenance (Epstein 1997). Bacteria must hydrolyze large macromolecules extracellularly and in some cases the absence of specific hydrolytic enzymes can hinder organic matter decomposition (Arnosti 2004). The uptake of HMW-DOC into ciliate food vacuoles, whether deliberate or fortuitous, would not require additional hydrolytic enzymes (and energy expenditures), allowing ciliates to effectively compete with bacteria for HMW-DOC. Ciliates are one of the most abundant groups of benthic bacterivorous protists (Fenchel 1967), thus, their role in processing sediment DOC could be significant. Ciliates also may benefit from the uptake of DOC, even at low ambient concentrations.

*Uronema marinum* is a bacterivorous ciliate commonly found in the sediments near Sapelo Island (First & Hollibaugh, In Prep). This ciliate has high growth rates in oxygenated seawater, but can also persist in anoxic environments (Fenchel and Findlay 1995). We used *U. marinum* was used as a model ciliate to test the hypotheses that: 1) bacterivorous ciliates are capable of direct ingestion of HMW-DOC at concentrations typical of salt marsh sediments, 2) the rate of HWM-DOC accumulation increases at lower prey concentrations, and 3) DOC ingestion can increase the growth and production rates of *U. marinum*. Bacteria and their

consumers provide the primary route for the reclamation of DOC into the food web (Azam et al. 1983). Understanding alternative routes of carbon flow will provide insight on food web efficiency and microbial trophodynamics.

## MATERIALS AND METHODS

**Culture establishment.** *U. marinum* was isolated from sandy subtidal sediments on Sapelo Island, Georgia, USA (31.389762 °N, 81.264268 °W). Proteose peptone (PP, ~ 1 g $l^{-1}$) was added the sediment to stimulate bacterial growth, which led to a bloom of *U. marinum* (Parker 1976). Cells were transferred with the natural bacterial assemblage into 30 ppt artificial seawater (ASW) (Mclachlan 1964) enriched with 1 g $l^{-1}$ of PP. The cultures were incubated at 22 °C in tissue culture flasks. Cultures were transferred into fresh media every 1 – 3 days, when the ciliate population was roughly $10^5$ cells $ml^{-1}$. No other protists were observed in the cultures after several transfers.

Ciliates used for experiments were in late-log or stationary growth. The media was screened through a 37 μm Nitex mesh to remove bacterial aggregates. Ciliates were washed by concentrating the media on a 5 μm Nuclepore polycarbonate filter and rinsing with several volumes of particle-free (0.22 μm filtered) ASW. The filter was not allowed to go dry during the rinse. Washing removed carbon-rich media and reduced the standing stock of bacteria. Antibiotics (0.1 mg $ml^{-1}$ gentamicin sulfate) were added to prevent further bacterial growth. This antibiotic treatment was effective at preventing the growth of bacteria in the enriched media described above, but did not impact the growth rate of *U. marinum*. Samples were held for 2 h prior to experimental manipulations to allow the ciliates to reduce the remaining bacteria in the culture.

Heat-killed bacteria were prepared for DOC uptake and grazing experiments to assure that bacterial prey were uniform across treatments. Bacteria were isolated from *U. marinum* cultures on ASW agar plates (10 g $l^{-1}$ peptone). One colony was suspended in seawater and killed by heating to 95°C for 20 min. The suspended bacteria were then washed with ASW containing antibiotics (1 mg $ml^{-1}$ gentamicin sulfate) and centrifuged. The supernatant was discarded and the cells were resuspended in the ASW containing antibiotics. This washing procedure was repeated for a total of three washes. Suspended cells were then filtered through a 5 μm pore size syringe filter to disperse or remove large aggregates. Microscope observations assured that the cells were well-dispersed and intact. Their inability to grow on agar plates indicated that this treatment was sufficient to kill bacteria and suppress further bacterial growth.

**Dextran uptake.** Fluorescein isothiocyanate (FITC) labeled dextran (average molecular weight 2,000 kDa, Sigma-Aldrich) was used as an analog for high molecular weight (HMW) DOC. The FITC-dextran was prepared in 10X stock solutions and syringe-filtered (0.22 μm) immediately before use. The FITC-dextran was added to triplicate *U. marinum* cultures at final concentrations ranging from 0.1 to 100 mg $l^{-1}$ (3 μm – 3 mM DOC); ASW was added to one triplicate set as a negative control. One formalin-killed control (4% final concentration) was run at each concentration to account for the background fluorescence of the media and passive adsorption of dextran on ciliate cells. The samples were incubated for 90 min in the dark at 25°C on a shaker table. Incubations were stopped by formalin addition (2% final concentration). Accumulation of FITC-dextran leads to an increase of the fluorescent signal in the ciliate relative to the background fluorescence. The fluorescence of individual ciliates was measured using a flow cytometer (Dako Cyan) with a 488 nm laser excitation. The ciliates were gated according to their

side scatter and forward scatter signals, as these measurements did not vary in response to the treatments. The fluorescent emission signals (FL1) for approximately 5,000 ciliates were recorded for each treatment replicate and control. Epifluorescence and laser scanning confocal microscopy were used to verify the accumulation of FITC-dextran in ciliate food vacuoles. Cells were imaged at 1000x with a combination of fluorescence emission in the green light spectrum and transmitted light from a 488 nm argon/krypton laser.

The relative rate of HMW-DOC accumulation in *U. marinum* was measured by incubating ciliates at three concentrations of FITC-dextran. Triplicate ciliate cultures were prepared in 50 ml conical centrifuge tubes as described above and incubated with 1, 10, and 100 mg $l^{-1}$ FITC-dextran for a up to 300 min. Samples of 1 ml were collected from each replicate periodically throughout the incubation period to determine the rate of FITC-dextran accumulation. Formalin-killed controls were also run to measure the background fluorescence of the solution. The fluorescent emission signal was recorded for approximately 5,000 ciliates as described above, subtracting the fluorescence of the killed control. To measure the relative accumulation of dextran over time, the final ciliate fluorescence was normalized to the initial concentration. The relative accumulation (*RA*) of FITC-dextran was calculated as the mean fluorescence at each time point ($T_i$) normalized to the mean fluorescence at the initial time point ($T_0$) according to the formula: $RA\ T\text{i} = \text{FL1}\ T\text{i} / \text{FL1}\ T_0$. Thus, a relative accumulation of 1 indicates that there was no increase in fluorescence over the incubation period (i.e. no uptake). We used this method because there are large differences in background fluorescence of the solutions. For example, absolute fluorescence of $T_0$ treatments of 100 mg $l^{-1}$ dextran was greater than final ($T_{300}$) fluorescence in 10 mg $l^{-1}$ solutions.

We also tested the hypothesis that DOC accumulation rate increases concurrently with higher bacterial grazing rates. Ciliate cultures were prepared as above and the washed culture was transferred into 50 ml conical centrifuge tubes. Two variables (bacteria and dextran concentration) were analyzed at three levels: low, medium, and high bacteria concentrations and 0, 10, and 100 mg $l^{-1}$ dextran. Heat-killed bacteria were prepared as described above and added to the cultures to yield 8.1, 15 and 110 x $10^5$ cells $ml^{-1}$ for low, medium, and high treatments, respectively. Treatments were immediately dispensed into 2 ml Eppendorf tubes. The samples were incubated for 90 min as described above. Ciliate and bacteria concentrations and ciliate fluorescence (FL1) were measured at both initial and final time points by flow cytometry. Additional samples were incubated for 26 h to assess ciliate growth in these treatments as described below. To calculate cell concentrations, the weight of the sample analyzed was converted to volume following a volume-weight relationship for ASW. Per-capita grazing rates were calculated as the loss of bacterial cells during the 90 min incubation per the mean ciliate concentration ($MC = C_{T0}\, e^{(\mu \Delta t/2)}$) where, $C_{T0}$ is the initial ciliate concentration (cells $ml^{-1}$) and $\mu$ is the growth rate ($\mu = \log [C_{90} \cdot C_0^{-1}] \cdot t^{-1}$) in hours (Gallegos et al. 1996). Ciliate growth rate ($\mu$, $d^{-1}$) was determined for the treatments after 26 h of incubation to assess the impact of these treatments on ciliate growth.

**Uptake of starch, glucose, and acetate.** The role of dissolved carbon compounds commonly found in salt marsh sediments was examined by measuring the growth and production rates of *U. marinum* incubated with starch, glucose, and acetate. Glucose constitutes over 80% of colloidal monosaccharides in diatom-dominated, intertidal sediments (Taylor et al. 1999). Acetate is an abundant, low molecular weight DOC in intertidal sediments, especially in anoxic zones (Holmer

1996). Soluble starch was used as representative HMW-DOC compound. Soluble starch, sodium acetate, and D-glucose were dissolved in filter-sterilized ASM; the starch solution was heated (~60°C) to speed dissolution. All solutions were prepared in cleaned and baked (550°C, 6 h) glassware. Solutions were syringe-filtered through a 0.22 μm membrane filter prior to use in the experiment and diluted to yield a final concentration of 3 mM DOC in all treatments, which is in the range observed in salt marsh surficial sediments (Weston et al. 2006).

Flow cytometric sorting was used to separate *U. marinum* from bacteria in cultures. The ciliates were gated on forward and side angle light scattering signals on a Dako MoFlo high speed cell sorter. Ciliates were sorted into bacteria-free ASW and held for 2 h prior to the experiment. The process of cell sorting had no observable impact on the growth or activity of *U. marinum*. The initial and final ciliate biomasses were determined by measuring microscope images of *U. marinum* captured at 400X on a Hamamatsu CCD digital camera. The length and width of at least 30 ciliates in each treatment were measured with image analysis software (Image Pro Plus 4.1) and used to calculate biovolume of ciliates (Wetzel & Likens 1991). Ciliate biovolume was converted to biomass using published relationships (Putt & Stoecker 1989). Image dimensions were calibrated using a stage micrometer and verified using 0.66 and 1.0 μm diameter fluorescent beads. Ciliate growth rate was calculated as above, except using the biomass concentration (μgC $ml^{-1}$) rather than cell concentration. Ciliate biomass was a more sensitive measure of growth as the cell volume of *U. marinum* varies during with growth stage (Parker 1976).

Treatments with bacteria were used to determine if DOC combined with bacteria can yield higher rates of ciliate growth and production. Treatments were prepared in autoclaved, 2 ml Ependorf tubes. Triplicates of each treatment were prepared by adding 100 μl of sorted *U.*

*marinum* to 800 µl of either starch, acetate or glucose solution; filter-sterilized ASW was used for control treatments. For treatments with bacteria, 100 µl of the bacterial suspension was added. Bacteria-free treatments received 100 µl of filter sterilized ASW with antibiotics. The final antibiotic concentration for all treatments was 0.1 mg $ml^{-1}$ of gentamicin sulfate. Initial ($T_0$) samples were chemically preserved with 0.22 µm filtered formalin (2% final concentration). The treatment samples were incubated in the dark at 22°C for 24.0 h, at which point the incubation was stopped by adding formalin. Treatments were stained with 4',6-diamidino-2-phenylindole (DAPI) and the concentrations of ciliates and bacteria in each treatment replicate were measured with a DAKO Cyan flow cytometer using a 405 nm laser.

## RESULTS

**Dextran uptake.** *U. marinum* incubated with FITC-labeled dextran were significantly more fluorescent than formalin killed controls at all concentrations tested (ANOVA, $P$ <0.001) (Fig. 5.1). Negative controls (with no dextran addition) did not show any fluorescence, indicating autofluorescence from the formalin was not detectable. Ciliates were able to accumulate dextran in food vacuoles at a concentration as low as 0.1 mg $l^{-1}$, and the fluorescence signal emitted by ciliates was strongly correlated to the concentration of dextran in solution (linear regression, $r^2$ = 0.99, df = 15, $P$ < 0.001). Fluorescence was concentrated in structures consistent with food vacuoles in shape, size, and location in the cell (Fig. 5.2). Examination by epifluorescence, confocal microscopy, and flow cytometry revealed no fluorescent particles or aggregates that could introduce the fluorescence signal into the food vacuole via phagocytosis of particles, indicating that the source of the fluorescence signal was dissolved or colloidal (<0.22 µm) FITC-dextran.

The relative rate of dextran accumulation was highly dependent on the dextran concentration (Fig. 5.3). The slope of the relationship between DOC relative accumulation and time was 0.003, 0.009 and 0.029 $min^{-1}$ for 1, 10 and 100 mg $l^{-1}$ FITC-dextran, respectively (linear regression, $r^2 > 0.9$, $P < 0.05$, df = 8, all cases). Ciliate fluorescence was significantly greater than the initial, background fluorescence after 60 minutes at all three dextran concentrations (ANOVA, $P < 0.05$, df = 20). The final percent enrichment after the 300 min incubation was 1.7 (± 0.07 SE), 3.9 (± 0.16), and 8.7 (± 0.51) for 1, 10, and 100 mg $l^{-1}$ dextran, respectively.

Dextran accumulation by ciliates was highest at intermediate bacterial concentrations (Fig. 4A) and was significantly greater than accumulation at both low and high bacteria concentrations (ANOVA, $P < 0.01$). There was no significant difference in relative accumulation of dextran between high and low bacteria treatments at both 10 and 100 mg $l^{-1}$ dextran (ANOVA, $P > 0.05$). Ciliate grazing rates increased with bacteria concentration, with the greatest per-capita grazing rates in the high bacteria concentration treatments (Fig. 5.4B). The growth rate of *U. marinum* was greatest in high bacterial treatments (Fig. 5.5). There was no significant difference in ciliate growth between low and medium bacteria treatments, nor was there any significant effect of FITC-dextran on ciliate growth rate at these bacteria concentrations (ANOVA, $P > 0.5$). The highest ciliate growth was measured in the no dextran, high bacteria treatments. This growth rate was significantly greater than in the 10 mg $l^{-1}$ FITC-dextran treatment (ANOVA, $P < 0.01$), but not the 100 mg $l^{-1}$ treatment.

**Utilization of starch, acetate, and glucose.** Ciliate growth rate, based on the change in concentration of cells over the incubation period, did not increase with starch, acetate, or glucose

treatments relative to the controls (Fig. 6A). The highest ciliate growth rates were observed in control samples without DOC addition. However, this higher growth rate in control treatment, both with and without bacteria, was not significantly greater than treatments with DOC addition (t-test, $p>0.05$, $df=4$). DOC addition increased biomass production by ciliates. The biomass production of *U. marinum* was slightly higher in treatments with starch and glucose than in no DOC controls in both bacteria enriched and bacteria-free treatments (Fig. 5.6B). This suggests that the DOC treatments led to increases in cell volume and biomass of *U. marinum*. However, the increase in biomass production rates were not significantly greater than controls in any treatment (t-test, $p>0.05$, $df=4$). Acetate did not appear to increase the biomass production for these ciliates incubated with bacteria.

## DISCUSSION

Several ciliates, including *U. marinum*, have been cultured under axenic conditions, hence their ability to ingest and metabolize DOC is well established (Soldo & Van Wagtendonk 1969, Hanna & Lilly 1974). We hypothesized that ciliates are capable of ingesting DOC at concentrations typical of salt marsh sediments and that DOC could supplement the energetic requirements of these ciliates. Direct uptake of DOC may be advantageous for ciliates in carbon-replete sediments, such as those in salt marshes. Salt marsh sediments receive organic carbon inputs from intertidal macrophytes (Schubauer & Hopkinson 1984) and benthic microalgae (Smith & Underwood 1998). A large portion of the aboveground biomass of common cordgrass, *Spartina alterniflora*, is ultimately buried in salt marsh sediments. Biomass in belowground root and rhizome structures also contributes carbon to fuel the benthic microbial food web (Schubauer & Hopkinson 1984). The breakdown of this plant matter leaves behind recalcitrant

organic compounds such as lignocellulose (Moran & Hodson 1990). Bacterial growth yield on these compounds is typically low (Newell et al. 1983). Additionally, large quantities of algal-derived exopolymers are released by benthic microalgae in shallow water sediments (Smith & Underwood 1998). Recalcitrant carbon compounds are also produced by bacteria from labile materials, such as sugars and amino acids (Ogawa et al. 2001). The uptake and hydrolysis of HMW and recalcitrant DOC by benthic ciliates may hasten the degradation of these compounds and increase benthic metabolism. The ingestion of macromolecules, in particular, may be advantageous to benthic protists as use of complex carbohydrates by bacteria requires specific extracellular hydrolytic enzymes (Arnosti 2004).

*U. marinum* was capable of ingesting dextran, a model HMW carbohydrate. Although dextran was dissolved and filtered to remove particles >0.22 μm, it is probable that a portion of this dextran existed as colloids (e.g. Verdungo et al. 2004). Therefore, the dextran source for these ciliates likely includes colloidal as well as dissolved organic carbon. The ingestion of fluorescently labeled dextran occurs almost instantaneously and is highly dependent on the ambient dextran concentration. Dextran appears to be ingested through the food vacuoles rather than via the formation of parasomal sacs (e.g. Radek & Hausmann 1996). Unexpectedly, higher prey concentrations did not correspond to the greater uptake of dextran. There could be several explanations for this observation. First, higher rates of digestion under bacteria-replete conditions may also degrade the fluorescence signal more rapidly. However, digestion rates and food vacuole cycling time do not vary significantly with prey concentration (Capriulo & Degnan 1991). Thus, the difference between ciliate uptake rates at different bacterial concentrations is not likely a function of metabolism. Second, lower prey concentrations relative to the high bacteria treatments may require more water to be processed per each food vacuole formed.

However, if this were the explanation, then ciliates in the lowest bacteria treatments should show the greatest enrichment in dextran. The most likely explanation for higher dextran uptake in intermediate bacteria treatments is that dense packing of bacteria in food vacuoles at high concentrations limit the food vacuole volume available for dissolved substances.

The ingestion of dextran did not increase ciliate growth rate at the concentrations tested. Dextran treatments actually yielded lower ciliate growth rates than control treatments without added dextran. This suggests that, with abundant bacterial prey, the processing of dextran incurs some energetic cost to ciliates resulting in lower growth rates. This energetic cost may be associated with the hydrolysis of nitrogen-poor carbon compounds. Conversely, the relatively low C:N ratio in marine bacteria provides an abundance of nitrogen for ciliate growth. For example, marine bacteria have a high relative contribution of nitrogen to their total biomass (Fukuda et al. 1998), whereas dextran and other carbohydrates do not provide nitrogen for biomass production.

*U. marinum* production rates were slightly higher with DOC than control treatments in both the presence and absence of bacteria. This increase in biomass was due to changes in *U. marinum* cell volume rather than increased cell concentrations. This supports the hypothesis that low nitrogen content of carbohydrates limits balanced growth and the cell reproduction (Gutierrez & Hungate 1957). Although DOC consumption does not appear to significantly increase the growth rate of *U. marinum*, other benthic ciliates (including larger taxa with lower rates of particle ingestion) may depend upon DOC to supplement growth requirements (Epstein 1997).

The ability to concentrate DOC in food vacuoles suggests that the process occurs simultaneously with particle ingestion. Assuming ciliate clearance rate is similar at all three

dextran concentrations, more dextran would accumulate in ciliates at higher dextran concentrations, as observed in this study. This also suggests that the process of dextran uptake is consequence of processing fluid via feeding currents, rather than deliberate transport across the cell membrane. The deposition of dextran in food vacuoles suggests that the HMW-DOC ingestion is a fortuitous process, perhaps a byproduct of interactions with receptors near the ciliate oral apparatus that bind to hydrophobic compounds on bacterial cell surfaces (Monger et al. 1999). Suspension-feeding ciliates like *U. marinum* create water currents that flow into the buccal cavity. Particles are sieved as water is passed through the paroral membrane and mechanical filtration is considered to be the major mechanism of particulate concentration (Fenchel 1980). However, chemical interactions increase the ingestion rates of particulate prey by protist bacterivores (Monger et al. 1999, Wilks & Sleigh 2004). The ability to concentrate and ingest dissolved or colloidal matter, which would not be retained on the paroral membrane (Fenchel 1980), suggests that molecular attraction also contributes to DOC endocytosis in these ciliates.

While the compounds tested did not appear to supplement ciliate growth, other consequences for carbon dynamics are possible. For instance, ciliate digestive enzymes could transform or hydrolyze recalcitrant DOC. Release of bacterial-labile carbon compounds, in turn, would increase bacterial production. In anoxic sediments, the release of low molecular weight (LMW) fermentation byproducts by ciliates stimulates terminal respiration rates of anaerobic bacteria (Biagini et al. 1998). The ingestion and processing of HWM-DOC by ciliates may be especially important during parts of the year where terminal respiration is limited by LMW-DOC (Weston & Joye 2005). The fermentation of HMW-DOC directly ingested by ciliates may stimulate sulfate reduction and denitrification. Rather than providing a direct benefit to ciliates,

the initial breakdown of HMW-DOC in protists' food vacuoles would benefit bacterivorous ciliates indirectly – through increased bacterial production. Thus, the ingestion of HMW-DOC by benthic ciliates may be an important process in salt marsh sediments.


## ACKNOWLEDGEMENTS

This work was supported by NSF Georgia Coastal Ecosystems LTER grant (OCE-9982133). J. Shields and C. Keith assisted in the confocal microscope operation. J. Nelson provided crucial assistance in the operation of the MoFlo and Dako flow cytometers and assisted in data analysis. M. Bernhard, M. Farmer, S. Joye and C. Meile provided guidance on the design of this project. M.R.F. was also supported by a UGA Graduate School Assistantship. This is contribution no. 961 to UGAMI.

## REFERENCES


Aomine M (1974) Studies on Mechanism of Uptake of D-Glucose by *Tetrahymena pyriformis* GL. Compar Biochem Physiol 47:1013-1021

Arnosti C (2004) Speed bumps and barricades in the carbon cycle: substrate structural effects on carbon cycling. Mar Chem 92:263-273

Azam F, Fenchel T, Field JG, Gray JS, Meyer-Reil LA, Thingstad F (1983) The ecological role of water-column microbes in the sea. Mar Ecol Prog Ser 10:257-263

Biagini GA, Finlay BJ, Lloyd D (1998) Protozoan stimulation of anaerobic microbial activity: enhancement of the rate of terminal decomposition of organic matter. FEMS Microbiol Ecol 27:1-8

Capriulo GM, Degnan C (1991) Effect of food concentration on digestion and vacuole passage time in the heterotrichous marine ciliate *Fibrea salina*. Mar Biol 110:199-202

Epstein SS (1997) Microbial food webs in marine sediments. II.s easonal changes in trophic interactions in a sandy tidal flat community. Microb Ecol 34:199-209

Fenchel T (1967) The ecology of marine microbenthos I. the quantitative importance of ciliates as compared with metazoans in various types of sediments. Ophelia 4:121-137

Fenchel T (1980) Suspension feeding in ciliated protozoa: structure and function of feeding organelles. Arch Protistenkd 123:239-260

Fenchel T, Finlay BJ (1995) Ecology and evolution in anoxic worlds. Oxford University Press, Oxford

Fukuda R, Ogawa H, Nagata T, Koike I (1998) Direct determination of carbon and nitrogen contents of natural bacterial assemblages in marine environments. Appl Environ Microbiol 64:3352-3358

Gallegos CL, Vant WN, Safi KA (1996) Microzooplankton grazing of phytoplankton in Manukau Harbour, New Zealand. New Zeal J Mar Fresh 30:423-434

Glaser D (1988) Simultaneous Consumption of bacteria and dissolved organic matter by *Tetrahymena pyriformis*. Micro Ecol 15:189-201

Gutierrez J, Hungate RE (1957) Interrelationship between certain bacteria and the rumen ciliate *Dasytricha ruminantium*. Science 126:511-511

Hanna BA, Lilly DM (1974) Growth of *Uronema marinum* in chemically defined medium. Mar Biol 26:153-160

Holmer M (1996) Composition and fate of dissolved organic carbon derived from phytoplankton detritus in coastal marine sediments. Mar Ecol Progr Ser 141:217-228

Legrand C, Carlsson P (1998) Uptake of high molecular weight dextran by the dinoflagellate *Alexandrium catenella*. Aquat Microb Ecol 16:81-86

McLachlan J (1964) Some considerations of growth of marine algae in artificial media. Can J Microbiol 10:769-&

Monger BC, Landry MR, Brown SL (1999) Feeding selection of heterotrophic marine nanoflagellates based on the surface hydrophobicity of their picoplankton prey. Limnol Oceanogr 44:1917-1927

Moran MA, Hodson RE (1990) Contributions of degrading *Spartina alterniflora* lignocellulose to the dissolved organic-carbon pool of a salt marsh. Mar Ecol Progr Ser 62:161-168

Newell RC, Linley EAS, Lucas MI (1983) Bacterial production and carbon conversion based on saltmarsh plant debris. Estuar Coast Shelf Sci 17:405-419

Ogawa H, Amagai Y, Koike I, Kaiser K, Benner R (2001) Production of refractory dissolved organic matter by bacteria. Science 292:917-920

Orias E, Hamilton EP, Orias JD (2000) *Tetrahymena* as a laboratory organism: useful strain, cell culture, and cell line maintenance. In: Asai DJ, Forney JD (eds) *Tetrahymena thermophila*, Vol 62. Academic Press, San Diego, p 189-211

Parker JG (1976) Cultural characteristics of marine ciliated protozoan, *Uronema marinum* Dujardin. J Exp Mar Biol Ecol 24:213-226

Putt M, Stoecker DK (1989) An experimentally determined carbon - volume ratio for marine oligotrichous ciliates from estuarine and coastal waters. Limnol Oceanogr 34:1097-1103

Radek R, Hausmann K (1996) Phagotrophy of ciliates. In: Hausmann K, Bradbury PC (eds) Ciliates: cells as organisms. Gustav Fischer, Stuttgart, p 197-219

Schubauer JP, Hopkinson CS (1984) Above-ground and belowground emergent macrophyte production and turnover in a coastal marsh ecosystem, Georgia. Limnol Oceanogr 29:1052-1065

Seaman GR (1961) Some aspects of phagotrophy in *Tetrahymena*. J Protozool 8:204-212

Sherr EB (1988) Direct use of high molecular weight polysaccharide by heterotrophic flagellates. Nature 335:348-351

Smith DJ, Underwood GJC (1998) Exopolymer production by intertidal epipelic diatoms. Limnol Oceanogr 43:1578-1591

Soldo AT, Van Wagtendonk J (1969) Nutrition of *Paramecium aurelia*, stock 299. J Protozool 16:500-506

Taylor IS, Paterson DM, Mehlert A (1999) The quantitative variability and monosaccharide composition of sediment carbohydrates associated with intertidal diatom assemblages. Biogeochemistry 45:303-327

Tiedtke A, Hünseler P, Rasmussen L (1988) Growth requirements of a new food-vacuole-less mutant of *Tetrahymena*. Eur J Protistol 23:350-353

Tranvik LJ, Sherr EB, Sherr BF (1993) Uptake and utilization of colloidal DOM by heterotrophic flagellates in seawater. Mar Ecol Progr Ser 92:301-309

Weston NB, Joye SB (2005) Temperature-driven decoupling of key phases of organic matter degradation in marine sediments. PNAS 102:17036-17040

Weston NB, Porubsky WP, Samarkin VA, Erickson M, MacAvoy SE, Joye SB (2006) Porewater stoichiometry of terminal metabolic products, sulfate, and dissolved organic carbon and nitrogen in estuarine intertidal creek-bank sediments. Biogeochemistry 77:375-408

Wetzel RG, Likens GE (1991) Limnological Analysis, Springer Verlag, New York

Wheeler JR (1976) Fractionation by molecular weight of organic substances in Georgia coastal water. Limnol Oceanogr 21:846-852

Wilks SA, Sleigh MA (2004) Lectin binding sites on *Euplotes mutabilis* (Tuffrau, 1960) and the implications for food particle selection. Eur J Protistol 40:153-162

**Figure 5.1.** Flow cytometric fluorescent signal (FL1) measured on ciliate populations in seawater enriched in several concentrations of FITC-labeled dextran. The box lines show the 25$^{th}$, 50$^{th}$ and 75$^{th}$ percentiles; bars and dots indicate the 10$^{th}$ and 5$^{th}$ percentiles of the data, respectively.

**Figure 5.1**

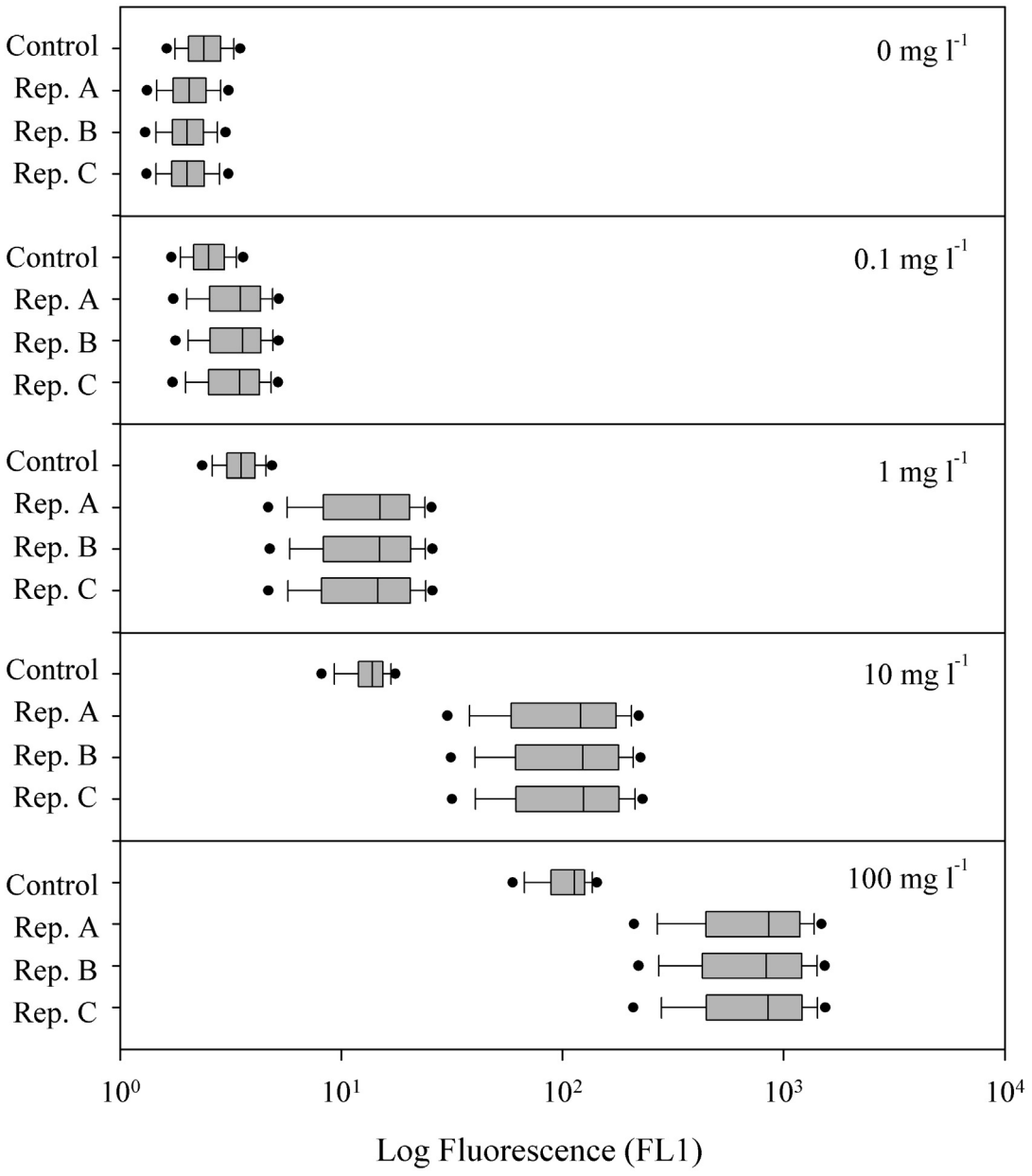
Control
Rep. A
Rep. B
Rep. C
0 mg l-1
0.1 mg l-1
1 mg l-1
10 mg l-1
100 mg l-1
10^0
10^1
10^2
10^3
10^4
Log Fluorescence (FL1)

**Figure 5.2.** Laser scanning confocal micrograph of *U. marinum* showing a fluorescent signal from FITC-dextran in food vacuoles located near the buccal cavity and the cell posterior. Scale bar = 10 μm.

**Figure 5.2**

**Figure 5.3.** Relative dextran accumulation rate (see text) in *U. marinum* at three FITC-dextran concentrations measured over a 300 min incubation period. Error bars show the standard error of the mean (n=3).

**Figure 5.3**

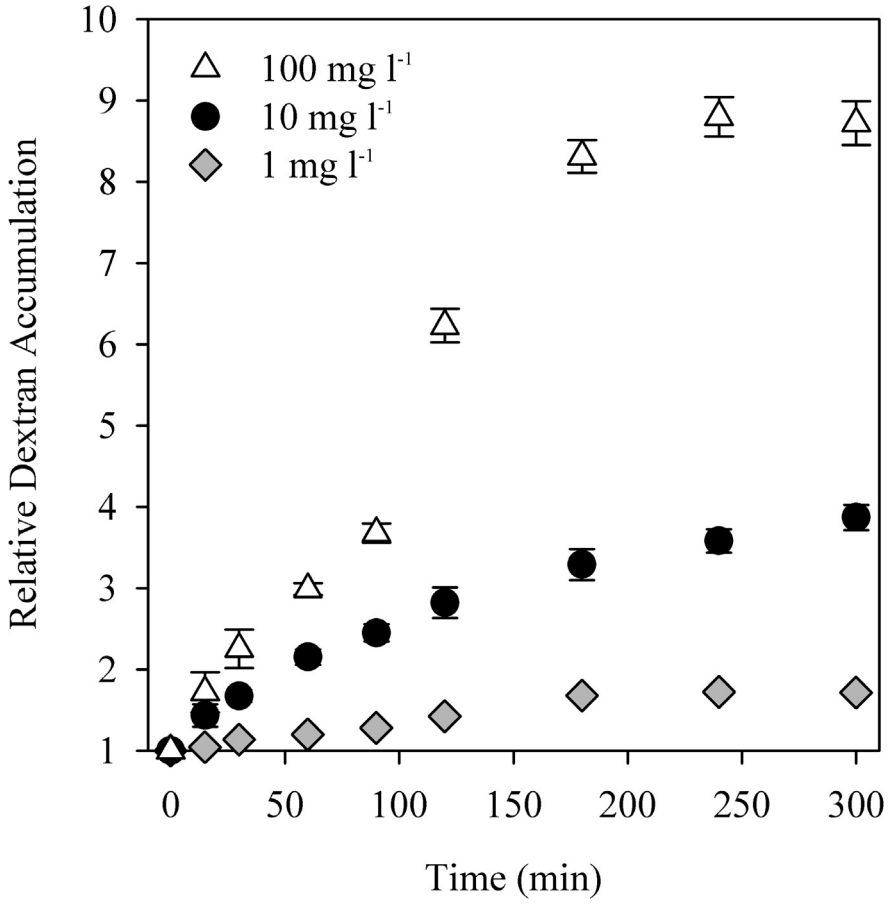
Relative Dextran Accumulation
Time (min)
100 mg l-1
10 mg l-1
1 mg l-1
10
9
8
7
6
5
4
3
2
1
0
50
100
150
200
250
300

**Figure 5.4.** A) Relative dextran accumulation rate in *U. marinum* treated with 0, 10, and 100 mg $l^{-1}$ dextran and low, medium and high bacteria concentrations. B) Per-capita ciliate grazing rates in all treatments. Error bars show the standard error of the mean (n=3). Asterisk indicates a significantly higher dextran accumulation (ANOVA, $p<0.05$)

**Figure 5.4**

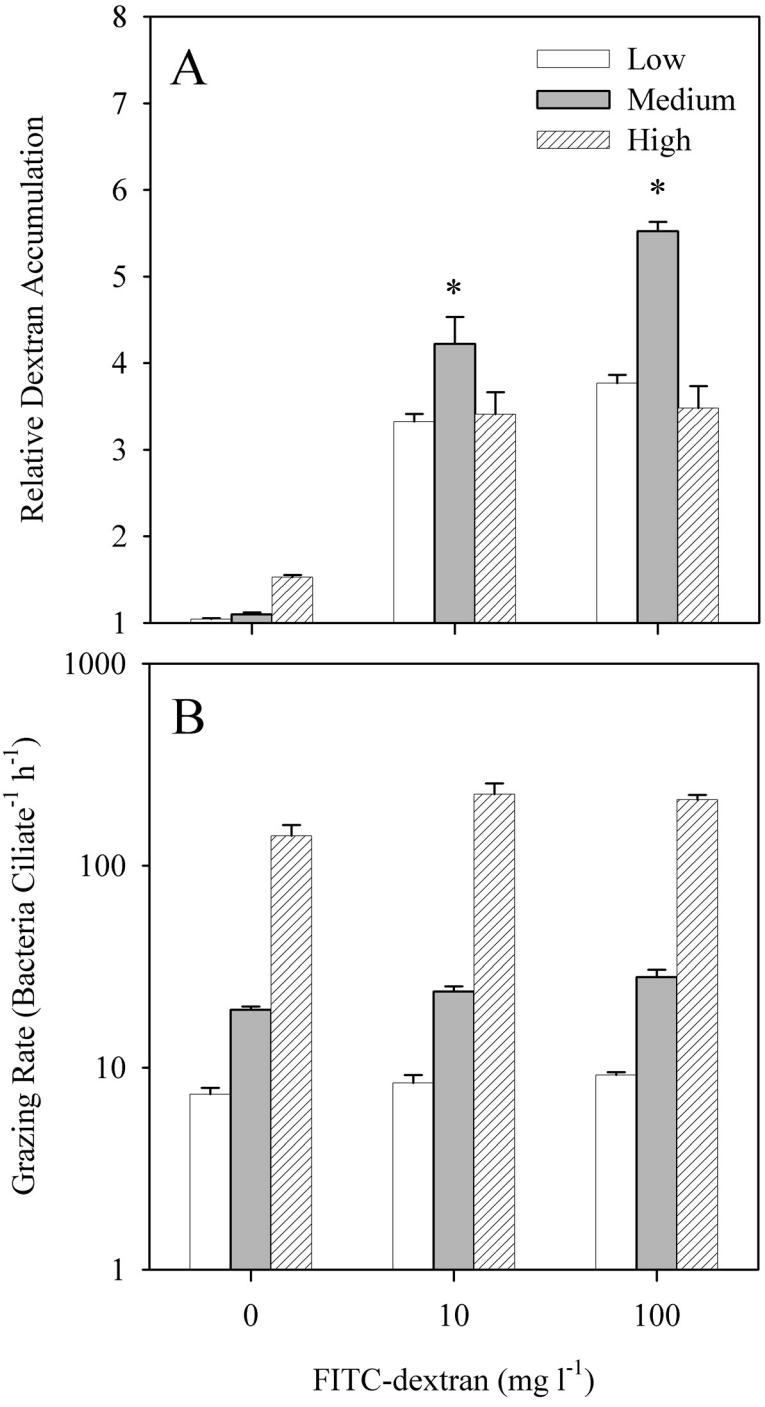
A
Low
Medium
High
Relative Dextran Accumulation
8
7
6
5
4
3
2
1
*
*
B
Grazing Rate (Bacteria Ciliate$^{-1}$ h$^{-1}$)
1000
100
10
1
0
10
100
FITC-dextran (mg l$^{-1}$)

**Figure 5.5.** *U. marinum* growth rate ($d^{-1}$) measured as the change in ciliate concentration over a 26 h incubation period. Ciliates were treated with low, medium, and high concentrations of bacteria and 0, 10, and 100 mg $l^{-1}$ FITC-dextran. Error bars show the standard error of the mean (n=3). Asterisk indicates a significantly higher ciliate growth rate (ANOVA, $p<0.05$).

**Figure 5.5**

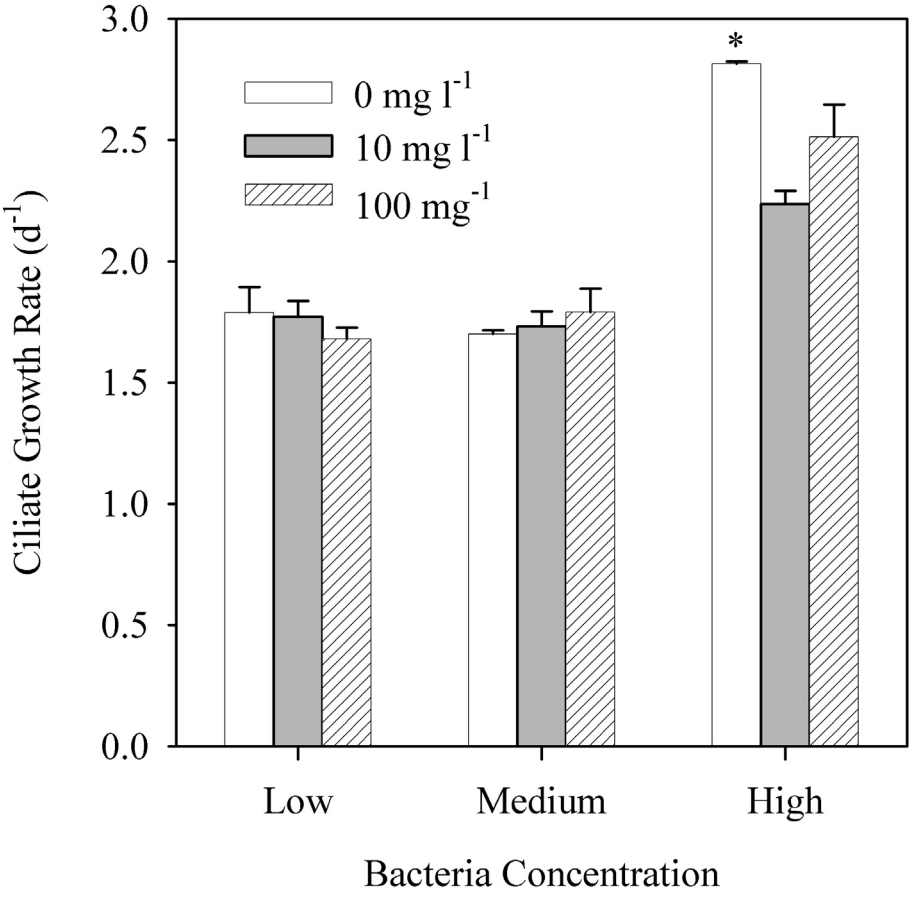
3.0
2.5
2.0
1.5
1.0
0.5
0.0
Ciliate Growth Rate (d-1)
0 mg l-1
10 mg l-1
100 mg-1
*
Low
Medium
High
Bacteria Concentration

**Figure 5.6.** A) *U. marinum* growth rate ($d^{-1}$) measured as the change in ciliate concentration over a 24 h incubation period. B) The biomass production rate (μg C $ml^{-1}$ $d^{-1}$) of *U. marinum.* The ciliates were incubated in control (no DOC addition), starch, acetate, and glucose treatments, with a final concentration of 3 mM DOC. Open bars show the growth rates without bacteria; gray bars are with bacteria. Error bars show the standard error of the mean (n=3).

**Figure 5.6**

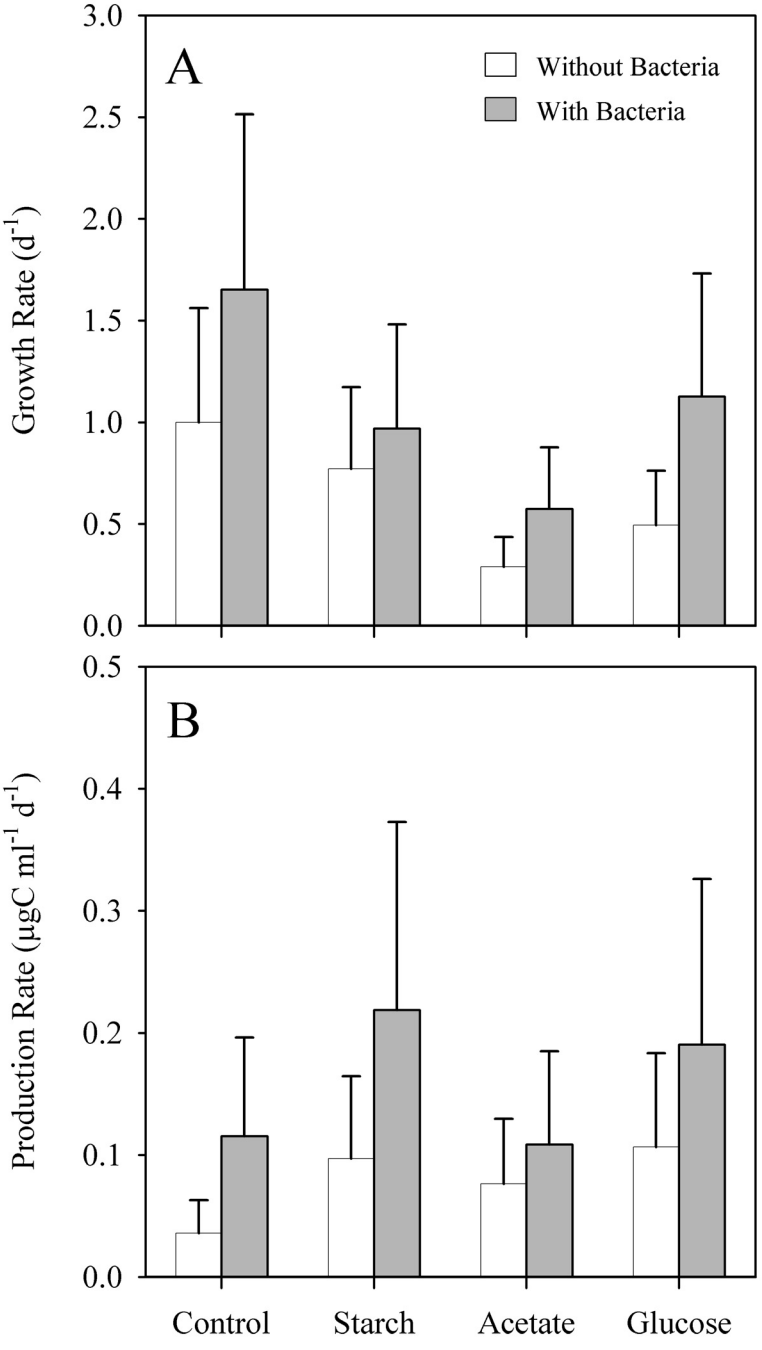
A
Without Bacteria
With Bacteria
Growth Rate (d-1)
3.0
2.5
2.0
1.5
1.0
0.5
0.0
B
Production Rate (µgC ml-1 d-1)
0.5
0.4
0.3
0.2
0.1
0.0
Control
Starch
Acetate
Glucose

# CHAPTER 6

## CONCLUSIONS

The term "secret garden" was used to describe the importance of benthic microalgae in shallow water coastal sediments (MacIntyre et al. 1996, Miller et al. 1996). The importance of bacteria, heterotrophic protists, and meiofauna as co-inhabitants of this "garden" suggests benthic microbial communities are better described as a "secret forest", harboring both producers and consumers. Similar to a temperate forest, there appears to be seasonal shift between the dominance of primary producers (BMA and *Spartina*) and the decomposers (bacteria) of organic matter. As described in **Chapter 2**, there was a period in the late summer/fall in which bacterial biomass dominated the total benthic biomass at all three locations that I studied. On a shorter time scale, there appeared to be fluctuations in the bacterial biomass over the course of a day (as reported in **Chapter 3**). These trends in bacterial biomass, and the factors that potential drive them, are discussed below.

### ARE BENTHIC BACTERIAL CONCENTRATIONS CONSTANT?

The high production, low grazing loss rates, and stable standing stocks of benthic bacteria are paradoxical. The goal of studying microbial food web structure and rates of bacterivory was to determine if bacterial production is uncoupled from grazing losses in sediments, either over short-term, diel cycles (due to varying grazing rates throughout the day) or long-term, seasonal cycles (due to greater relative abundances of heterotrophic protists).

Although the impact of protists grazing on bacteria varied throughout the day, there were no periods when grazing could substantially reduce bacterial biomass. Monthly monitoring revealed greater variations in the food web structure between sediment sampling locations than the variation that occurred at each location over the year. For example, protists were the most abundant (relative to the total biomass of the microbial food web) at Nannygoat Beach. Benthic bacterial biomass was lowest in these sediments, and bacterial turnover times were estimated to be approximately 10 d. In contrast, heterotrophic protists were <1% of the total biomass throughout the year in Marsh Landing sediments. Bacterial turnover times in Marsh Landing sediments were estimated to be >100 d in most of the monthly samples (Fig. 2.7).

The concentrations of benthic bacteria varied over daily and seasonal cycles. Bacteria concentrations ranged from 1.4 – 3.6 x $10^9$ cells $gws^{-1}$ (27 – 91 μg C $gws^{-1}$) over a day in Dean Creek intertidal sediments (Fig. 3.2). However, small-scale spatial variability may account for some of the differences between sampling times. Benthic bacterial biomass also fluctuated over the year at the three locations studied. The concentration of bacteria in Dean Creek subtidal sediments ranged from 1.3 to 7.0 x $10^9$ cells $gws^{-1}$ over a year (Fig. 2.2). This range of concentrations is not much greater than the range reported by Schmidt et al. (1998). However, changes in the mean bacterial cell size observed throughout the year resulted in bacterial biomass ranging over nearly one order of magnitude (26 – 253 μg C $gws^{-1}$) in Dean Creek sediments. The other locations also showed large variations in the biomass of benthic bacteria over the year. These data suggest that concentrations of benthic bacteria are not constant (sensu Schmidt et al. 1998), but instead are variable over time. Variations in bacterial cell biomass between sample times and locations indicates that the carbon stored in bacterial biomass may fluctuate more than

the bacterial concentration. Therefore, even when bacterial concentrations are constant, the total carbon stored by benthic bacteria may still be variable.

Variations in bacterial concentrations, as well as total bacterial biomass, may explain situations where bacterial production exceeds grazing losses. Yet, no periods were evident in my studies when grazing would exceed bacterial production and reduce the bacterial standing stocks. The inability to control bacterial biomass is not due to the low per-capita ingestion rates of bacterivorous protists. The cell specific ingestion rate of bacterivorous protists measured in this study (range, 3 – 15 x $10^2$ cells individual$^{-1}$ h$^{-1}$) is at the high end of the values reported in salt marsh sediments (Kemp 1988) and surface waters (Sherr et al. 1988). Instead, the relatively low abundance of bacterivorous protists limits grazing pressure and the flux of bacteria carbon into the food web via the microbial loop (Fig. 3.5). Potential factors limiting the abundance of benthic bacterivores are addressed below.

## CONTROLS ON BENTHIC BACTERIVORES

Bacteria are several orders of magnitude more abundant in sediments than in pelagic environments (when scaled to sediment porosity). However, the concentration of small heterotrophic protists (i.e. flagellates and small ciliates) is approximately the same in benthic and pelagic environments (see Fig. 6.1). What are the fundamental processes in sediments that set the lower relative abundance of bacterivores? Two likely processes preventing a higher abundance of benthic bacterivores are the low growth efficiencies of protists in anoxic environments and top-down predation pressure from omnivorous protists and meiofauna.

Anoxic environments are known to have truncated food webs due to the low growth yields of fermentation by eukaryotic consumers (Fenchel & Finlay 1995). In general, there are

fewer than three trophic levels in anaerobic communities due to the low carbon transfer efficiencies (Fenchel & Finlay 1990). Furthermore, many metazoans and larger animals are unable to exist for long time periods in anoxic sediments (Fenchel & Finlay 1995). Therefore, the large omnivorous protists and meiofauna inhabiting anoxic regions are effectively the top trophic level within the sediments. Some of the large protists observed in this study (e.g. Karyorelictid ciliates) are able to ingest bacterivorous flagellates and ciliates (Carey 1992). Likewise, nematodes are able to ingest a wide range of bacterivorous ciliates (Hamels et al 2001). Thus, in anoxic sediments, populations of heterotrophic flagellates and small ciliates are potentially limited by predation from omnivorous protists and meiofauna.

While bacterivorous protists are relatively scarce compared to benthic bacteria, selectively consuming bacterivorous protists provides larger omnivorous organisms with a significant energetic advantage. The following calculation demonstrates the advantage to nematodes of preying upon bacterivorous protists. Nematodes are estimated to consume as many as $5 \times 10^2$ bacteria individual$^{-1}$ h$^{-1}$ (Epstein & Shiaris 1992). The mean bacterial biomass calculated from monthly observations at locations in this study is $0.023 \pm 0.01$ pg cell$^{-1}$ (± SD, range observed: 0.014 to 0.043 pg cell$^{-1}$). Given the estimated ingestion rate of bacteria, nematodes would be able to consume 12 pg C h$^{-1}$ (range: 7 to 22 pg C h$^{-1}$). Small flagellates and ciliates that are approximately 20 x 15 μm in dimension have a carbon content of 350 pg C cell$^{-1}$. Thus, the ingestion of a single flagellate would equal the amount of bacteria carbon consumed over 30 h (range: 16 – 50 h). The higher carbon content in protists, as well as a higher nutritional quality (e.g. Klein Breteler et al. 1999), suggest that selectively consuming phagotrophic protists would be energetically advantageous for benthic omnivores.

Consuming bacterivorous protists is can be particularly advantageous for omnivores during periods when bacterial biomass exceeds microalgal biomass, such as in the late summer and fall in the Sapelo Island salt marsh sediments I studied. During periods of high abundance, BMA may be the preferred food source of omnivorous protists and meiofauna. When BMA became proportionally less abundant than bacteria, omnivorous protists and meiofauna may selectively consume bacterivorous flagellates and small ciliates. In other coastal marine sediments, the grazing rates on bacteria and BMA were estimated to be insufficient to support the metabolic requirements of large ciliates during parts of the year (Epstein 1997). In this case, bacterivorous protists may be the "missing component" in the diet of omnivorous ciliates. With reduced abundance of bacterivorous protists, the rates of nutrient regeneration will also decline. This could potentially explain the buildup of inactive bacterial biomass during this time period, most evident in Dean Creek sediments (See Fig. 2.2).

## IMPLICATIONS OF NON-UNIFORM DISTRIBUTIONS OF MICROBENTHOS

The application of the FLEC technique to monitor spatial distributions of microbenthos described in **Chapter 4** revealed that: 1) enzymatically-active microbenthos were found throughout the 2 cm examined; and 2) microbenthos were significantly clumped throughout the day at all spatial scales. The majority of microbenthos were benthic diatoms. This determination was based on cell size, cell morphology, and microscope observations of sediments from this location. Subsurface accumulation of many benthic diatoms is commonly observed (Pinckney & Zingmark 1993). BMA below the top 1 – 2 mm of the surface are functionally described as 'photosynthetically inactive biomass' (Kelly et al. 2001). The cells observed in at these depths in the FLEC cores are not dead or dormant, as the fluorescent stain used in this investigation only

labels cells with intact enzymes and membranes. The factors driving benthic algae deep into the sediments are unclear, but the behavior could allow algae to access nutrients deeper in the sediments (Kingston 2002). In this case, the aggregation of BMA near heterotrophic protists would provide close proximity to regenerated nutrients.

The clumped distribution of microbenthos has several implications. First, concentrations of the benthic microorganisms (measured per sediment weight, volume, or surface area) may not reflect their ecological importance. For example, I reported the concentrations of benthic protists per weight of wet sediment in **Chapters 2** and **3**, based on methods that homogenized sediments by stirring before they were chemically fixed. The relatively low concentrations of heterotrophic protists I found relative to bacteria and BMA biomass suggest their role in the benthic microbial food web is reduced relative to pelagic environments. However, aggregation of benthic protists in zones of high microbial activity will lead to a greater impact than suggested by their average abundance. In this case, the typical roles of benthic protists in aquatic food webs (nutrient regeneration, etc.) will be important to specific microenvironments and organisms within these 'zones of influence'.

Similarly to concentrations of organisms, rates of microbiological processes in sediments (e.g. bacterial production, photosynthesis), are often reported as bulk averages per unit area, volume, or weight of sediment. These rates measurements, therefore, integrate the heterogeneity in sediments, mixing zones of relatively low microbial activity with zones of high activity and potentially underestimating cell-specific activities. With uneven distributions of microbial activity, the ingestion rates of protists and meiofauna will depend upon the time spent near areas of dense prey versus the time spent in zones where prey are scarce.

Lastly, symbiotic associations among microbenthos may be a key feature of anoxic sediments. Symbiotic relationships between microbenthos and prokaryotes occurred more frequently in anoxic sediments compared to sediments with higher oxygen concentrations (Bernhard et al. 2000). The aggregation of flagellates with prokaryotic ectobionts suggests that the host can locate favorable microenvironments occurring within the sediments (Bernhard et al. 2003). Non-random aggregation patterns described in **Chapter 4** indicate that potentially symbiotic or commensal relationships among microbenthos may exist in these salt marsh sediments.

## POSITIVE FEEDBACKS OF THE MICROBIAL LOOP

Phagotrophic protists have been shown to stimulate the activities of bacteria and the rates of organic matter consumption (Gruber et al. 2006). This occurs via increasing rates of nutrient regeneration and by grazing bacterial populations that are in stationary growth phases. Remineralization of high molecular weight polysaccharides was accelerated by phagotrophic flagellates (Sherr et al. 1982). In wastewater treatment plant effluent, both the oxygen demand and the concentration of dissolved organics are reduced in the presence of high densities of phagotrophic protists (Curds 1982). Additionally, bacterivores may play a role in shaping the dissolved organic carbon pool (and bacterial production rates) by egesting labile carbon compounds (Kujawinski et al. 2002).

The common benthic ciliate, *Uronema marinum*, was capable of ingesting dextran, a model high molecular weight organic carbon compound **(Chapter 5)**. Bacterivorous ciliates are common in the sediments examined here and elsewhere (Fenchel 1967, Fernandez-Leborans et al. 2001), so their activities have implications for overall sediment metabolism. I found that

ingestion of DOC did not improve the growth rates of these ciliates. However, transformation of high molecular weight DOC in protists' food vacuoles may affect the lability of the DOC pool and thus facilitate DOC use by bacteria. Terminal respiration rates in sediments can be limited by the supply of low-molecular weight DOC during summer (Weston & Joye 2005). Release of these compounds resulting from the fermentation of particulate and high molecular weight DOC by bacterivorous protists (Biagini et al. 1998), may thus be a critical source of labile carbon during the summer months when heterotrophic protists are abundant. In this study, heterotrophic protists were generally most abundant in summer months (**Chapter 2**). Consequently, the release of labile carbon may benefit bacterivorous protists due to increased bacterial production.

## REFERENCES


Bernhard JM, Buck KR, Farmer MA, Bowser SS (2000) The Santa Barbara Basin is a symbiosis oasis. Nature 403:77-80

Bernhard JM, Visscher PT, Bowser SS (2003) Submillimeter life positions of bacteria, protists, and metazoans in laminated sediments of the Santa Barbara Basin. Limnol Oceanogr 48:813-828

Biagini GA, Finlay BJ, Lloyd D (1998) Protozoan stimulation of anaerobic microbial activity: enhancement of the rate of terminal decomposition of organic matter. FEMS Microbiol Ecol 27:1-8

Carey PG (1992) Marine interstitial ciliates: an illustrated key, 2nd ed., Chapman and Hall, Norwell, MA

Curds CR (1982) The Ecology and role of protozoa in aerobic sewage-treatment processes. Ann Rev Microbiol 36:27-46

Epstein SS (1997) Microbial food webs in marine sediments. 2. seasonal changes in trophic interactions in a sandy tidal flat community. Microb Ecol 34:199-209

Epstein SS, Shiaris MP (1992) Rates of microbenthic and meiobenthic bacterivory in a temperate muddy tidal flat community. Appl Environ Microbiol 58:2426-2431

Fenchel T (1967) The ecology of marine microbenthos I. The quatitative importance of ciliates as compared with metazoans in various types of sediments. Ophelia 4:121-137

Fenchel T, Finlay B (1990) Anaerobic free-living protozoa: growth efficiencies and the structure of anaerobic communities. FEMS Microbiol Ecol 74:269-275

Fenchel T, Finlay BJ (1995) Ecology and evolution in anoxic worlds. Oxford University Press, Oxford

Fernandez-Leborans G, Valganon B, Perez E (2001) Characterization of the protistan communities inhabiting the benthic area of an inner estuary. Bull Mar Sci 68:451-467

Gruber DF, Simjouw JP, Seitzinger SP, Taghon GL (2006) Dynamics and characterization of refractory dissolved organic matter produced by a pure bacterial culture in an experimental predator-prey system. Appl Environ Microbiol 72:4184-4191

Kelly JA, Honeywill C, Paterson DM (2001) Microscale analysis of chlorophyll-*a* in cohesive, intertidal sediments: the implications of microphytobenthos distribution. J Mar Biol Assoc U K 81:151-162

Kemp PF (1988) Bacterivory by benthic ciliates: significance as a carbon source and impact on sediment bacteria. Mar Ecol Progr Ser 49:163-169

Kingston MB (2002) Effect of subsurface nutrient supplies on the vertical migration of *Euglena proxima* (Euglenophyta). J Phycol 38:872-880

Klein Breteler WCM, Schogt N, Baas M, Schouten S, Kraay GW (1999) Trophic upgrading of food quality by protozoans enhancing copepod growth: role of essential lipids. Mar Biol 135:191-198

Kujawinski EB, Farrington JW, Moffett JW (2002) Evidence for grazing-mediated production of dissolved surface-active material by marine protists. Mar Chem 77:133-142

Legrand C, Carlsson P (1998) Uptake of high molecular weight dextran by the dinoflagellate Alexandrium catenella. Aquat Microb Ecol 16:81-86

MacIntyre HL, Geider RJ, Miller DC (1996) Microphytobenthos: the ecological role of the "secret garden" of unvegetated, shallow-water marine habitats. I. Distribution, abundance and primary production. Estuaries 19:186-201

Miller DC, Geider RJ, MacIntyre HL (1996) Microphytobenthos: The ecological role of the "secret garden" of unvegetated, shallow-water marine habitats. II. role in sediment stability and shallow-water food webs. Estuaries 19:202-212

Pinckney J, Zingmark RG (1993) Biomass and production of benthic microalgal communities in estuarine habitats. Estuaries 16:887-897

Schmidt JL, Deming JW, Jumars PA, Keil RG (1998) Constancy of bacterial abundance in surficial marine sediments. Limnol Oceanogr 43:976-982

Sherr BF, Sherr EB, Berman T (1982) Decomposition of organic detritus - a selective role for microflagellate protozoa. Limnol Oceanogr 27:765-769

Sherr BF, Sherr EB, Rassoulzadegan F (1988) Rates of digestion of bacteria by marine phagotrophic protozoa: temperature dependence. Appl Environ Microbiol 54:1091-1095

Sherr EB (1988) Direct use of high molecular-weight polysaccharide by heterotrophic flagellates. Nature 335:348-351

Tranvik LJ, Sherr EB, Sherr BF (1993) Uptake and utilization of colloidal DOM by heterotrophic flagellates in seawater. Mar Ecol Prog Ser 92:301-309

Weston NB, Joye SB (2005) Temperature-driven decoupling of key phases of organic matter degradation in marine sediments. PNAS 102:17036-17040

**Figure 6.1** Concentrations of bacteria and bacterivorous protists (mostly flagellates, although small ciliates are included) in this study. The concentrations were determined per weight of wet sediment and adjusted to porewater volume. The range of concentrations of marine pelagic bacteria and flagellates are shown by the bar. See **Chapter 2** for details and the literature sources.

**Figure 6.1**

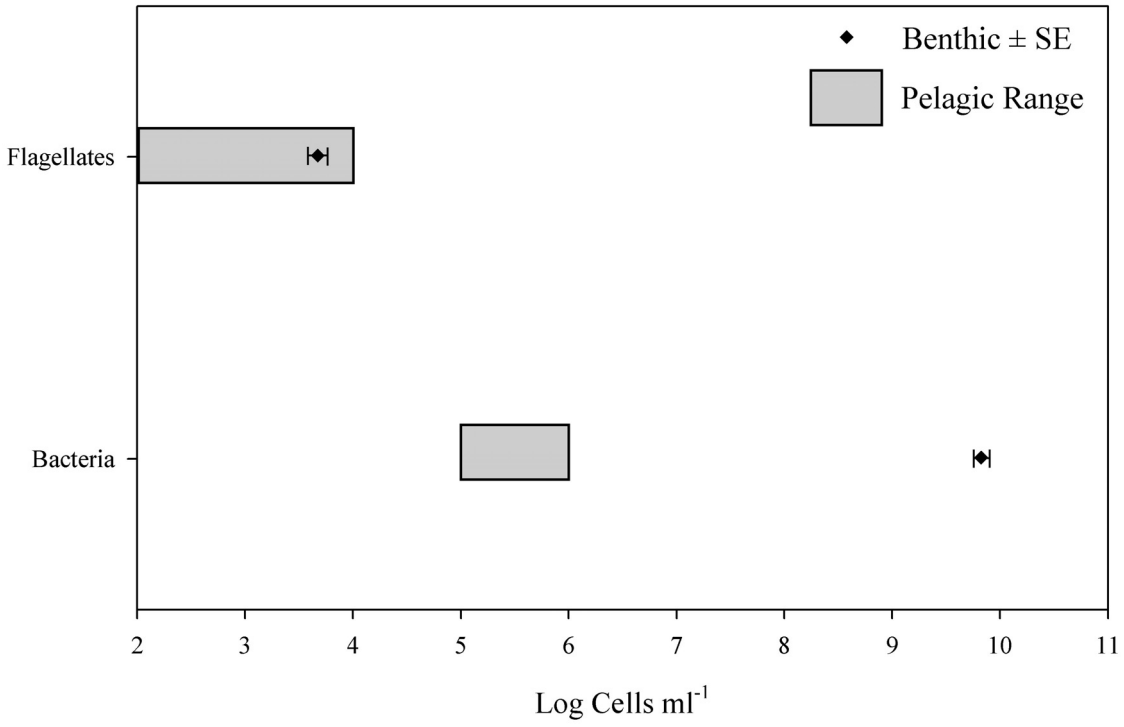
Benthic ± SE
Pelagic Range
Flagellates
Bacteria
2
3
4
5
6
7
8
9
10
11
Log Cells ml-1